Separation of readily biodegradable aminocarboxylate complexes by electrodriven methods

Lebogang Maureen Katata

"Dissertation presented in partial fulfillment for the degree of Doctor of Science at the University of Stellenbosch"

Promoter: **Professor Andrew M. Crouch**

March 2008

“DECLARATION

I, the undersigned, hereby declare that the work contained in this dissertation is my own original work and that I have not previously in its entirety or in part submitted it at any university for a degree.

Signature:……. Date:……..**”**

Abstract

Aminopolycarboxylic acids (APCAs) are chelating agents widely used to inactivate various metal ions by complex formation in industrial and household applications. Ethylenediaminetetraacetic acid (EDTA) and diethylenetriaminepentaacetic acid (DTPA) are the widely used agents. Their use is under scrutiny due to their persistence in the environment because they cannot readily biodegrade. This led to the introduction of readily biodegradable agents namely ethylenediaminedisuccinic acid (EDDS) and iminodisuccinic acid (IDS) as alternatives especially to EDTA. Therefore, there was an interest to study the separation of EDDS, IDS and other APCAs using a simple, quick and accurate method.

Capillary electrophoresis was used to determine the separation and speciation of iminodisuccinic acid with various metal ions at various pH levels. Speciation modelling was also utilized to compare and validate the presence and distribution of metal-ligand species. The obtained CE results were compared with speciation profiles and a reasonable agreement was obtained.

The degradation studies at various time intervals for the metal-ligand (ML) complexes of DTPA, S,S-EDDS, IDS and R,S-IDS with various metal ions (Cd^{2+}, Cr^{3+}, Cu^{2+}, Fe^{3+}, Mn^{2+}, Pb^{2+} and Zn^{2+}) at pH 7 and 9 was evaluated using CE. New peaks were observed in some ML complexes when the pH was changed from pH 9 to 7. Sharp peaks were seen for CuL (L = DTPA, S,S-EDDS, IDS and R,S-IDS), FeDTPA and FeEDDS at both pH's. While small broad peaks were observed for FeIDS, CrL and MnL complexes. CuDTPA and CuEDDS complexes showed a greater stability over some considerable time as compared to CuIDS, CuR,S-IDS and other metal complexes at pH 9.

This work also investigated the effect of various cationic electroosmotic flow (EOF) modifiers and counter anions on the CE separation of EDTA, EDDS and IDS as Cu(II) complexes. The performance of the modifiers was evaluated in terms of migration times, resolution and plate numbers. The best results were observed when

Tetradecyltrimethylammonium bromide (TTAB) and Cetyltrimethylammonium bromide (CTAB) was used as modifiers in order to reverse the EOF in the fused silica capillary. This resulted in short analysis time and better peak shapes. The effect of different counteranions attached to EOF modifiers on the separation was also shown. It was also found that the counter anions of EOF modifiers used influences the separation of the complexes. The EOF modifiers namely Cetyltrimethylammonium chloride (CTAC) and Tetradecyltrimethylammonium chloride (TTAC) were further utilized for the determination of EDTA in South African river waters and industrial effluents.

A method for the simultaneous separation of Fe (III) complexed with EDTA, S,S'-EDDS and IDS was developed by CE and high-performance liquid chromatography (HPLC). The recalcitrant EDTA is used in combination with readily biodegradable analogues like EDDS and IDS in many commercial products. The methodology performance was evaluated in terms of linearity, limit of detection (LOD), limit of quantitation (LOQ) and reproducibility for both CE and HPLC methods. The LOD values obtained from HPLC were low when compared with CE. The applicability of both methods was demonstrated for the analysis of cosmetic products such as foam bath and shower cream. The results obtained by both CE and HPLC were found to be comparable and are in good agreement.

Opsomming

Aminopolikarboksiel sure (APCAs) is komplekseer middels wat algemeen gebruik word om verskillende metaal ione te deaktifeer deur kompleks vorming in industriële en huishoudige toepassings. Etileendiamientetraasynsuur (EDTA) en dietileentriamienpentaasyn suur (DTPA) is die mees algemene APCA's. Hul gebruik word deesdae noukerig ondersoek as gevolg van hul volharding in die omgewing. Daar is 'n intense soektog na bio-afbreekbare agente soos etieleendiamiendisuksien suur (EDDS) and iminodisuksien suur (IDS) wat as plaasvervangers kan dien vir nie-afbreekbare EDTA. Daar is dus 'n behoefte om te kyk na eenvoudige, vinnige en noukeurige metodes vir die bepaling van EDTA, EDTA , IDS en ander APCA's.

Kapillere elektroforese (CE) was gebruik vir die skeiding en spesiering van iminodisuksien suur met verskillende metale by verskillende pH's. Spesiasie modellering was ook gebruik om die teenwoordigheid en verspreiding van metaal- spesies te vergelyk. Die CE uitslae was met die spesiasie profiele vergelyk en 'n redelike ooreenkoms was gevind.

Die degraderings studies as 'n funksie van tyd was met CE bestudeer vir verskillende metal-ligand (ML) samestellings van DTPA, S,S-EDDS, IDS en R,S-IDS met verskillende metal ione (Cd^{2+}, Cr^{3+}, Cu^{2+}, Fe^{3+}, Mn^{2+}, Pb^{2+} en Zn^{2+}) by pH 7 en 9. Nuwe pieke was opgemerk in sommige ML samestellings wanneer die pH van pH 9 na 7 verander. Hoë pieke was vir CuL (L = DTPA, S,S-EDDS, IDS and R,S-IDS), FeEDTA en FeEDDS by alle pH's gevind. Lae, breë pieke was vir FeIDS, CrL en MnL komplekse gevind. CuDTPA en CuEDDS komplekse het 'n goeie stabiliteit gewys oor 'n redelike tyd as dit met CuIDS, CuR,S-IDS en ander metal komplekses by pH 9 vergelyk word.

In hierdie werk was die effek van verskillende kationiese elektro-osmotiese stroom (EOF) modifiseerders ook ondersoek. Veral die effek wat teen ioone op die CE skeidings het van EDTA, EDDS en IDS asook Cu(II) komplekse was ondersoek. Die effek van die modifiseerders was ondersoek en ge-evalueer in terme van migrasie tye, resolusie en

plaat getalle. Die beste skeidingskondisies was bereik wanneer tetradesieltrimetielammonium bromied (TTAB) and setieltrimetielammonium bromied (CTAB) as modifiseerders gebruik word. Hierdie kondisies het ook aanleiding gegee tot korter ondersoek tye en beter piekvorme. Die effek van verskillende teen ioone wat aan die EOF modifiseerders gekoppel was het ook interresante resultate opgelewer. Die EOF modifiseerders setieltrimetielammonium chloried (CTAC) en tetradesieltrimetielammonium chloried (TTAC) was ook gebruik vir die bepaling van EDTA in Suid Afrikaanse rivier waters en industrieel afloop.

'n Metode vir die gelyktydige skeiding van Fe(III) met EDTA, S,S'-EDDS en IDS was met behulp van CE en hoedruk vloeistof chromatography (HPLC) ontwikkel. Die metodologie was ondersoek ingevolge lineariteit, limiet van deteksie (LOD), limiet van kwantifisering (LOQ) en die herhaalbaarheid van CE en die HPLC metodes. Die LOD waardes verkry vanaf HPLC was swakker vergeleke met die' verkry deur CE. Die toepaslikheid van al die metodes was vir die ontleding van kosmetiese produkte soos bad skuim en stortbad room getoets. Die uitslae deur CE en HPLC was vergelykbaar en 'n goeie ooreenkoms was gevind.

Acknowledgments

This road has been long and hard but I would like to give all thanks to God the creator for the gift of life and also giving me the strength to write up this thesis.

My greatest debt of gratitude is to my supervisor Prof Andrew. M Crouch for his patience and support throughout my years of study. Without his guidance and encouragement this work would have been very difficult. *Modimo a go tshegofatse.*

I would also like to thank Astrid Buica, Dr Frederic Lynen and Dr Andre de Villiers for their valuable discussions and support on capillary electrophoresis.

Dr Velupula Nagaraju and Dr Mosidi Makgae are gratefully acknowledged for their careful review of the manuscript and their valuable criticism and comments that led to its improvement.

My sincere appreciation is expressed to all the members of my family for their love, understanding and unconditional support through the tough times. Warmest thanks to all my friends and colleagues. You all had an impact on my life in many ways.

Financial support from the University of Stellenbosch, National Research Foundation (NRF) of South Africa and the Tertiary Education Support Program (TESP) of Eskom are acknowledged.

This work is dedicated to Atlegang and my family because of their love and inspiration.

Contents

List of Abbreviations

APCAs	- Aminopolycarboxylic acids
AAS	- Atomic Absorption Spectroscopy
CE	- Capillary Electrophoresis
CTAB	- Cetyltrimethylammonium bromide
CTAC	- Cetyltrimethylammonium chloride
DCTA	- Trans-1, 2-diaminocyclohexane-N, N, N', N'-tetraacetic
DTPA	- Diethylenetriamine pentaacetic acid
EDDM	- Ethylenediamine dimalonic acid
EDDS	- Ethylenediamine disuccinic acid
EDTA	- Ethylenediamine tetraacetic acid
EGTA	- Ethyleneglycolcolbis (2-aminoethyl ether) N, N, N', N'-tetraacetic acid
EOF	- Electroosmotic flow
GC	- Gas Chromatography
HPLC	- High Performance Liquid Chromatography
ICP	- Inductively Coupled Plasma
ICP-MS	- Inductively Coupled Plasma source with a Mass Spectrometer
IDS	- Iminodisuccinic acid
JESS	- Joint Expert Speciation System
LOD	- Limit of detection
LOQ	- Limit of quantitation
NTA	- Nitrilotriacetic acid
TTHA	- Triethylenetetramine-N, N, N', N'', N''', N'''-hexaacetic acid

TTAC - Tetradecyltrimethylammonium chloride

UV - Ultraviolet

List of Tables

List of Figures

Chapter 1

Introduction

1.1 Properties and uses of chelating agents

Chelate is the term that originates from the Greek "*chele*" meaning lobster or crab's claw and was first applied in 1920 by Morgan and Drew [1]. Chelating agents are multidentate ligands ("*ligare*" is a term in Latin = to bind) that bind metal ions similar to a claw holding an object. Metal ions form coordinate covalent bonds with molecules or anions having lone pairs of electrons and this is called complex formation. Ligands can occupy one, two or more positions in the inner coordination sphere of the central ion and are referred to as monodentate, bidendate and so on. Complex ions are formed from a metal ion with Lewis bases attached to it by coordinate covalent bonds [2]. The stability of complex ions is expressed by means of stability constant. The more stable the complex, the greater is the stability constant that is the smaller the tendency of the complex ion to dissociate into its constituent ions [3], thus forming an inert complex. However in labile complexes, the metal ion can be readily exchanged. Because of the stability of chelates, polydentate ligands are often used to remove metal ions from a chemical system [2]. Reviews on crystallography of chelants showed that their interaction with cation leads to the formation of heterocyclic rings, as illustrated in Figure 1.1. The structure of NTA allows for a total of four possible ligand sites and that of EDTA allows for a total of six.

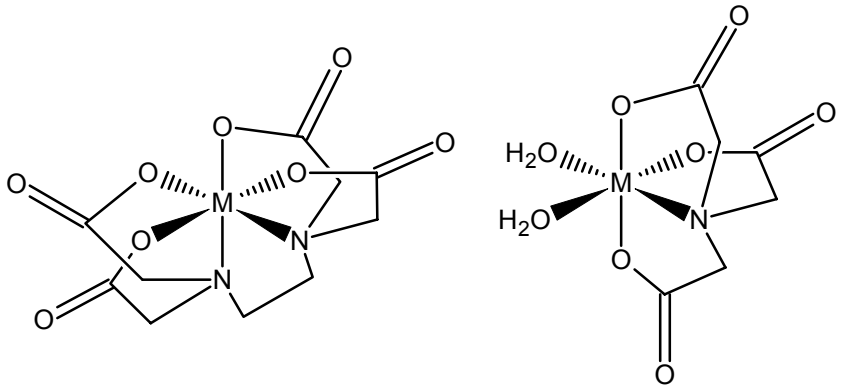

Figure 1.1: Ideal octahedral structures of metal-EDTA and metal-NTA complexes.

Aminopolycarboxylates (APCAs) and phosphonates are mostly used chelating agents for complexation of metal ions in many processes and are also ubiquitous in the environment. In this study our interest involves the use of APCAs and they are characterized by one or more tertiary or secondary amines and two or more carboxylic acid groups. Their main uses are the following: (i) to prevent the formation of metal precipitates, (ii) to hinder unwanted chemical reactions caused by metal ion in catalysis, (iii) to remove ions from systems or (iv) to make metal ions more available by keeping them in solution. They are also preferred for many applications because of their stability, chelation strength and activity over a wide range pH and temperature.

Figure 1.2 shows structures of some of the APCAs chelating agents. EDDS, IDS and MGDA have received recently some attention as possible replacements for EDTA and DTPA. EDTA offers a considerable versatility in industrial and household uses as compared to other ligands worldwide [4]. It has also been extensively used for more than 60 years.

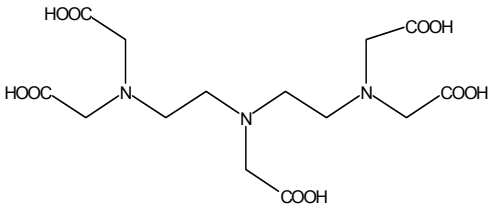

Diethylenetriaminepentaacetic acid (**DTPA**)

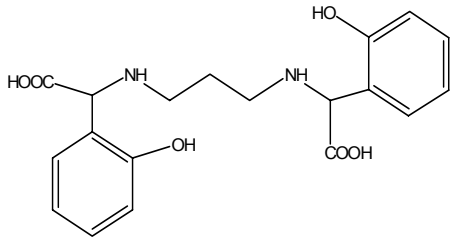

Ethylynediamine(o-hydroxyphenylaceti) acid (**EDDHA**)

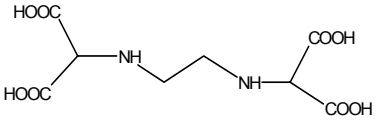

Ethylenediaminedimalonic acid (**EDDM**)

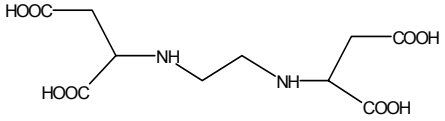

Ethylenediaminedisuccinic acid (**EDDS**)

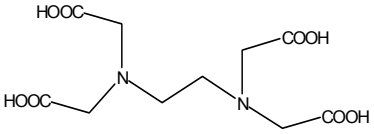

Ethylenediaminetetraacetic acid (**EDTA**)

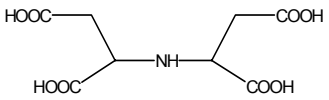

Iminodisuccinic acid (**IDS**)

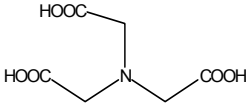

Nitrilotriacetic acid (**NTA**)

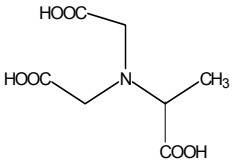

Methylglycinediacetic acid (**MGDA**)

Figure 1.2: Molecular structures of aminopolycarboxylic acids

A summary of different uses of EDTA and its ligands world wide is given in Table 1.1. EDTA is released into the environment through wastewaters since it is used predominantly in aqueous medium. The applications include decontaminating nuclear reactor systems, cleaning various kinds of boilers, softening boiler and process water. There are also medicinal uses that include treating Alzheimer's disease by the complex active of aluminium [5], treating ulcers and periathritis. In consumer products EDTA is used to complex trace metals in order to prevent catalytic reactions leading to rancidity, loss of flavour and discolouration in food products and also to control metals that destabilize cosmetics and pharmaceuticals [6]. EDTA is used medically to remove toxic metals (e.g. lead in children) and in dental procedures [7].

Table 1.1: Uses of chelating agents

Area	Compound	Use
Detergents	APCAs	complexation of Ca, Mg and heavy metals
Photo industry	EDTA, PDTA	oxidising agent
Pulp and paper	APCAs	complexation of heavy metals
Food	EDTA	stabilizer, antioxidant, Fe-fortification
Agriculture	EDTA, EDDHA	Fe, Cu and Zn fertilizers
Oil production	EDTA	inhibition of mineral precipitation
Medicine	APCAs	treatment of metal poisoning and chelation therapy
Soil remediation	APCAs	extraction of heavy metals and phytoremediation
Textile industry	APCAs	bleach stabilizer
Personal care	EDTA	stabilizer and antioxidant

Figure 1.3 illustrates the latest available data on the consumption of chelating agents [8]. The total worldwide use of synthetic APCAs i.e. EDTA, DTPA and NTA was 200 00 tons in 2000 [9]. These chelating agents are of great interest because of their use. Their concentrations are found in natural systems (e.g. wastewaters, surface and drinking water). Their widespread use has raised major concerns with the amounts of APCAs that are released to the environment. This is due to the slow removal or biodegradability of EDTA under many environmental conditions and has led to its highest concentration of 1120 µg/L in some European surface waters [9, 10]. Elevated concentrations of chelating agents increase the transport of metals e.g. Zn, Cd, Cr, Ni, Pb and Fe in soils [11] and enhance the undesired transport of radioactive metals away from disposal sites [12]. Theoretically the mobilized toxic heavy metals and radionuclides can be accumulated by plants and transferred to human beings through the food chain or can cause problems in the preparation of drinking water. Many European countries have banned EDTA for use in detergents but it is still used extensively in foodstuffs [13].

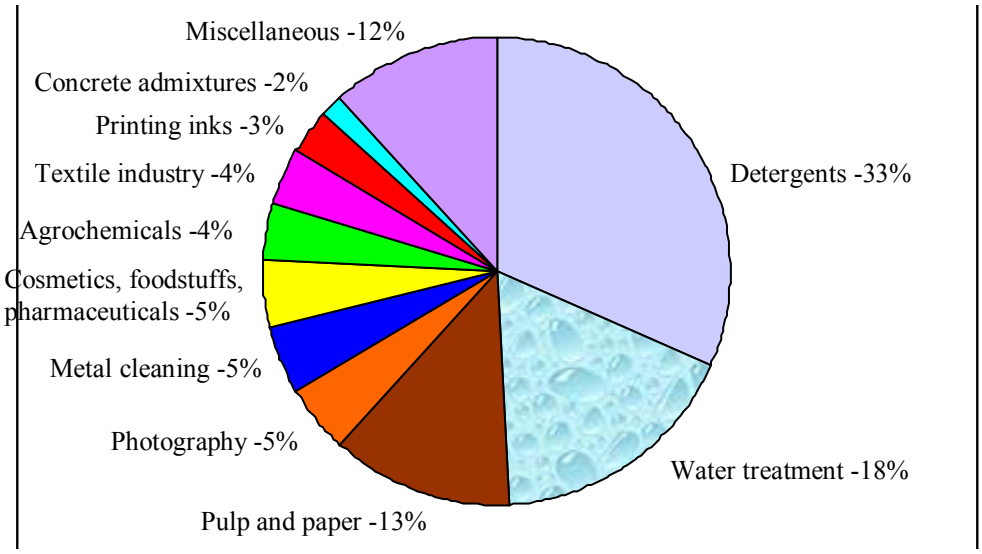

Figure 1.3: Industrial and household uses of ligands as a percentage of world market.

The ranges of concentration of EDTA found in natural waters are shown in Table 1.2. A highest value of 1120 µg/L has been found in England. The concentrations of EDTA in surface waters were measured in the Midwestern United States were reported for the Illinois River (51 µg/L) and the Des Plains River (76 µg/L) [4]. All of these rivers receive significant input of wastewater treatment effluents that were released upstream of the river measurement points had EDTA between 170 – 436 µg/L. EDTA was also detected in drinking water from an alluvial aquifer at 8 µg/L, a concentration of 158 µg/L nearby surface waters also indicated the migration of EDTA[14].

Table 1.2: Concentrations of EDTA in natural waters [14, 15].

Range of concentration (μg/L)	Type of fresh water	Location
158	River	France
14 - 1120	River	England
3.4 - 22.2	River	Germany
9.1 - 28	Lake	Germany
900	River	Jordan
2.0 - 45	River	Switzerland
5.85	Sea	Greece
2.6 - 29.2	Surface	Netherlands
1.7 - 44	Lake	Finland

1.2 Biodegradation of chelating agents

Current environmental legislation is increasingly moving towards phasing out of potentially harmful non-readily biodegradable chelating agents and the introduction of environmentally more benign readily biodegradable chelating agents. Biodegradation models could be useful in the early development of new chemicals because biodegradability could then become an integral part of the design process itself [16].

Biodegradation is the process by which microorganisms (bacteria, fungi and algae) break down organic materials into simpler fragments. The organic matter provides the bacteria with energy and building blocks from which more bacteria is produced. When biodegradation is complete, the end products are mostly carbon dioxide and water. Some of the scientists in the Procter & Gamble (P&G) company study the fate of the ingredients of their products so that they can comply with the EEC's Detergents Biodegradability. Their main concerns are the following:

- Where does the product go?
- How much goes there?
- How long does it stay there? and
- What happens to it while it is there?

People around the world use P&G's products to shampoo hair or use Ariel detergent to wash clothes. After each use of these products, the water disappears down the drain and ends up in the environment (see Figure 1.4) [17]. These products and their ingredients travel through sewers to the local wastewater treatment plant, where various processes shown in Fig 1.4 acts on them. Treated waste water is then released into surface water and, in some circumstances sewers directly discharge these products in the environment. Yet after wastewater treatment, some ingredients in the household product may still reach the environment. P&G's environmental safety organization helps to develop the understanding and to ensure that their products and ingredients do not harm the environment.

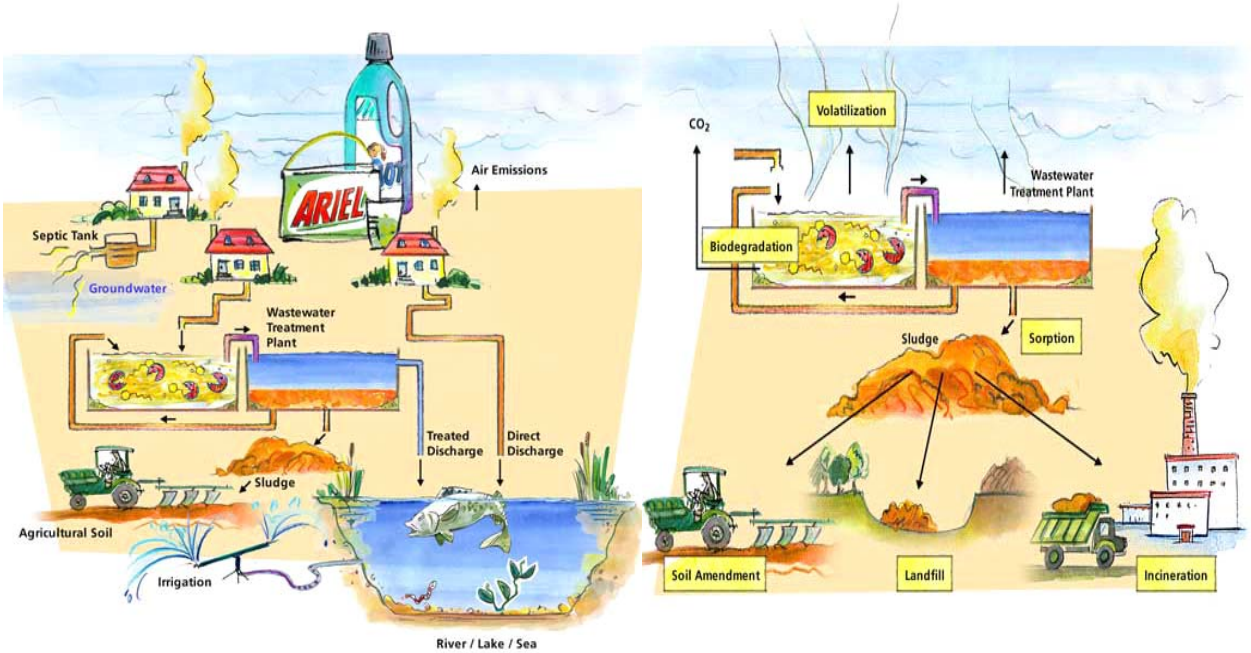

(a)What Happens to Products after Use? (b) Where do Chemicals Go?

Figure 1.4: The fate of the household products after being released into the environment.

Chemicals which have a structure susceptible to enzyme reaction are more readily biodegradable, since the biodegradation is a reaction in which chemicals are included in microorganisms in an activated sludge and undergo metabolic reaction through enzyme reaction. [18]. There is a relationship between biodegradability and molecular structure presented in accordance with the Law Concerning the Examination and Regulation of Manufacture of Chemical Substances. Satoshi et al [18] discovered biodegradable chelating agents which are suitable for photographic processing. Furthermore they discovered that of aminopolycarboxylic acid type chelating structures having (i) secondary amine, (ii) monoamine based and (iii) amide bond are specifically advantageous for biodegradability. The Chemical Substances Control Law (CSCL) which was enforced in Japan by the year 1973, was introduced in order to protect the human health from the impact caused by chemical pollutants via the environment [19]. This law requires the biodegradability test of chemicals before being introduced to the markets. Therefore a chemical that passes the criterion of biodegradability in the MITI (Japanese Ministry of International Trade and Industry) test protocol is judged to be a safe chemical when released in the environment. Table 1.3 shows the relationship between biodegradability and the molecular structure, while Figure 1.5 shows biodegradability test results of chelating agents employing the MITI test method which has been accepted by OECD (the Organization for Economic Cooperation and Development).

Table 1.3: Relationship between molecular structure and biodegradability

Amine	Biodegradability decreases in the order of primary, secondary and tertiary.
Alkane	Biodegradability decreases in the order of straight, branched and quaternary chain.
Halogen	Biodegradability decreases with substitution of halogen.
Molecular weight	Biodegradability decreases with an increase in molecular weight.

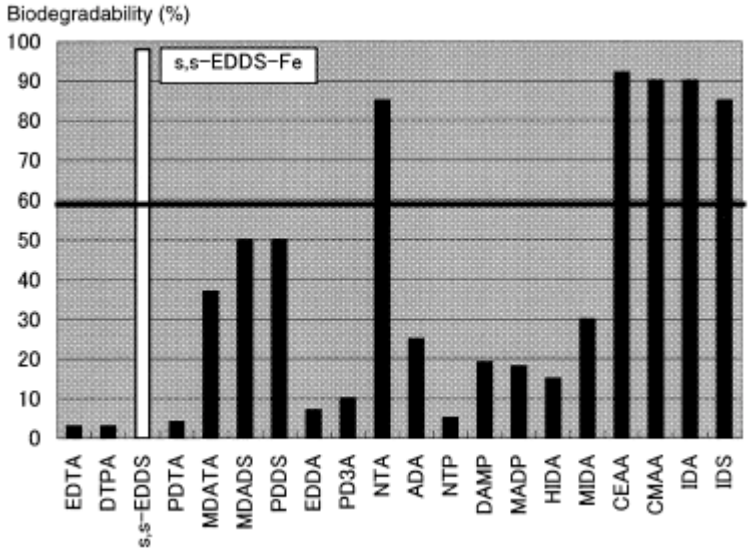

Figure 1.5: Biodegradability of chelating agents using MITI test [18]

It is thus of interest to understand the biodegradation of APCAs and their metal complexes. Many articles have been published on the investigation of their biodegradability.

1.2.1 The biodegradation process of EDTA

EDTA was thought to be resistant to biodegradation for a long time [10] and does not comply with the OECD ready-biodegradability criteria [20]. However there is some evidence that under certain conditions it may be degraded. In surface waters, the removal of EDTA as a ferric chelate has shown to photodegrade under UV light [21]. Kari and Giger [21] also point out that the studies on the photodegradability of EDTA in the environment should also take into account the cloud cover and the suspended material in the waters, since these are factors that condition the intensity of light received by water. Other studies have also demonstrated that EDTA and its metal chelates can be degraded by specially enriched bacterial cultures and in wastewater treatment plants receiving EDTA-containing effluents [10]. Nörtemann suggested catabolic pathways of EDTA in bacteria. The approach considered uncomplexed EDTA entrance to the cell, and the loss of an acetyl group as the first step in the intracellular oxidation was shown. It has also

been demonstrated that the bacterial strain DSM 9103 (located in the *Rhizobium-Agrobacterium* branch), degrades EDTA as a sole carbon source and it is able to perform the cellular uptake of the metallic complex Ca(II)-EDTA, with intracellular calcium polyphosphates accumulation [22].

It is necessary to point out that both the metal-chelate speciation and the bacterial species are the determining factors in the ability to degrade the compound. Thus, in certain cases there is only the ability to degrade metal-chelate complexes of low stability constant. Kluner et al. also investigated the influence of metal ions on the metabolism of EDTA by whole cells and cell-free extracts of strain BNC1. The suggested catabolic pathway is shown in Figure 1.6, while the exact opposite occurs when the Fe(III)-EDTA complex with a high stability constant is degraded [23]. Thomas et al. investigated the degradation of metal-EDTA complexes using an enriched microbial population from a river and liquid effluent sludge [24]. The consortium was enriched on Fe(III)-EDTA and it slowly degraded metal-EDTA complexes in the order Fe(III)-EDTA > CuEDTA> CoEDTA> NiEDTA> CdEDTA during a 28-day incubation. Furthermore, from the data available for the intracellular catabolism of EDTA, no generalizing pattern with respect to the influence of metal speciation on degradation can be deduced.

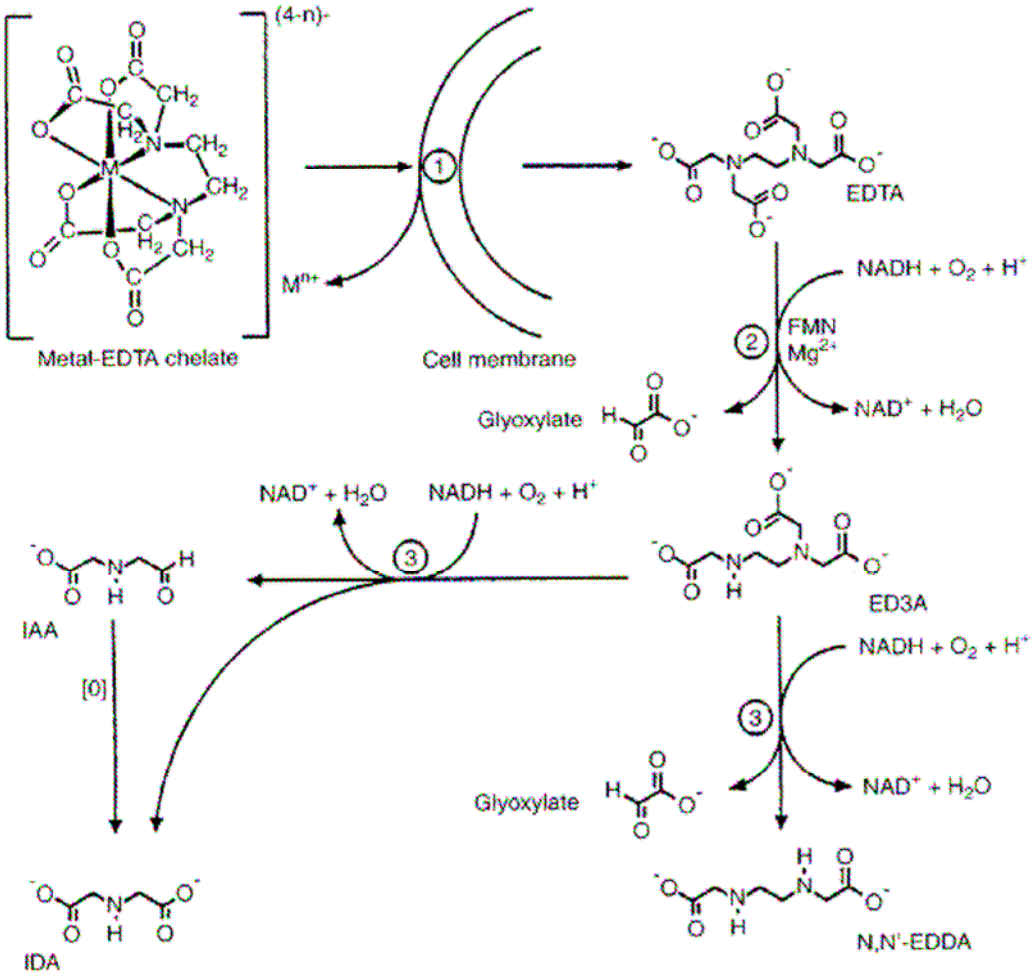

Figure 1.6: Proposed catabolic steps of EDTA pathway by strain BNC1. The first catabolic enzyme appears to be an EDTA monooxygenase since it requires O_2, NADH, and FMN for its activity and yields glyoxylate and ethylenediaminetriacetate (ED3A) as products. The latter is further degraded via N,N'-ethylenediaminediacetate. N,N'-EDDA,N,N-ethylenediaminediacetate, 1AA (iminoacetalaldehydeacetate), IDA (iminodiacetate). 1. Transport enzyme, 2. EDTA monooxygenase, 3. ED3A monooxygenases, n is the positive charge of the metal ion [23].

1.2.2 The biodegradation process of DTPA

There are no microorganisms that have been described which are able to grow with DTPA as sole source of carbon and energy. However, DTPA can be unspecifically

oxidized to ketopiperazinepolycarboxylates (KPPC), dead-end metabolites which can be detected in several surface waters and drinking waters [4]. It was concluded that only one acetyl group was cleaved from DTPA yielding uncompletely substituted APCAs and glyoxylate as products. This was based on the extensive enrichment experiments carried out with various samples, e.g. sewage sludge from the pulp and paper industry. Although glyoxylate should be degradable as a source of carbon and energy, no significant bacterial growth was observed.

1.2.3 The biodegradation process of EDDS

EDDS was first mentioned in a patent in 1964. It was synthesized from ethylenediamine and maleic anhydride producing a mixture of stereoisomers and is a structural isomer of EDTA [25]. It has two chiral centers, giving rise to three stereoisomers i.e. [S,S]-, [S,R]- or [R,S]-EDDS and [R,R]-EDDS. The biodegradation of these stereoisomers have been investigated extensively by various authors [26, 27]. In these studies the [S,S]-isomer was found to be readily degradable whereas the [R,R] remained undegraded in conventional test systems (e.g. OECD 301B), and the mixed stereoisomers were converted slowly and incompletely. As a consequence, the [S,S]-stereoisomer of EDDS has substituted traditional chelant agents in a number of consumer products [28, 29]. The bacterial strain DSM 9103 was able to utilize EDDS as a sole source of carbon, nitrogen, and energy [30]. Out of the three stereo-isomers, [S,S]- and [R,S]-EDDS were accepted as substrates by the lyase, whereas [R,R]-EDDS remained unchanged in assays with both cell-free extracts and pure enzyme. The enzyme catalyzed the transformation of free [S,S]-EDDS and of metal-[S,S]-EDDS complexes with stability constant lower than 10, such as Mg-, Ca-, BaEDDS and to a small extent also of MnEDDS, whereas Fe(III)-, Ni-, Cu-, Co- and ZnEDDS were not transformed. These results demonstrate that the [S,S]-EDDS-degrading enzyme is a lyase catalyzing an elimination reaction by splitting a C-N-bond between one succinyl residue and the ethylenediamine part of the molecule. A proposed biodegradation pathway for the isomers of EDDS is illustrated in Figure 1.7. It has also been reported that [S,S]-EDDS can be produced naturally by a number of actinomycete microbes [31, 32]. Jaworska et al. proposed an environmental risk assessment for the use

of EDDS in detergent applications [28]. The projected use volumes in detergent applications was predicted that the steady-state concentration of EDDS in rivers was below 5 µg/l due to rapid biodegradation.

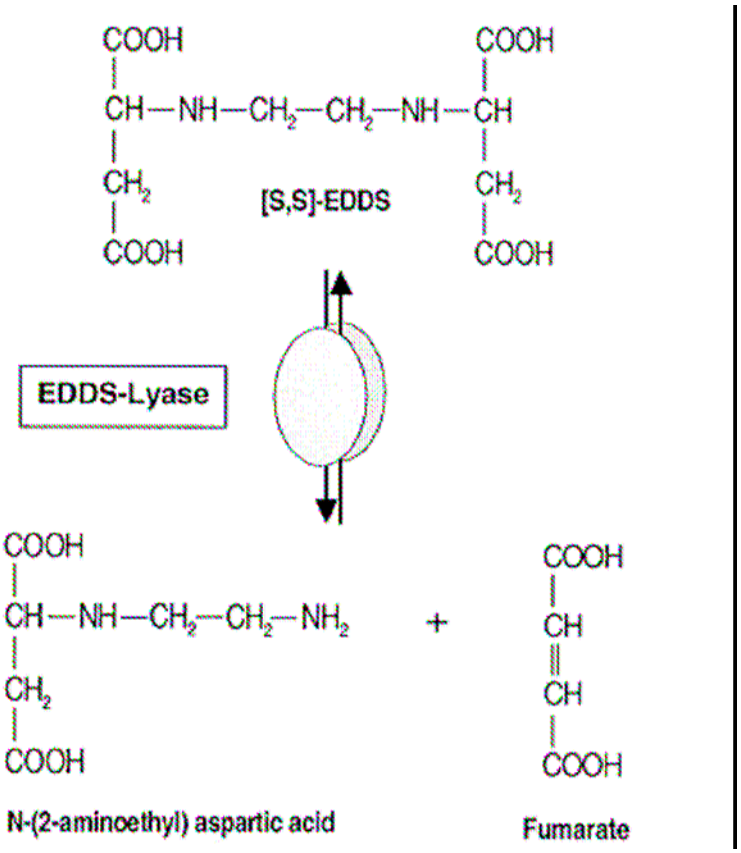

Figure 1.7: Reversible reaction catalyzed by the EDDS-lyase in the EDTA-degrading bacterial strain DSM 9103 [30].

1.2.4 IDS biodegradation

IDS is a medium chelating agent as compared to EDTA, DTPA and EDDS. It can be synthesized from maleic anhydride, ammonia and sodium hydroxide [33]. This synthesis route produces a mixture of 50% [R,S]-, 25% [S,S]- and 25% [R,R]-IDS. The biodegradation tests according to the OECD guidelines for testing of chemicals were done for the three stereoisomers of iminodisuccinate (IDS). The strain referred to as Ralstonia sp. SLRS7 was isolated from activated sludge and used two of the three

isomers, i.e. [R,S]- and [S,S]-IDS as sole source of carbon, nitrogen and energy [34]. An IDS-degrading lyase was isolated from cell-free extract and catalysed IDS. A proposed biodegradation pathway for the isomers of IDS is illustrated in Figure 1.8. The pure enzyme degraded [S,S]-IDS with formation of fumaric acid and L-aspartic acid without requirement of any cofactors. In addition, it catalysed also the degradation of [R,S]-IDS, however only D-aspartic acid was liberated besides fumaric acid. The [R,R]-IDS isomer was not transformed by the enzyme. These results demonstrate that the IDS-degrading enzyme is a carbon-nitrogen lyase that catalyses a cleavage reaction of the C-N bond between the succinic and the aspartic acid residue. Interestingly, this non-hydrolytic cleavage of [R,S]-IDS led only to the formation of D-aspartic acid, indicating that the S-configuration of IDS is mandatory for the cleavage reaction. The S-configuration was also observed for EDDS-degradation by strain DSM 9103 [30].

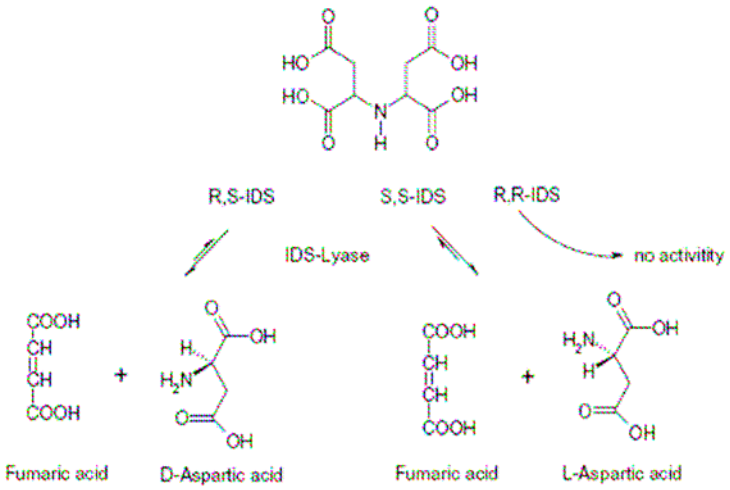

Figure 1.8: Initial transformation of IDS by *Ralstonia sp.SLRS7* [34].

It can be expected that after intended use, IDS occurs most likely as metal-complex in waste water treatment facilities or the environment. The strain SLRS7 degraded well Ca-, Mg-, Mn-, and also Fe-[S,S]-IDS, whereas the degradation of Cu-[S,S]-IDS was poor. The results strongly suggested that the strain biodegrade metal complexes with low $pK_{Me\text{-}IDS}$ values more easily. Such relationship between the complex formation constant and the

biodegradability of the different metal complexes was also observed for EDDS by Witschel and Egli [30].

1.3 Analytical methods for study metal chelate complexes

An overview of some of the available methods for the analytical determination of aminopolycarboxylates is discussed below. The methods include gas and liquid chromatography, capillary electrophoresis, spectrophotometry, electrochemical methods, atomic absorption spectrometry and titrimetric assays. APCAs occur in natural waters predominantly in the form of metal complexes [35]. Adequate analytical assays have to be chosen according to the sample matrix to be analyzed and the respective research problem.

1.3.1 Gas Chromatography

Gas chromatography (GC) has been used for many decades as a separation technique. The technique requires the analytes to be volatile or vaporizable, while APCAs lack this property. Analysis of APCAs by GC is possible when they are converted to another chemical form (derivatization) [36].

The sample preparation of APCAs involves their conversion to readily volatile alkyl ester derivatives, like methyl [37], ethyl [38], n-propyl [39], isopropyl [40] or n-butyl esters [41]. The derivatization step makes sample preparation tedious and time consuming. When APCAs exist as metal complexes, their derivatization is more difficult, therefore metal complexes must be decomposed prior to derivatization by decreasing the pH value causing a conversion of the APCAs into their free acid forms. GC methods are unfortunately not suitable for the determination of individual aminopolycarboxylate-metal species and determine only the integral content of all existing species of specific aminopolycarboxylic acid. In most cases, derivatization is preceded by a concentration step to increase the sensitivity of the overall process.

In principle, two approaches exist: (i) concentration of the APCAs as anions on an anion exchanger (e.g. SAX) at pH 2-3, elution with formic acid and evaporation of the eluate at 100-110°C to dryness [42], and (ii) simple evaporation of the acidified aqueous sample to dryness at 100-115°C [39]. After derivatization followed by water addition, the resulting APCA alkyl esters can be extracted from aqueous phase and purified by liquid-liquid extraction with an organic solvent like toluene [38]. Usually, the final injection in GC is preceded by drying the extract over Na_2SO_4 and reduction of the sample volume by partial evaporation. Earlier studies often involved the use of flame ionization detectors (FID) [43, 44]. They have been almost completely replaced in current studies by mass-selective [37, 39] or nitrogen-sensitive detectors [38, 45] that have become state-of-the-art due to their increased sensitivity. An international standard procedure has been published on the analysis of aqueous samples, it allows the simultaneous determination of EDTA, DTPA, NTA, β-ADA, 1,3-PDTA and MGDA [4].

1.3.2 Electrochemical Methods

The determinations of APCAS using electrochemical methods have been developed in the past, these are potentiometry, voltammetry and polarography [36]. The predominant number of methods refers to the determination of EDTA and NTA, only a small portion takes DTPA into account. Methods for EDTA analysis include polarography [46], differential pulse polarography (DPP) [47], potentiometry [48] and potentiometric stripping analysis (PSA) [49]. A major drawback of the discussed methods is their poor selectivity and robustness. Methods for natural and waste water analysis using voltammetry developed by Voulagoropoulos et al provide the lowest detection limits (0.1 µg/L) ever presented for EDTA determination [50]. In addition, it is reported that PSA methods is affected by the nature of the electrolyte present in solution and its concentration [49]. Generally, these electrochemical methods [49, 50] prove superiority to earlier ones in terms of sensitivity. Selectivity is poor in some electrochemical methods and simultaneous determination of chelating agents complicated. In natural waters, ligands e.g. humic substances or other anthropogenic complexing agents, anions and cations often present during the analysis can interfere. Due to the poor selectivity, more

recent papers propose to use electrochemical methods as a summation parameter in screening tests [51, 52]. On the other hand, most electrochemical methods are simple, inexpensive, rapid and sensitive.

1.3.3 Spectrophotometry

A number of spectrophotometric methods have been published on the determination of APCAs [36, 53]. The spectrophotometric methods measure the amount of metal-chelate complex either directly or indirectly. Most of these procedures do not differentiate between complexing agents, are subject to interferences and are not sensitive enough for trace analysis. Due to their comparably poor selectivity, these methods are mostly suitable for the determination of the general complexing capacity of a sample.

1.3.4 Atomic Absorption Spectrometry

Some procedures for indirect determination of APCA's by atomic absorption spectroscopy (AAS) have been reported [54, 55]. For example in EDTA analysis, EDTA is first converted to its Cu(II)-EDTA complex and then the complexed copper is determined by AAS. Major problems related to this approach are in particular the separation of Cu(II)-EDTA from non-complexed copper ions in the solution, and also interferences by other metal ions having an impact on the generation of the Cu(II)-EDTA complex [54]. These approaches offer detection limits down to the low mg/L range depending on the method. However, although such techniques are comparably fast and simple, they suffer from poor selectivity when the sample also contains other complexing agents. Therefore, the use of AAS methods is limited when it comes to wastewaters and natural water samples, they only allow the determination of a general complexing capacity.

1.3.5 Titrimetry

Some titrimetric methods are available for the determination of APCAs [36, 56]. The procedures have same disadvantages as the spectrophotometric methods. Therefore, considerable concessions are to be made with respect to sensitivity and selectivity. In addition, matrix-containing samples often cause problems in end-point recognition.

1.3.6 Liquid Chromatography

Another method for the determination of APCAs is liquid chromatography (LC). LC offers benefits that no derivatization of the analytes for increased volatility is necessary as compared to GC. The analytes can be directly injected into the separating column. The determination of APCAs by LC has been applied in many different sample matrices [36], including drinking water [14], surface water [57], wastewater [58] etc. The LC separation of APCAs is normally performed on reversed-phase (RP) columns [14] or by ion chromatography (IC) on an anion exchange column [59]. The reversed-phase technique usually involves the addition of the ion-pair reagent to the mobile phase to convert the target compounds into neutral components. Ultraviolet (UV) is the most commonly used detection method. APCAs to be analyzed are converted into a highly stable defined metal complex with favorable UV absorption characteristics and Cu(II) and Fe(III) are usually used as metal ions [60-62]. For this purpose the addition of excess metal ions, prior to analysis [60], during analysis [63] or after [58] the analysis of the samples is important. In addition to UV detection, some studies were performed using electrochemical [64], fluorescence [65] and mass-spectrometric detection [66] and also ICP-MS coupling [67].

1.3.7 Capillary Electrophoresis

The principle of CE is based on the different migration velocities of electrically charged particles in an electric field and its particular benefits are high separation efficiency and short analysis times. CE is a comparably new technique because the equipment was commercially available since around 1988 and its distribution is still limited.

A Swedish chemist Arne Tiselius first developed electrophoresis as a separation technique in the mid-1930's for the study of serum proteins [68]. Electrophoresis (In Greek, *elektron* meaning electron and *phoresis* being carrying) is a separation based on the differential rate of migration of charged species in a buffer solution in the presence of an electric field. This technique has been traditionally performed on glass plates coated with anti-convective media, such as agarose gels. Unfortunately slab gel electrophoresis suffers from long analysis times, low efficiencies and difficulties in detection and automation. This led to the development of electrophoretic separation in narrow-bore capillaries, since these are anti-convective. Hjerten described the initial work in open tube electrophoresis in 1967 [69]. In the early 1980's Jorgenson and Lukacs advanced the technique by using 75 μm fused silica capillaries. The fundamental theories were developed by Jorgensen, where he demonstrated the potential for high performance capillary electrophoresis (HPCE) as an analytical technique [70].

There are different modes of CE, namely capillary zone electrophoresis (CZE), micellar electrokinetic capillary chromatography (MEKC), capillary electrochromatography (CEC), capillary gel electrophoresis (CGE), capillary isoelectric focusing (CIEF) and capillary isotachophoresis (CITP). In CZE, the separation is based on differences in the electrophoretic mobilities of the solutes, resulting in different velocities of migration of ionic species in the electrophoretic buffer filled in the capillary [71]. The separation of neutral species as well as charged ones by MEKC is accomplished by the use of surfactants in the running buffer. Neutral compounds can be trapped in micelles of an ionic surfactant and thus can migrate either with or against the electroosmotic flow (EOF). EOF is caused by the influence of an electric field on a charged double layer formed on the interface between bulk electrolyte solution and a capillary wall (more detailed explanation can be found in chapter 5). Addition of cationic surfactants like CTAB is a very convenient method to reverse the direction of EOF [72]. The CEC mode involves the packing of the capillary with a chromatographic packing which can retain solutes and the separation of neutral compounds is based on the normal distribution equilibria upon which conventional chromatography depends. CGE is based on differences in solute size, as analytes migrate through the pores of the gel filled capillary

and it is useful for the separation of oligomers such as oligonucleotides. CIEF is a high resolution electrophoretic technique to separate peptides and proteins on the basis of their isoelectric point. While CITP is a "moving boundary" electrophoretic technique and the separation is performed in a discontinuous buffer system. Sample components condense between leading and terminating constituents, producing a steady-state migrating configuration composed of consecutive sample zones [73].

CE is often the preferred technique, particularly considering the high selectivity and lower operating costs compared to HPLC. The advantages and limitations of CE are given in Table 1.4.

Table 1.4: Advantages and limitations of capillary electrophoresis [74].

Advantages	**Limitations**
▪ High separation efficiency and precision ▪ Simple and ease of automation ▪ High sample throughput due to short analysis times ▪ Low costs (for labour, solvent volumes, waste disposal, stationary phases e.g. chiral separations) ▪ Nanoliter sample amounts possible ▪ Little or no sample pre-treatment necessary	Reasons to consider alternative separation techniques : ▪ Analytes highly volatile and stable at high temperatures? Consider GC ▪ Concentration of analytes of interest in the range of 1 mg/L? Otherwise: consider other possible detection methods or other techniques such as LC ▪ Analytes soluble in polar solvent (preferably water)? Otherwise: consider LC (there is non-aqueous CE but not much experience) ▪ MS coupling desirable or essentially needed (identification, selectivity enhancement, structure analysis)? Consider LC-MS

The main components of a typical CE instrument consist of a high voltage power supply, two buffer reservoirs, a capillary and a detector. This is depicted schematically below in Figure 1.9. However, the basic instrumentation for CE can be enhanced with the use of autosamplers, multiple injection devices, sample and capillary temperature control, programmable power supply, multiple detectors, fraction collection and computer interfacing [74].

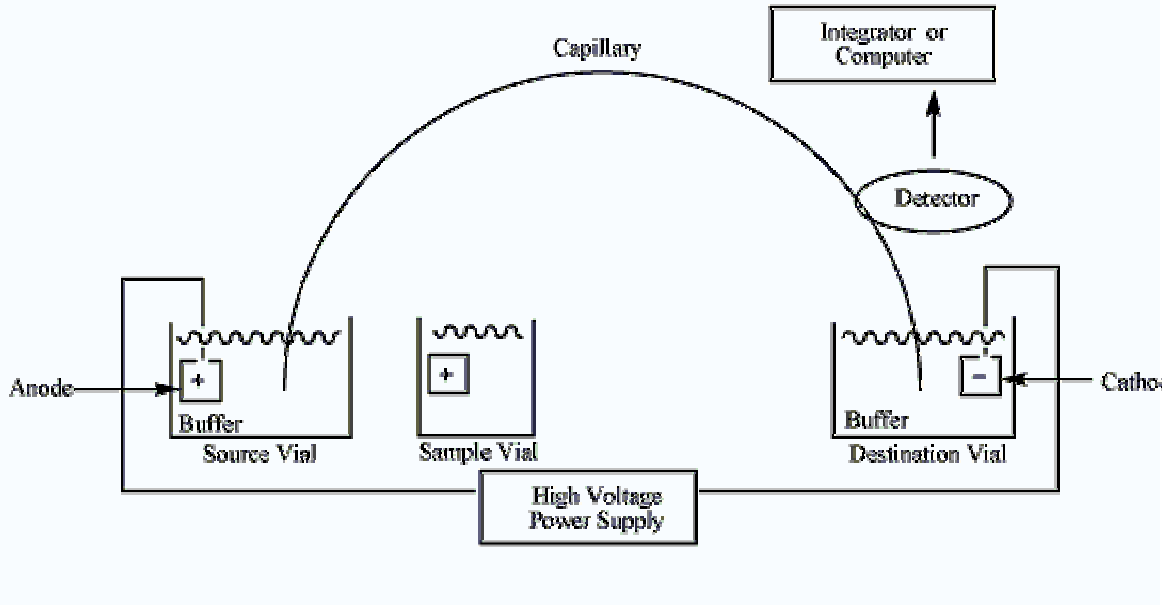

Figure 1.9: Schematic representation of capillary electrophoresis instrumentation

In order to carry out a separation, the capillary is first filled with buffer solution. The capillary consist of fused silica (amorphous SiO_2) coated with polyimide to prevent breaking of the capillary. Capillaries are typically 10 to 100 cm long with the inner diameter ranging from 25 to 100 µm. Narrow-bore capillaries are used so that very high voltages can be applied. One of the buffer vials is replaced by a sample vial and the sample is then injected into the beginning of the capillary either hydrodynamically (by applying a pressure difference) or electrokinetically (by applying high voltages during a short time period). The capillary end dips into the buffer solution again at the beginning of the separation so that the electrophoretic separation can take place out of the injected sample zone.

The majority of commercial systems use UV-Vis absorbance as their primary mode of detection. Typical detection limits for small ions obtained by use of different detection techniques [75] are summarized in Table 1.5. A small section of the capillary itself is used as the detection cell. In order to obtain the identity of sample components, capillary electrophoresis can be directly coupled with mass spectrometers. In most systems, the capillary outlet is introduced into an ion source that utilizes electrospray ionization (ESI). The resulting ions are then analyzed by the mass spectrometer. This set-up requires volatile buffer solutions, which will affect the range of separation modes that can be employed and the degree of resolution that can be achieved.

Table 1.5: Comparison of common detection techniques used for small-ion analysis [75].

Detection method	LOD ($mol\ L^{-1}$)	Main advantages	Main drawbacks
UV–visible absorption			
Indirect	10^{-4}–10^{-5}	Universal	Low sensitivity
Direct	10^{-6}–10^{-7}	Selective	Often requires derivatization
Fluorescence			
Indirect	10^{-5}–10^{-6}	Universal	Limited number of fluorophores
Direct	10^{-6}–10^{-9}	Sensitive, selective	Requires derivatization
Chemiluminescence	10^{-6}–10^{-12}	Ultrasensitive	Limited number of analytes and reagents
Conductivity	10^{-5}–10^{-7}	Universal,	Limited choice of miniaturization buffer
Amperometry	10^{-7}–10^{-9}	Sensitive,	Maintenance of Selective electrodes
Potentiometry	10^{-5}–10^{-7}	Universal	Maintenance of electrodes
ICP–MS	10^{-6}–10^{-9}	Sensitive, selective	Identification
ESI–MS	10^{-5}–10^{-7}	Selective, identification	Limited choice of buffer, sensitivity

During the separation the applied electric power is converted into Joule heating (typical currents: 1-200 µA, converted electric power: up to 7W). Hence the buffer solution and capillary are heated up. The Joule heat has to be led away as efficiently as possible. Thus

capillaries with small inner diameter and therefore high surface-volume ratio are used. These narrow bore capillaries strongly reduce radial diffusion and convection as well.

A high potential is applied across the capillary by means of a pair of electrodes located at either end of the buffer. This potential causes ions of the sample to migrate toward one or the other of the electrodes. The rate of migration of a given species depends upon its charge and also upon its size. Separations are then based upon differences in charge-to-size ratios for the various analytes in a sample. The larger this ratio, the faster an ion migrates in the electrical field [76]. The mobility μ (m^2 V^{-1} s^{-1}) of a species can be calculated by its velocity v (m s^{-1}) in the in the electric field divided by the electric field strength E (V m^{-1}) (equation 1.1).

$$\mu = \frac{v}{E} \qquad [1.1]$$

The velocity results from the migration time t_m and the distance l from capillary inlet to the detector (equation 1.2).

$$v = \frac{l}{t_m} \qquad [1.2]$$

This distance is also called the effective capillary length. The electric field strength is the quotient of the voltage U and the total capillary length L (equation 1.3). The mobility can be calculated using (equation 1.4).

$$E = \frac{U}{L} \qquad [1.3]$$

$$\mu = \frac{l.L}{t_m.U} \qquad [1.4]$$

EOF arises due to the electric double layer that is formed at the surface of the silica capillary wall. The capillary surface has a net negative charge owing to the dissociation of the functional groups on the capillary surface and this change depends on the pH of the solution. Mobile positive ions present at the capillary surface are attracted to the negative electrode and solvent molecules are transported concurrently. For fused silica, the EOF is

strongly controlled by the numerous silanol groups (SiOH) that can exist in anionic form (SiO^-). EOF becomes significant above pH 4. At high pH, where the silanol groups are predominantly deprotonated, the EOF is greater than at low pH where they become protonated. EOF causes movement of nearly all species, regardless of charge, in the same direction. Under normal conditions (i.e. negatively charged surface), the flow is from the anode to the cathode.

Figure 1.10 demonstrates a flat flow profile which is a further key feature of EOF in CE and also the parabolic flow profile generated by an external pump used for HPLC. EOF has a flat profile because of its driving force (i.e. applied electrical field) is uniformly distributed along and across the capillary. This means that no pressure drops are encountered and the flow velocity is uniform across the capillary. This contrasts with the pressure-driven flow in HPLC in which frictional forces at the column walls cause a drop across the column, yielding a parabolic or laminar flow profile. The flat profile of EOF is important because it minimizes zone broadening leading to high separation efficiencies that allow separations on the basis of mobility differences.

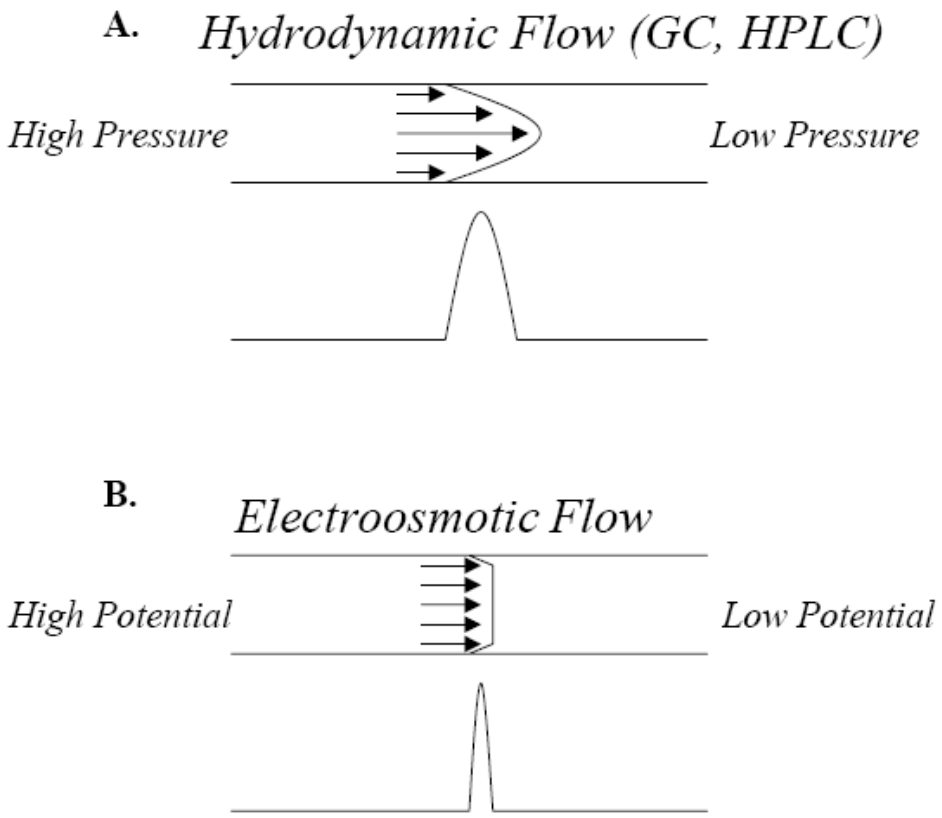

Figure 1.10: Comparison of (A) Hydrodynamic flow profile and (B) Electroosmotic flow profile.

Efficiency in terms of the number of the theoretical plates can be calculated directly from an electropherogram using the following equation:

$$N = 5.54\left(\frac{t_m}{w_{1/2}}\right)^2 \qquad [1.6]$$

The overall performance in CE separations can be described by resolution (R_s), which is a quantitative measure of the degree of separation. This parameter is defined in analogy to chromatography as well. The resolution R_s can be calculated as migration time difference related to the mean peak base width (equation 1.7) for two (consecutive) peaks:

$$R_s = 2\left(\frac{t_2 - t_1}{w_2 + w_1}\right) \qquad [1.7]$$

where t_1 and t_2 are the migration times of two peaks eluting in succession, w_1 and w_2 the corresponding peak widths.

In recent years, capillary electrophoresis (CE) has evolved to an alternative separation technique to HPLC, allowing the determination of the speciation of complexing agents. Complexing agents are used in particular as an electrolyte additive for the modification of the ion mobility of metal cations [77, 78]. Electrophoretic assays for APCAs (i.e. mostly EDTA, NTA, DPTA) include all possible variations like the determination of free acids [79, 80], the determination following conversion of all existing complex species into a single defined metal complex [79, 81] and also the differentiated determination of individual metal complex species [82, 83]. The application of micellar electrokinetic capillary chromatography (MEKC) has also been described [84]. Published application ranges include biological fluids [81], detergent formulations [85], natural [82] and wastewater [86], radioactive waste solutions [87], wood pulp [88] and cosmetics [89].

The detection is predominantly done with UV detectors. Occasionally, laser-induced fluorescence (LIF) detectors [90], electrochemical detectors [4] and mass spectrometers [81, 91] are used. Sensitivity can be considerably increased by mass-spectrometric detection. The detection limits for these techniques are usually low in the mg/L range. Sheppard and Henion reported on a detection limit of 150ng EDTA/L when using CE-ion spray MS/MS coupling [81]. LIF detection after conversion of EDTA or DTPA into ternary complexes with 8-hydroxyquinoline-5-sulfonic acid (HQS) and lutetium or thorium allowed to achieve detection limits in the low µg/L range [90]. Sample preparation procedures described for individual applications often involve only a dilution step or filtration of the sample solution.

Purpose of the study

Governmental and regulatory authorities are generally against chemicals which pose a threat to the environment. Legislation such as Commission for the Protection of the Marine Environment of the North-East Atlantic (OSPAR) recommends that only

environmentally friendly chemical agents be permitted in future. *S*,*S*′-ethylenediaminedisuccinic acid (EDDS) and iminodisuccinic acid (IDS) are readily biodegradable complexing agents that have recently replaced recalcitrant ethylenediaminetetraacetic acid (EDTA) in some commercial products for example in cosmetics and detergents. In some cases a combination of EDTA and EDDS or IDS are used. This is because EDTA and other APCAs are not readily biodegradable in standard tests. The present study attempts to evaluate the potential use of CE as an analytical tool for the speciation analysis as well as the analytical quantification of various APCAs. This will include

- The separation and speciation of iminodisuccinic acid with various metal ions at various pH levels using capillary electrophoresis and also to use speciation modelling to compare and further validate the presence and distribution of metal-ligand species. No CE method has been reported for the separation of IDS and its metal ions and speciation of this newly biodegradable chelating agent. It is important to find a rapid and accurate method for the determination of biodegradable agents.
- The study of changes that might occur at various time intervals for the metal-ligand complexes of chelating agents namely diethylenetriaminepentaacetate (DTPA), ethylenediaminedisuccinate (S,S-EDDS), iminodisuccinate (IDS) and R,S-IDS with various metal ions (Cd^{2+}, Cr^{3+}, Cu^{2+}, Fe^{3+}, Mn^{2+}, Pb^{2+} and Zn^{2+}) at pH 7 and 9. Three readily biodegradable chelating agents will be compared with a recalcitrant DTPA.
- The effect of various cationic electroosmotic flow (EOF) modifiers and counterions on the separation of aminopolycarboxylic acids i.e. EDTA, EDDS and IDS as Cu(II) complexes by capillary electrophoresis (CE) with on-column UV detection. The performance of the modifiers will be evaluated in terms of migration times, resolution and plate numbers. Only limited studies for the separation of APCAs have been reported but none was done for readily biodegradable ligands.
- The investigation of the possible use of CE for the separation of Cu^{2+}, Cr^{3+}, Fe^{3+}, Mn^{2+} and Pb^{2+} metal ions complexed with chelating agents namely IDS, EDDS and EDTA. The effect of background electrolyte parameters such as electrolyte nature, pH and concentration upon the electrophoretic behaviour of metal complexes will be

investigated. A mixture of two of Good's buffers i.e. 2-(N-morpholino)ethanesulfonic acid monohydrate (MES) and 3-morpholino-2-hydroxypropane-sulfonicacid (MOPSO) was selected as the running buffer because of their non-complexing effects as opposed to tetraborate buffer. Based on the results obtained from the above mentioned investigation, a method will be developed for the simultaneous determination of EDTA, EDDS and IDS as their Fe(III) complexes.

- The applications of the established methods for the analysis of the EDTA and IDS complexes in cosmetics like shower cream, foam bath and also in environmental water samples will be studied.

This thesis consists of chapters devoted to the following topics depicted in a chart below:

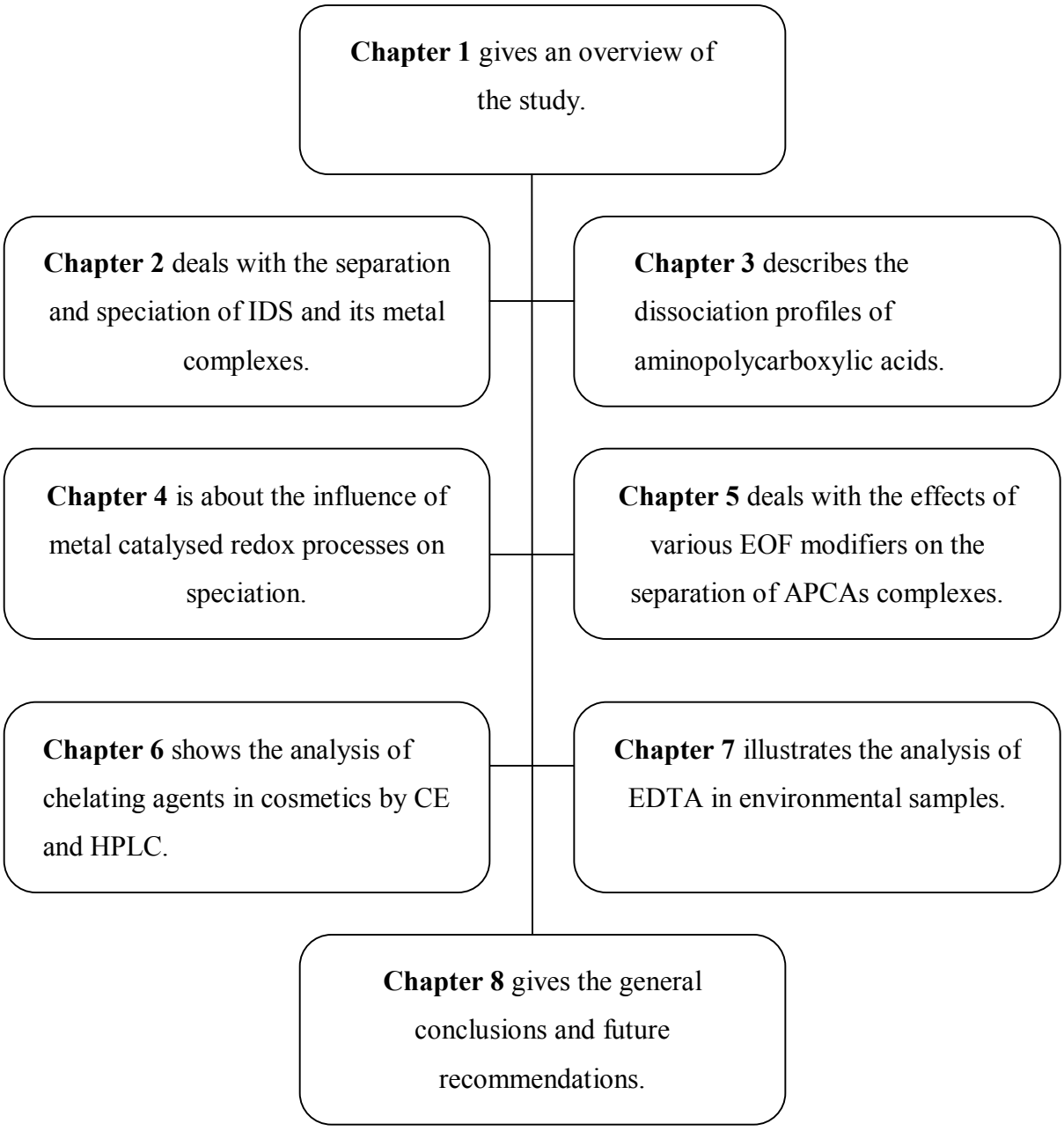
Chapter 1 gives an overview of the study.
Chapter 2 deals with the separation and speciation of IDS and its metal complexes.
Chapter 3 describes the dissociation profiles of aminopolycarboxylic acids.
Chapter 4 is about the influence of metal catalysed redox processes on speciation.
Chapter 5 deals with the effects of various EOF modifiers on the separation of APCAs complexes.
Chapter 6 shows the analysis of chelating agents in cosmetics by CE and HPLC.
Chapter 7 illustrates the analysis of EDTA in environmental samples.
Chapter 8 gives the general conclusions and future recommendations.

Bibliography

[1] Morgan G. T, Drew H. D. K, ***J Chem Soc***, 1920, 117, 1456-1465.

[2] Ebbing, ***General Chemistry***, 4th edition, Houghton Mifflin Company, 1993, 981-983.

[3] Basset J, Denney R. C, ***Vogel's textbook of quantitative inorganic analysis***, 4th Edition, Inc, New York, London, 1978.

[4] Nowack B, VanBriesen J, ***Biogeochemistry of Chelating Agents***, ACS Symposium Series, 2005, Vol. 910.

[5] Yaeger L. L, ***Rejuvenation***, 1983, 11, 76-80.

[6] Whittaker P, Vanderveen J. E, Dinovi M. J, Kuznesof P. M, Dunkel V. C, ***Regulatory Toxicol. Pharmacol***, 1993, 18, 419-427.

[7] Mayfiled L, Soderholm G, Norderyd O, Attstrom R. J, ***J Clinical Periodontology***, 1998, 25, 707-714.

[8] Oviedo C, Rodríguez J, ***Quim. Nova,*** 2003, 26 (6), 901-905.

[9] Schmidt C. K, Fleig M, Sacher F, Brauch H, ***J Environ.Pollut***, 2004, 131, 107-124.

[10] Nörtemann B, ***Appl. Microbiol. Biotechnol***, 1999, 51, 751-759.

[11] Li Z, Shuman L. M, ***Sci. Total Environ***, 1996, 191, 95-107.

[12] Means J. L, Alexander C. A, ***Nucl. Chem. Waste Management***, 1981, 2, 183-196.

[13] Williams D. R, ***Chem. Br***, 1998**,** *1,* 48-50.

[14] Loyaux-Lawniczak S, Douch J, Behra P, ***Fresenius J. Anal. Chem***, 1999, 364, 727-731.

[15] Sillanpää M, ***Rev. Environ. Contam. Toxicol***, 1997, 132, 85.

[16] Loonen H, Lindgren F, Hansen B, Karcher W, Niemelä J, Hiromatsu K, Takatsuki M, Peijnenburg W, Rorije E, Struij J, ***Environ. Toxic. Chem***, 1999, 18(8), 1763-1768.

[17] http://www.scienceinthebox.com.

[18] Satoshi O, Kenji I, Satoru K, ***Konica Technical report***, 2003, 16, 13-18.

[19] Hiromatsu K, Yakabe Y, Katagiri K, Nishihara T, ***Chemosphere***, 2000, 41,

1749-1754.

[20] OECD Guidelines for Testing of Chemicals, 1996, Section 3: Degradation and Accumulation, OECD, Paris.

[21] Kari F, Giger W, ***Environ. Sci. Technol*, 1995**, *29*, 2814-2827.

[22] Witschel M, Egli T, Zehnder A, Wehrli E, Spycher M, ***Microbiology***,1999, *145*, 973.

[23] Klüner T, Hempel D. C, Nörtemann B; ***Appl. Microbiol. Biotechnol***, 1998, *49*, 194-201.

[24] Thomas R. A. P, Lawlor M, Bailey M, Macaskie L. E, ***App.Environ.Microb***, 1998, 64(4), 1319-1322.

[25] Kezerian C, Ramsey W M, 1964, US Patent 3158635.

[26] Schowanek D, Feijtel T. C. J, Perkins C. M, Hartman F. A, Federle T. W, Larson R. J, ***Chemosphere***, 1997, 34, 2375-2391.

[27] Takashi R, Fujimoto N, Suzuki M, Endo T, ***Biosci.Biotech.Biochem***, 1997, 61, 1957-1959.

[28] Jaworska J. S, Schowanek D, Feijtel, T. C J, ***Chemosphere,*** 1999, 38, 3597-3625.

[29] Knepper T. P, ***Trends Anal. Chem,*** 2003, *22*, 708-724.

[30] Witschel M, Egli T, ***Biodegradation*,** 1998, 8, 419–428.

[31] Kovalyova I. B, Mitrofanova N. D, Martynenko L. I, Samohina M. V, Felin M. G, ***J. Inorg.Chem***, 1991, 36, 3.

[32] Stegmann E, Pelzer S, Wilken K, Wohlleben W J, ***Biotechnol***, 2001, 92, 195-204.

[33] Bayer: Imminodisuccinate, Iminodisuccic acid sodium salt, Product literature from www.bayer.com, 2001.

[34] Cokesa Ž, Lakner S, Knackmuss H-J, Rieger P-G, ***Biodegradation***, 2004, 15, 229-239.

[35] Nowack B, ***Environ.Sci.Technol***, 2002, 36, 4009-4016.

[36] Sillanpää M, Sihvonen M.-L, ***Talanta***, 1997, 44, 1487-1497.

[37] Nishikawa Y, Okumura T, ***J Chromatogr A***, 1995, 690(1), 109-118.

[38] Tuulos-Tikka S, Sillanpää M, Rämo J, ***Intern J Environ.Anal.Chem***, 2000, 77(3), 221-232.

[39] Raksit A, ***J.AOAC.Int***, 2002, 85(1), 50-55.

[40] Randt C, Wittlinger R, Merz W, ***Fresenius J.Anal.Chem***, 1993, 346(6-9), 728-731.

[41] Nguyen D.L, Bruchet A, Aprino P.J, ***J.High.Res.Chromatogr***, 1994, 17(3), 153-159.

[42] Lee H.-B, Peart T. E, Kaise K. L. E, ***J Chromatogr A***, 1996, 738, 91-99.

[43] Rudling L, ***Water. Res***, 1972, 6(7), 871-876.

[44] Gardiner J, ***Analyst***, 1977, 102(1211), 120-123.

[45] Sillanpää M, Vickackaite V, Rämö J, Niinisto L, ***Analyst***, 1998, 123, 2161-2165.

[46] Nomura T, Nakagawa G, ***J. Electroanal. Chem***, 1980, 111, 319.

[47] Stolzberg R. J, ***Anal. Chim. Acta***, 1977, 92, 139-148.

[48] Hadjiioannou T. P, Koupparis M. A, Efstathiou G. E, ***Anal. Chim. Acta***, 1977, 88, 281-287.

[49] Fayyad M, Tutunji M, Taha Z, ***Analyt. Lett***, 1988, 21, 1425.

[50] Voulgaropoulos A,Tzivanakis N, ***Electroanalysis***, 1992, 4, 647.

[51] Schön P, Bauer K.-H, Wiskamp V, ***Fresenuis J. Anal. Chem***, 1997, 358, 699-702.

[52] Esser S, Wenclawiak B. W, Gabelmann H, ***Fresenius J. Anal. Chem***, 2000, 368, 250-255.

[53] Fujita Y, Mori I, Matsuo T, ***Anal. Sci***, 1998, 14(6), 1157-1159.

[54] Kunkel R, Manahan S. E, ***Anal. Chem***, 1973, 45(8), 1465-1468.

[55] Güclü K, Hugül M, Dermirci-Cekic S, Apak R, ***Talanta***, 2000, 53, 213-222.

[56] Clinckemaile G. G, ***Anal. Chim. Acta***, 1968, 43, 520-522.

[57] Ye L, Lucy C. A, ***J Chromatogr A***, 1996, 739, 307-315.

[58] Bedsworth W. W, Sedlak D. L, ***J Chromatogr A***, 2001, 905, 157-162.

[59] Miller M. L, McCord B. R, Martz R, Budowle B, ***J.Anal.Toxicol***, 1997, 21, 521-528.

[60] Bergers P. J. M, DeGroot A. C, ***Water. Res***, 1994, 28, 639-642.

[61] Tandy S, Schulin R, Nowack B, ***J.Chromat Science***, 2006, 44(2), 82-85.

[62] Kord A. S,Tumanova I, Matier W. L, ***J Pharmaceut.Biomed.Anal***, 1995, 13, 575.

[63] Chinnik C. C. T, ***Analyst***, 1981, 106, 1203-1207.

[64] Taylor D. L, Jardine P. M, ***J Environ.Qual***, 1995, 24(4), 789-792.

[65] Ye L, Lucy C. A, ***Anal Chem***, 1995, 67, 2534-2538.

[66] Baron D, Hering J. G, ***J Environ.Qual***, 1998, 27, 844-850.

[67] Ammann A. A, ***J Chromatogr A***, 2002, 947, 205-216.

[68] Tiselius. A, ***Trans.Faraday Soc.***, 1937, 33, 524.

[69] Hjerten. S, ***Chromatogr.Rev***, 1967, 9, 122.

[70] Jorgenson. J.W, Lucacz. K.D, ***Anal Chem***, 1981, 53, 1298-1302.

[71] Goodall. D et al***, LC-GC***, 8 (8), 788-799.

[72] Heiger. D. N, ***High performance Capillary Electrophoresis***, Hewlett Packard Company, 1992, 3rd edition, Printed in France.

[73] Li S. F. Y., ***Capillary Electrophoresis: Principles, Practice and Applications***, Amsterdam: Elseiver, 1992, 4-12.

[74] Wätzig H, Günter S, ***Clin Chem Lab Med,*** 2003; 41(6), 724–738.

[75] Szpunar-Lobinska, et al, ***Fresenius J Anal Chem***, 1995, 351, 351-377.

[76] Padarauskas. A, ***Anal Bioanal Chem***, 2006, 384, 132–144.

[77] Baraj B, Martinez M, Satre A, Aguilar M, ***J Chromatogr A***, 1995, 695(1), 103-112.

[78] Timerbaev A. R, Semenova O. P, Petrukhin O. M, ***J Chromatogr A***, 2002, 943, 263-274.

[79] O'Keeffe M, Dunemann L, Theobald A, Svehla G, ***Anal.Chim.Acta***, 1995, 306, 91-97.

[80] Owens G, Ferguson V. K, McLaughlin J, Singleton I, Reid R. J, Smith F. A, ***Environ. Sci. Technol***, 2000, 34, 885-891.

[81] Sheppard R. L, Henion J, ***Electrophoresis,*** 1997, 18, 287-291.

[82] Laamanen P-L, Busi S, Lahtinen M, Matilainen R, ***J Chromatogr A***, 2005, 1095, 164-171.

[83] Carbonaro R. F, Stone A. T, ***Anal. Chem***, 2005, 77(1), 155-164.

[84] Harvey S. D, ***J Chromatogr***, 1996, 736, 333-340.

[85] Wiley J. P, ***J Chromatogr A***, 1995, 692, 267-274.

[86] Buchberger W, Mülleder S, ***Mikrochim Acta***, 1995, 119, 103-111.

[87] Okemgbo A. A, Hill H. H, Metcalf S. G, Bachelor M, ***Anal. Chim. Acta***, 1999, 396, 105-116.

[88] Nagaraju V, Goje T, Crouch A. M, ***Anal. Sci***, 2007, 23, 493- 496.

[89] Katata L, Nagaraju V, Crouch A. M, ***Anal. Chim. Acta,*** 2006, 579, 177-184.

[90] Ye L, Wong J. E, Lucy C. A, ***Anal Chem***, 1997, 69, 1837-1843.

[91] Sheppard R. L, Henion J, ***Anal Chem***, 1997, 69, 2901-2907.

[1]Chapter 2

Speciation and separation of Iminodisuccinate complexes by CE

2.1 Introduction

Capillary Electrophoresis has attained large attention in the recent years and is particularly effective in separating ionic species [1]. Short analysis times, high resolution and low electrolyte and sample consumption are the main advantages of CE compared to other separation methods like ion chromatography [2]. The separations of transition metal ions with chelating agents like EDTA [3, 4], DTPA [5, 6] by CE have been reported. According to the International Union of Pure and Applied Chemistry (IUPAC) speciation of an individual element refers to its occurrence in or distribution among different species [7]. Chemical speciation defines the isotopic composition, concentration, electronic or oxidation state of each of the species actually present in a chemical sample. A recent report indicates that the speciation of metal complexes of the polyaminocarboxylate type is viable [8].

IDS is a readily biodegradable ligand produced by Bayer [9] and classified as a medium strength chelating agent. It can be used in various industrial applications for complexing different metal ions. In this work, the speciation and separation behaviour of selected transition metal ions with IDS at various pH levels and IDS concentration values is reported. The CE results were used to validate the speciation modeling results obtained using Joint Expert Speciation System (JESS).

[1] a. Part of the work described in this chapter has been presented as a poster at the 36th Convention of the South African Chemical Institute, Port Elizabeth, South Africa, 1-5 July 2002, L M Katata and A. M Crouch.
b. Part of the work described in this chapter has been presented as a poster at the International Symposium on Analytical Science, University of Stellenbosch, South Africa (Analytika), 4-10 December 2002, A. M Crouch, L. E Khotseng, L M Katata and P Sandra.
c. Part of the work described in this chapter has been published in Chemical Speciation and Bioavailability, 2006, 18(3), 85-93, M Polhuis, L. M. Katata and A. M. Crouch.

2.2 Experimental Details

2.2.1 Instrumentation

All separations were performed on a Hewlett-Packard^{3D} CE instrument (Agilent Technologies, Waldbronn, Germany) equipped with a diode array UV-visible detector. A bare fused silica capillary (Composite Metal Services Ltd., Worcester, UK) of 50μm i.d. with the total length of 50 cm and the detection window burned 8.5 cm from the capillary end. Absorbances were monitored at 200 and 214 nm for the detection of analytes. The pH of solutions was measured with a Jenway 4330 pH meter. All experiments were conducted at 25 °C.

2.2.2 Reagents and solutions

All chemicals were of analytical grade. Deionised water with a resistivity of 18 MΩ.cm (Millipore) was used throughout. Stock solutions of 1000 ppm Cd^{2+}, Cr^{3+}, Cu^{2+}, Fe^{3+}, Pb^{2+}, Zn^{2+} and IDS ligand were used to prepare dilute metal-chelate solutions. The working electrolyte was prepared daily from stock solutions containing 10 mM tetraborate buffer for IDS analysis and 30 mM tetraborate for MIDS complexes. 0.3 mM CTAB was used as a surfactant. The electrolyte was filtered through a 0.45-μm membrane filter prior to use.

2.2.3 Procedure for Electrophoresis

The fused silica capillary was rinsed with 0.1 M NaOH for 10 minutes, then with deionized water for another 10 minutes and equilibrated with the borate buffer solution for a further 10 minutes. Between each injection the entire capillary was filled with the buffer solution and flushed for 5 minutes. The flush cycle is used to wash the capillary in order to remove the traces of old sample and buffer. Both ends of the capillary were dipped in two separate vials filled with the same buffer solution. The sample solution was introduced into the anodic end of the capillary by applying a 50 mbar pressure for 2

seconds (hydrodynamic injection). A potential of –20kV was then applied for separation. All CE analysis were done four times.

2.2.4 Modelling

Speciation model diagrams for IDS and metal-IDS complexes were produced using the Joint Expert Speciation System (JESS) [10-12] in the laboratory under the supervision of Professor D.R. Williams (University of Wales, Cardiff). Chemical speciation modeling is based upon the principles of chemical equilibria as governed by thermodynamics and coordination chemistry. It represents the chemical reactions occurring between fundamental components present within a system. It is a non-invasive technique that is ideally suited to study extremely complex reactions at sub-parts per billion levels.

JESS is a computer package written in Fortran 77, used for modelling chemical systems in solution and performing numerical analyses on the corresponding experimental data, for example input stability constants determined using potentiometric titration. The package has been designed to solve problems requiring specialist knowledge of chemical speciation and overcomes many existing problems with solution chemistry databases. The system is fully interactive. The reactions can be expressed in almost any form and can be associated with any number of equilibrium constants, enthalpy, entropy and Gibbs-free energy values. The supplementary data such as background electrolyte, ionic strength, temperature, method determination and original literature reference are also stored. Thermodynamic database being distributed with JESS contains over 1200 reactions and over 20 000 equilibrium constants, with these data spanning interactions in aqueous solution of some 100 metal ions with more than 650 ligands [10].

This program calculates the speciation of a ligand from a database containing the relevant thermodynamic parameters for that ligand, and offers significant insight into the expected distribution behaviour of the ligand in different pH environments. The user can interactively select the desired ligand and metal(s), which must be speciated, given by a series of commands. The user can also specify the conditions under which the data is to

be modelled, e.g. ionic strength of the medium, temperature, concentration of reactants and desired pH range over which the speciation is to be calculated. The final output data correspond to pH and the respective species that have been modelled over the pH range of interest. The output can then be readily manipulated and graphed in most spreadsheets and graphics programs for facile visual representation of the speciation curves.

2.3 Results and Discussion

2.3.1 Separation of metal-IDS complexes at various pH levels

The metal-ligand complexes can be classified as substitution-labile or substitution-inert based upon time scales of complex association and dissociation relative to time scales required for CE analysis (usually 5-20 min) [3]. Substitution-labile complexes associate and dissociate faster than the time scale for a typical CE separation ($t_{rxn} << t_{CE}$). This means the speciation of metal ions and ligand present in the original sample is lost during the analysis. In the case of substitution-inert complexes, they associate and dissociate slower than the time scale for CE ($t_{rxn} >> t_{CE}$). The M-IDS complexes can be categorised under the substitution-labile complexes according to Carbonaro and Stone [3].

M-IDS complexes are normally formed by dissolving equimolar amounts of metal and ligand. At a 1:1 ratio most metal-ligand complexes could not be detected due to their lability. In this study some metal-IDS complexes were prepared by mixing the cation stock solution with an excess of IDS in a 1:4 ratio metal to ligand. IDS is a medium complexing agent compared to EDDS and EDTA. Therefore it forms weaker complexes with transition metals than EDDS, EDTA or DTPA. The chelates absorb less at wavelengths higher than 230 nm and are stable over a broad range of pH. When IDS complexes with bivalent and trivalent cations, metal-IDS chelates possess a net negative charge. Fast analysis times were observed for ML complexes used in this study when a surfactant and a negative voltage was used during analysis.This property of net negative charge can be used to separate the complexes by CE. The CE results for the speciation of IDS, CdIDS, CrIDS, CuIDS, FeIDS, PbIDS and ZnIDS is outlined below.

IDS

A separation of 2 mM H_4IDS illustrated in Figure 2.1A was determined at pH 10. Figure 2.1B gives the electropherograms of the selected pH levels at 10, 9 and 7 (a-c). Possible species present over the entire pH ranges are H_4IDS, H_5IDS^+, H_3IDS^-, H_2IDS^{2-}, $HIDS^{3-}$ and IDS^{4-}. Their reaction equations are given in Table 2.1.

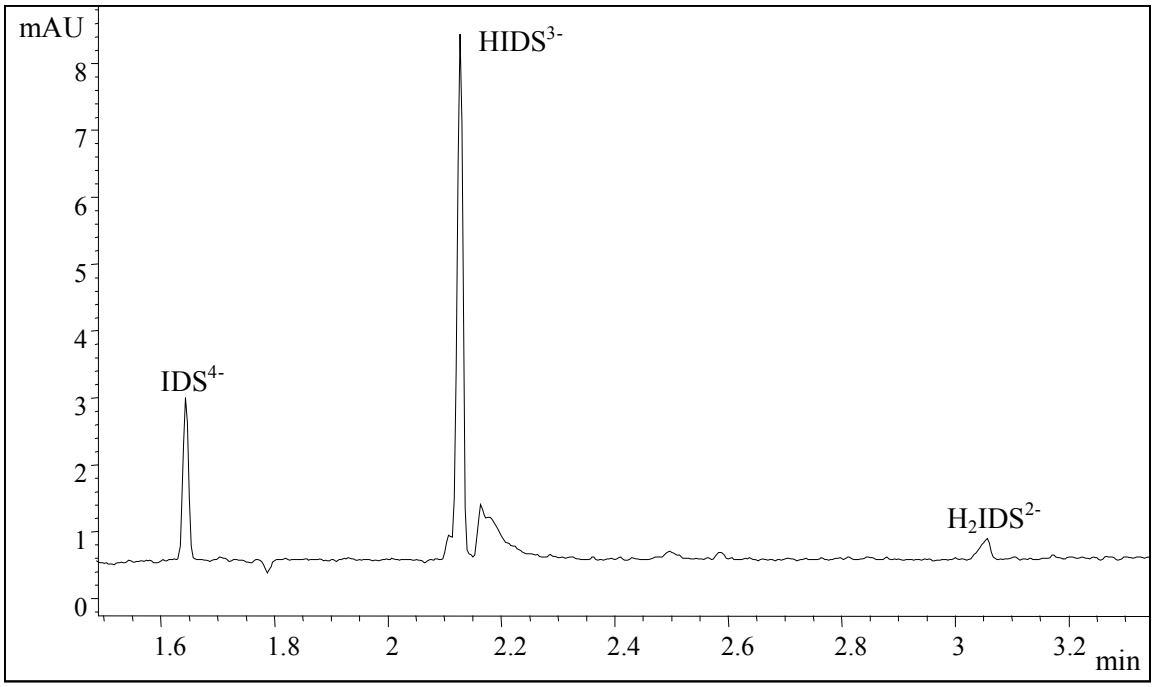

Figure 2.2A: Electropherogram of 2mM H_4IDS monitored at 200 nm. Conditions: 10 mM tetraborate buffer and 0.3 mM CTAB as a modifier at pH 10, applied voltage -20 kV, temperature 25 ºC, hydrodynamic injection 50 mbar for 2 s.

Table 2.1: The protonation constants and stability constants of IDS [9] compared to EDDS [10], EDTA [14] and DTPA [14] and their metal complexes.

Reaction	IDS	EDDS	EDTA	DTPA
	H_4L	H_4L	H_4L	H_5L
H^+				
$L^{x-} + H^+ \leftrightarrow HL^{1-x}$	10.52	10.00	10.37	10.79
$HL^{1-x} + H^+ \leftrightarrow H_2L^{2-x}$	4.55	6.84	6.13	8.60
$H_2L^{2-x} + H^+ \leftrightarrow H_3L^{3-x}$	3.53	3.86	2.69	4.28
$H_3L^{3-x} + H^+ \leftrightarrow H_4L^{4-x}$	2.43	2.95	2.00	2.70
$H_4L^{4-x} + H^+ \leftrightarrow H_5L^{5-x}$	1.52	1.40	1.50	2.00
Cu^{2+}				
$Cu^{2+} + L^{x-} \leftrightarrow CuL^{2-x}$	14.30	18.40	18.78	21.20
$CuL^{2-x} + H^+ \leftrightarrow CuHL^{3-x}$	4.39	3.60	3.10	4.80
$CuHL^{3-x} + H^+ \leftrightarrow CuH_2L^{4-x}$	3.13	3.60	2.00	2.96
$CuOHL^{1-x} + H^+ \leftrightarrow CuL^{2-x}$	10.40	11.00	11.40	
Fe^{3+}				
$Fe^{3+} + L^{x-} \leftrightarrow FeL^{3-x}$	16.10	22.0	25.10	28.0
$Fe^{3-x} + H^+ \leftrightarrow FeHL^{4-x}$	3.89		1.30	3.56
$FeOHL^{2-x} + H^+ \leftrightarrow FeL^{3-x}$	5.30		7.37	9.66
Zn^{2+}				
$Zn^{2+} + L^{x-} \leftrightarrow ZnL^{2-x}$	13.00	13.58	16.60	18.60
$ZnL^{2-x} + H^+ \leftrightarrow ZnHL^{3-x}$	4.41	3.67	3.00	5.60
$ZnOHL^{1-x} + H^+ \leftrightarrow ZnL^{2-x}$	11.26	11.30	11.60	
Mn^{2+}				
$Mn^{2+} + L^{x-} \leftrightarrow MnL^{2-x}$	7.30	8.95	13.89	15.20
$MnOHL^{1-x} + H^+ \leftrightarrow MnL^{2-x}$	11.26			
Cr^{3+}				
$Cr^{3+} + L^{x-} \leftrightarrow CrL^{2-x}$	9.30			28.30
Pb^{2+}				
$Pb^{2+} + L^{x-} \leftrightarrow PbL^{2-x}$	12.40	12.70		18.60
Cd^{2+}				
$Cd^{2+} + L^{x-} \leftrightarrow CdL^{2-x}$	13.50	10.90		19.00

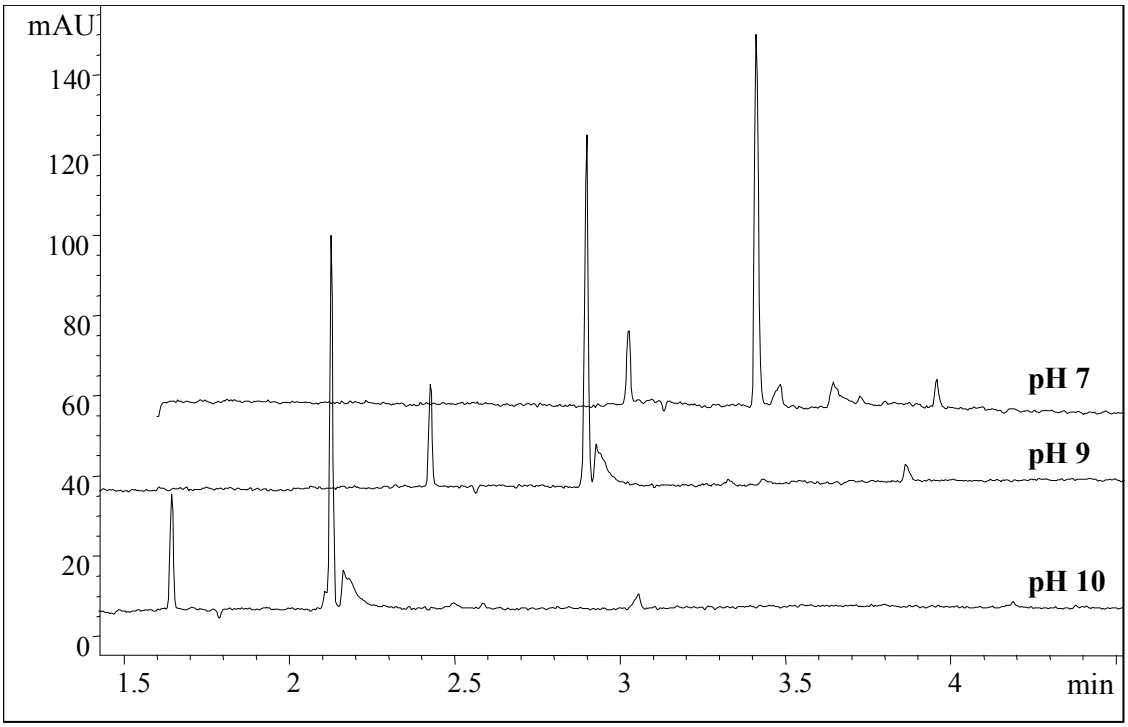

Figure 2.1B: Electropherograms (stacked) of 2mM H_4IDS monitored at various pH levels. For peak identification and conditions please refer to Fig. 2.1A. Please note that the all electropherograms have the same scale of 1.5 min.

In alkaline medium, at pH 10, four peaks were evident. The first and second peaks are due to high concentrations of IDS^{4-} and $HIDS^{3-}$ species, respectively, while the third is an un-assigned artefact and fourth peak is to due to low concentration of H_2IDS^{2-} present in the aqueous solution according to the speciation plot shown in Fig. 2.2. It is expected that H_2IDS^{2-} dominates speciation below pH 5, while H_3IDS^{-} is the dominant species at pH above 2.

A plot of corrected peak areas vs pH of IDS is shown in Figure 2.2A. Quantification of the obtained CE results was accomplished by using peak areas divided by migration times (i.e. corrected peak area) rather than peak area alone. This allowed for any variation of run times and gave better reproducibility than peak area alone. The same quantification was used for all CE results in all the chapters in the thesis. A reasonable agreement between experimental CE (Fig. 2.2A) and modeled speciation results (shown in Fig. 2.2B) was observed. Speciation distribution diagram is a powerful tool for the assessment of the concentrations of the species present as a function of pH as the ligand strongly depends on the pH of the solution. The obtained CE results showed that not all species in Table 2.1 can be analysed using the current methods, as some are positively charged.

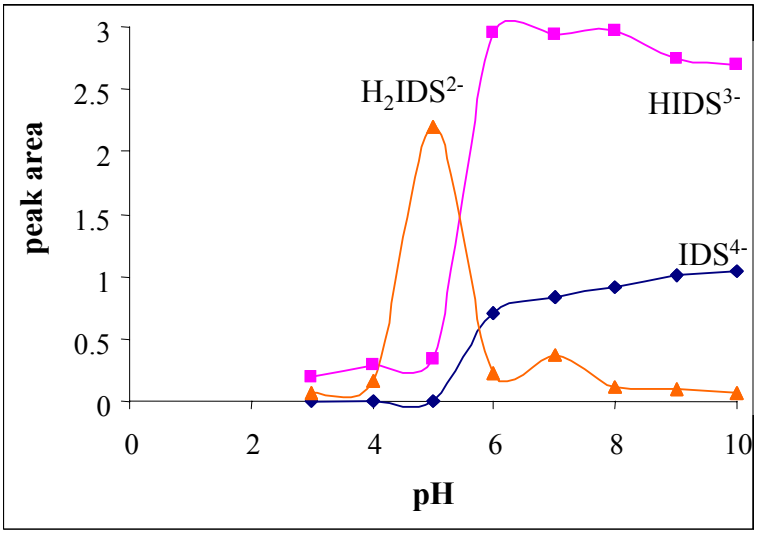

Figure 2.2A: 2 mM H_4IDS peak area as a function of pH. Conditions same as in Fig. 2.1A.

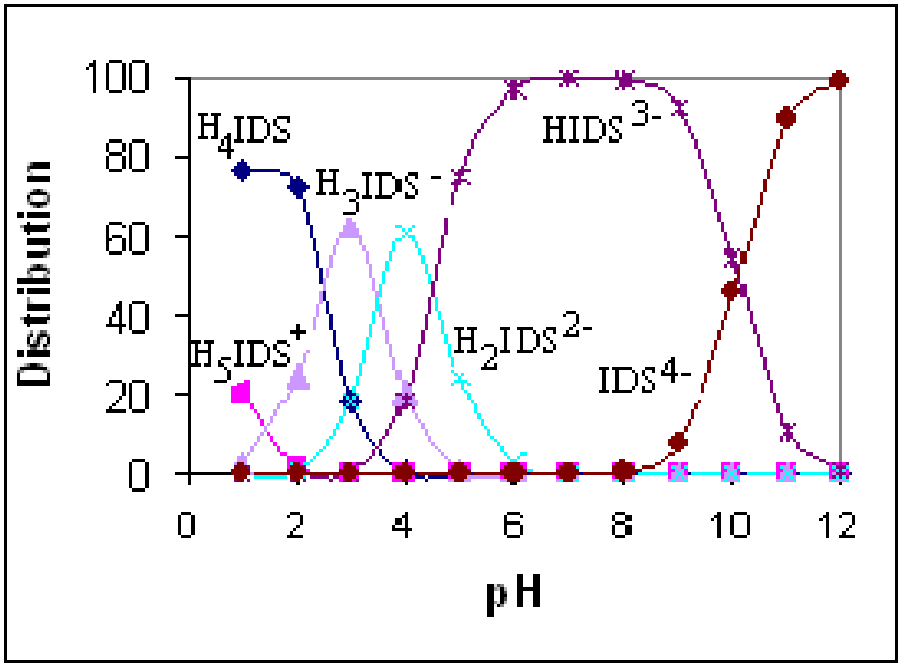

Figure 2.2B: Speciation profile of H_4IDS as function of pH; T = 25 ºC, I = 0.1 M.

CdIDS

The CE results for CdIDS complex in a 1:2 metal to ligand (M:L) ratio is given in Figure 2.3A at pH 10. Protonated species are formed under acidic conditions whereas an increase in pH enhances the tendency of hydroxyl species. The first and second peaks are due to IDS^{4-} and $CdIDS^{2-}$, respectively. The peaks were identified injecting ligand, Cd^{2+},$CdIDS^{2-}$ and analyzing them individually. Each species was also identified by spiking them in the sample. A small sharp peak for the CdIDS complex could not be detected at pH levels 3 and 4 (shown in Fig. 2.3B). The equilibrium between free metal ion and M-IDS depends on factors such as stability constants of the complexes, pH and IDS concentration. The more complete the complexation of metal ion, the sharper will be the peak of the complex formed [6]. IDS and nitrate peaks were observed over all pH ranges because of the high concentration of IDS in the sample mixture.

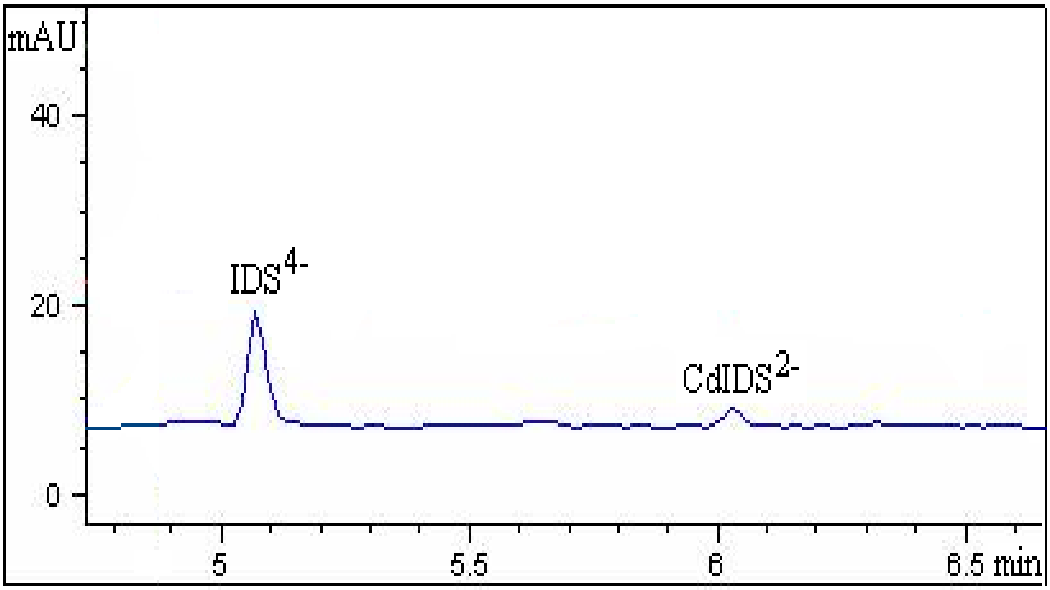

Figure 2.3A: Electropherogram of CdIDS monitored at 200 nm. Conditions: 30 mM tetraborate buffer and 0.3 mM CTAB as a modifier at pH 10, applied voltage -20 kV, temperature 25 ºC, hydrodynamic injection 50 mbar for 2 s.

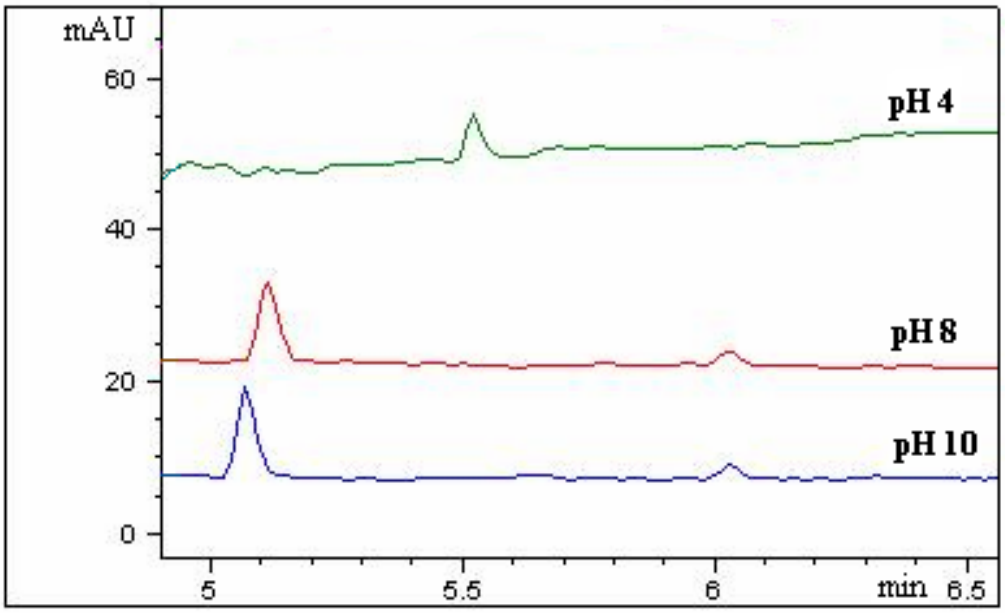

Figure 2.3B: Electropherograms of CdIDS at various pH levels monitored at 200 nm. For peak identification and conditions please refer to Fig. 2.3A

The peak areas of CdIDS seem to increase at high pH as depicted in the Fig. 2.4A. This is attributed to the strong complexation of CdIDS at high pH. CE results showed a moderate comparison with speciation results. The discrepancy between the JESS and experimental plot may be that the complex is more unstable at pH 8-10 than at pH 7. The probable CdIDS species that can form according to theoretical speciation data illustrated in Figure 2.4B are CdH_2IDS, $CdHIDS^-$ and $CdIDS^{2-}$, depending on the pH.

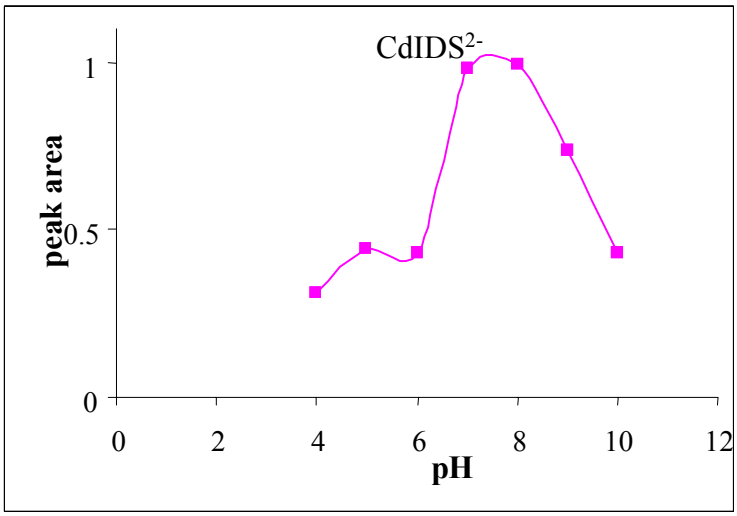

Figure 2.4A: CdIDS peak area as a function of pH. Conditions same as in Fig. 2.3A.

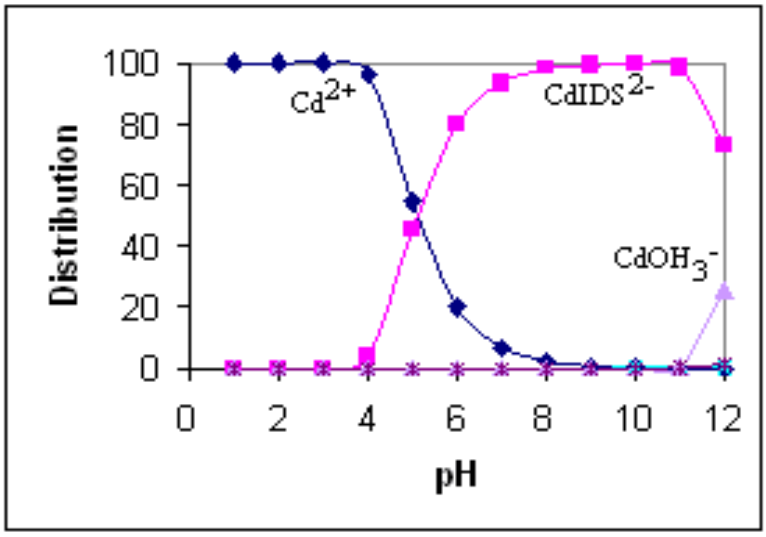

Figure 2.4B: Speciation profile of CdIDS as function of pH; T = 25 ºC, I = 0.1 M.

CrIDS

Figure 2.5A shows the separation of CrIDS in the electropherogram. The influence of pH vs the peak area is also seen in Figure 2.6. The peak was small and broad because of its low log K value of 9.3. Complexes with low equilibrium constants are labile and its difficult to analyse using CE. The IDS peak showed an increase at high pH levels, while CrIDS decreased. The CE results could not be compared with the speciation data because there is no JESS speciation data available for CrIDS.

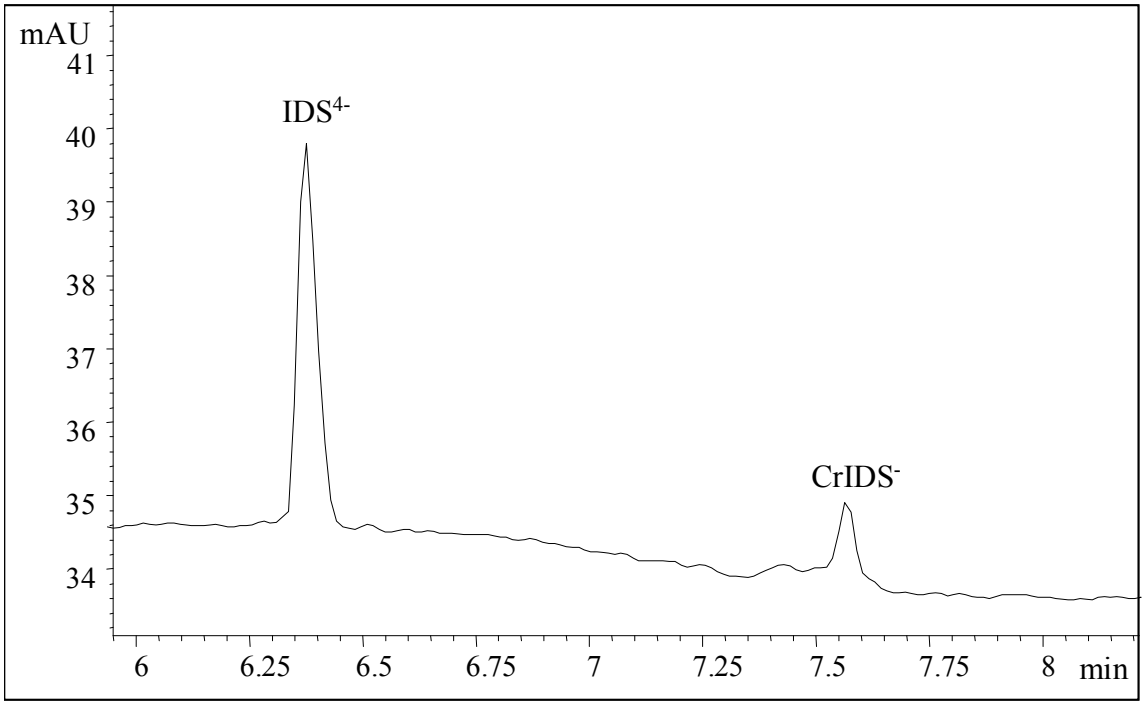

Figure 2.5A: Electropherogram of CrIDS monitored at 200 nm. Conditions same as in Fig. 2.3A.

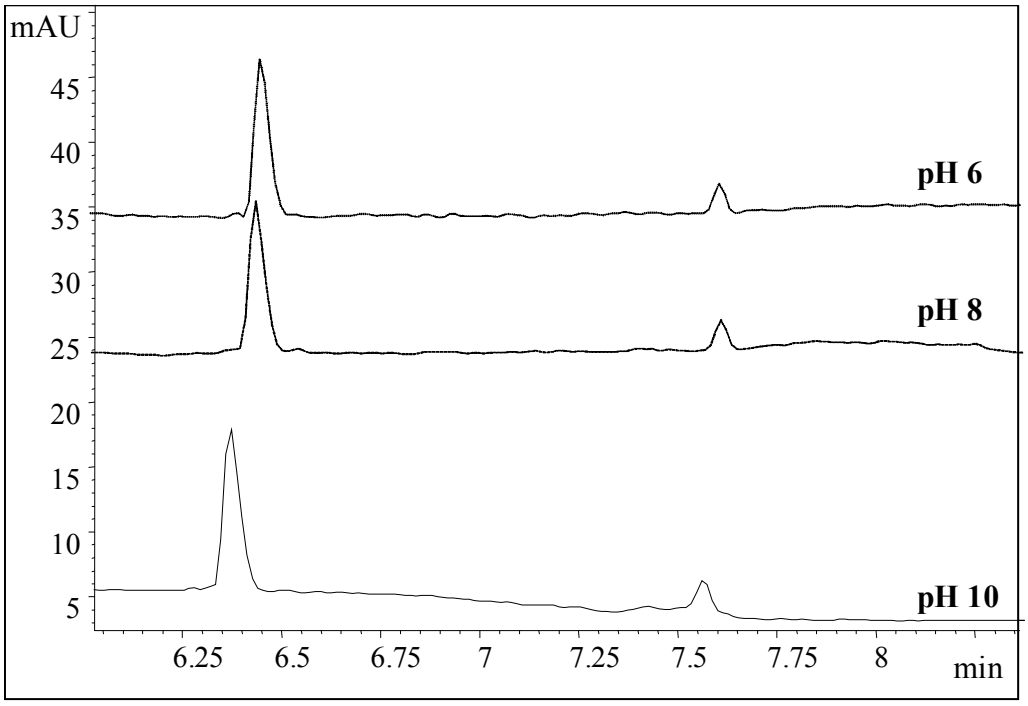

Figure 2.5B: Electropherograms (stacked) of CrIDS monitored at various pH levels. For peak identification and conditions please refer to Fig. 2.3A.

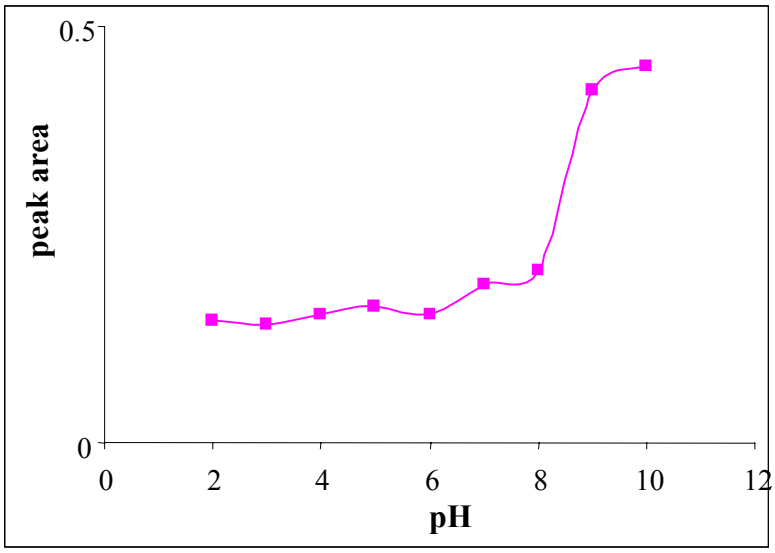

Figure 2.6: CrIDS peak area as a function of pH. Conditions same as in Fig. 2.3A.

CuIDS

Cu^{2+} normally forms strong ML complexes with most ligands like EDTA [4], DTPA [6] and EDDS [13] due to its high stability constant. The stability of CuIDS complex was not as strong as hoped for and this was seen (Fig. 2.7B) over a wide range of pH levels between 10 and 2. The CuIDS complex showed a sharper peak compared to other metal-IDS chelates analysed. An increase in the peak area of CuIDS at pH 10 is illustrated in Figure 2.8A. The experimental results differed significantly from the modeled results (Fig. 2.8B) due to the lability the complex in the buffer used in this method. CuIDS is stable at high pH levels and all the possible species present are given in Table 2.1.

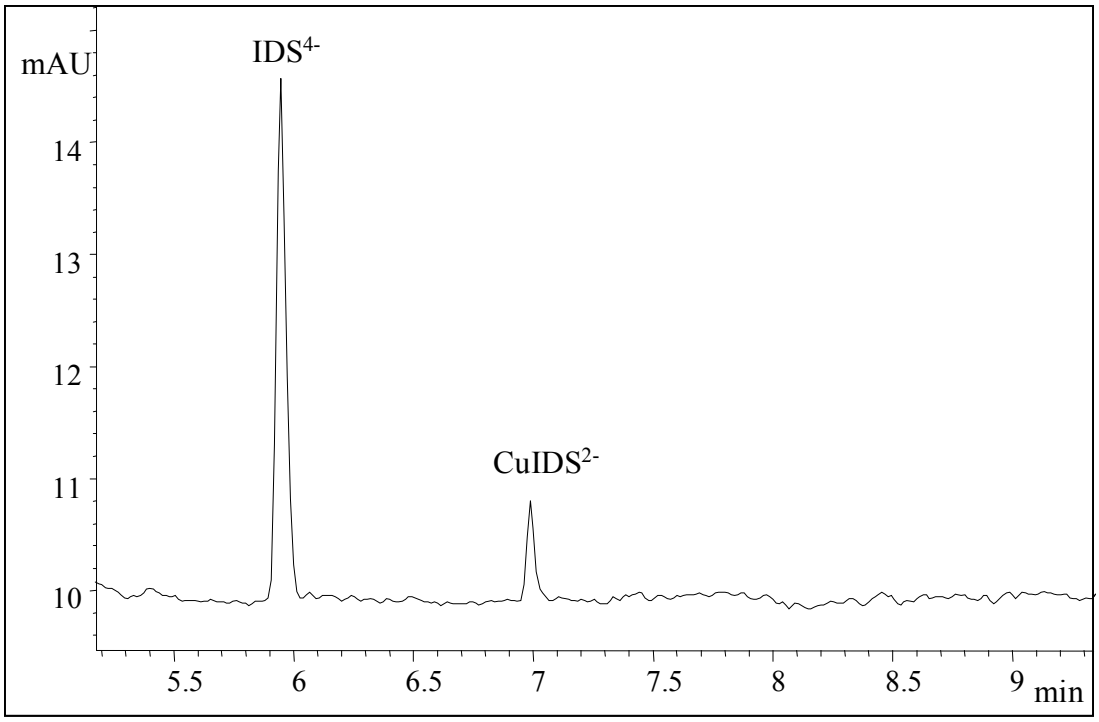

Figure 2.7A: Electropherogram of CuIDS monitored at 200 nm. Conditions same as in Fig. 2.3A.

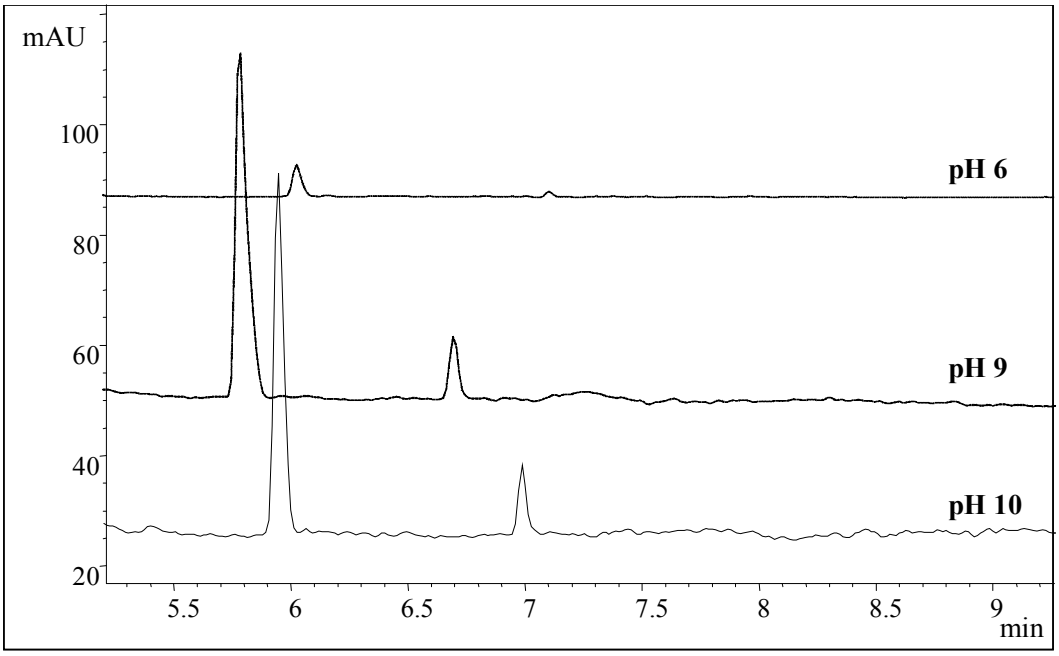

Figure 2.7B: Electropherograms (stacked) of CuIDS monitored at various pH levels. For peak identification and conditions please refer to Fig. 2.7A.

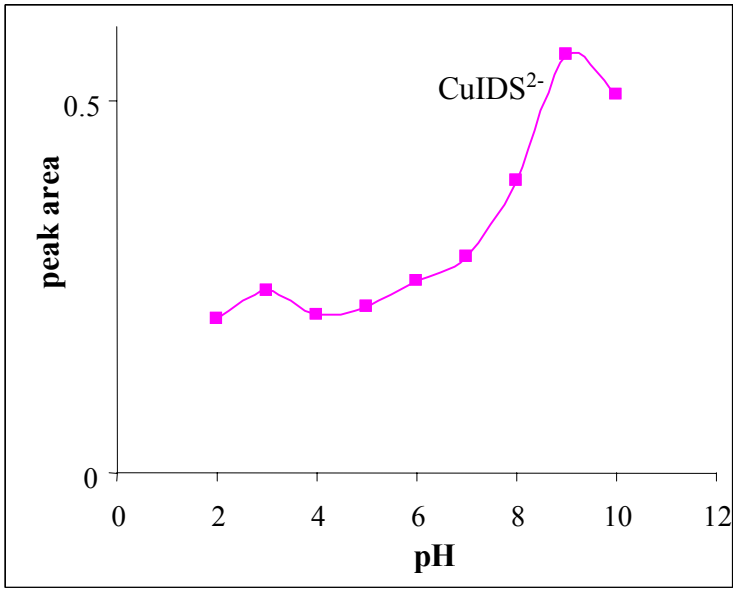

Figure 2.8A: CuIDS peak area as a function of pH. Conditions same as in Fig. 2.3A.

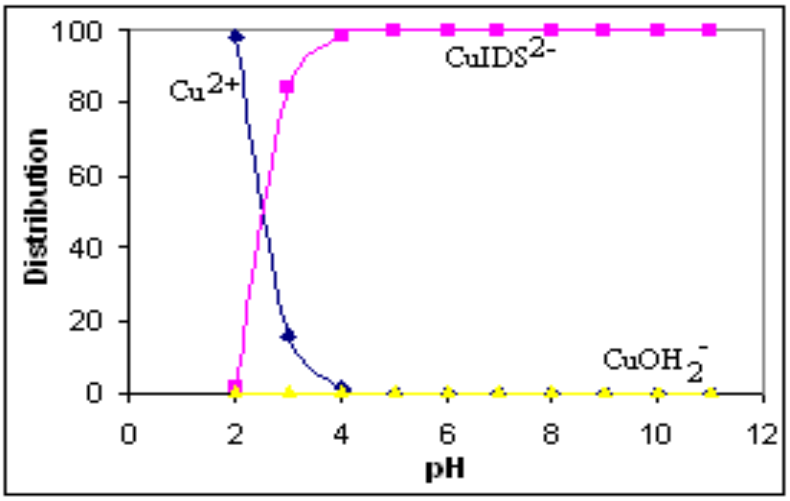

Figure 2.8B: Speciation profile of CuIDS as function of pH; T = 25 ºC, I = 0.1 M.

FeIDS

Fe tends to form hydroxy species at high pH levels, so an unidentified small peak was seen at pH 9 and 10. FeIDS is said to be stable within pH 5 and 7 but the CE results showed a very small peak. The reason could be the lability of Fe^{3+} when complexed with IDS, even though it has a high log K value of 16.1. The peaks that could clearly be detected were nitrate and IDS peaks (Fig. 2.9A). A graph of pH vs peak area is given in Fig. 2.10. According to the speciation plot, FeIDS complex is expected in the acidic pH region of 3-6 [9]. The results were not comparable with the speciation data from the literature. No JESS data is available for $FeIDS^-$ complex.

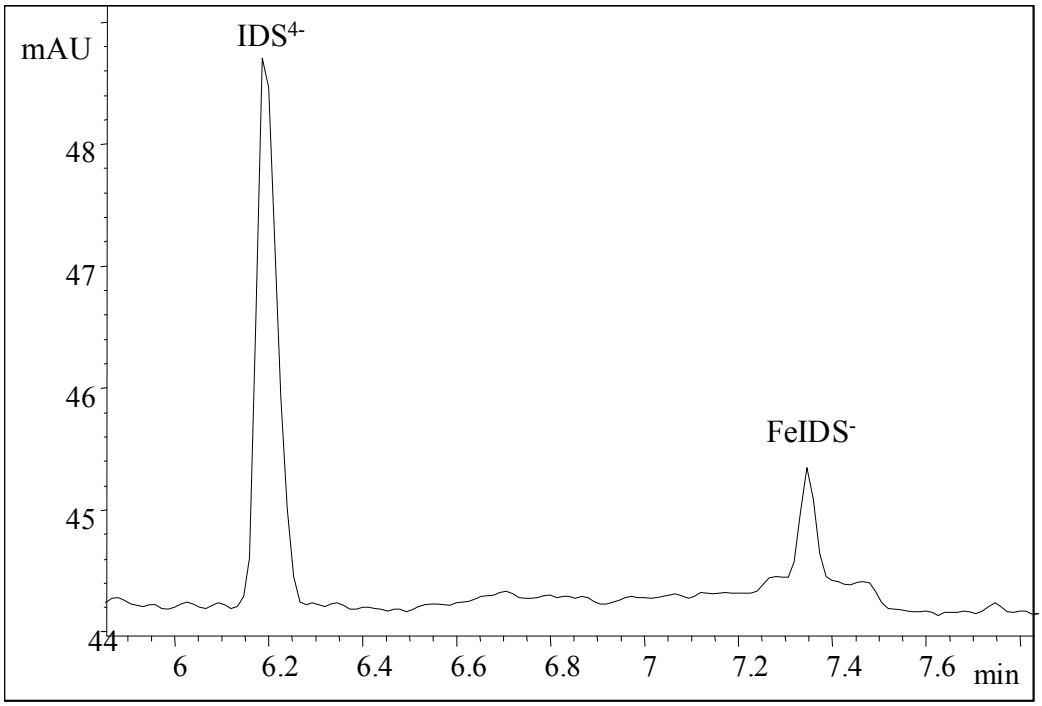

Figure 2.9A: Electropherogram of FeIDS monitored at 200 nm. Conditions same as in Fig. 2.3A.

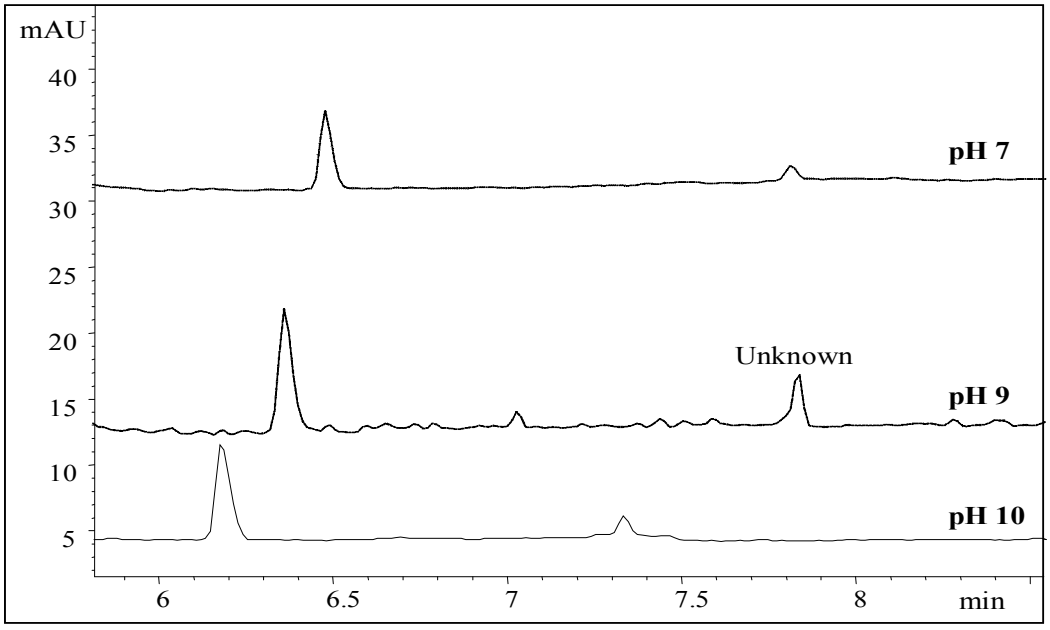

Figure 2.9B: Electropherograms (stacked) of FeIDS monitored at various pH levels. For peak identification and conditions please refer to Fig. 2.9A.

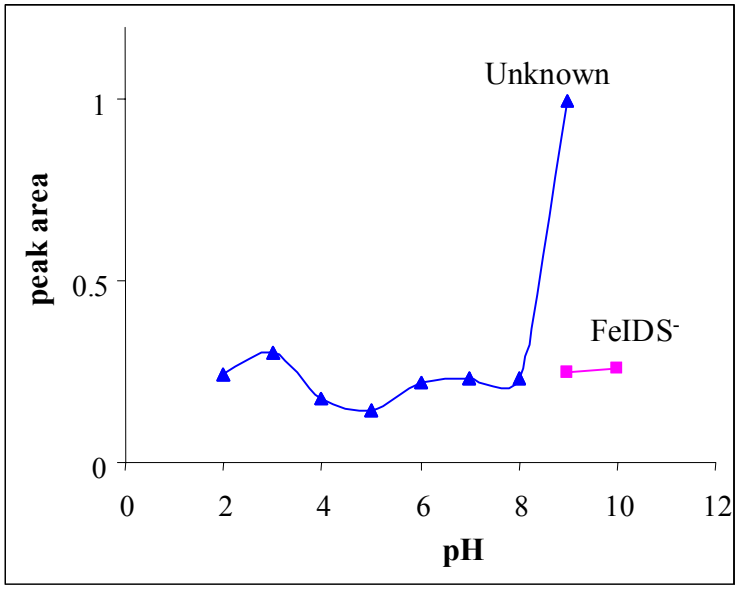

Figure 2.10: A graph of FeIDS peak area as a function of pH. Conditions same as in Fig. 2.3A.

MnIDS

Mn^{2+} was complexed with IDS to form MnIDS complex and the CE results are shown in Figure 2.11A. A graph of pH vs corrected peak areas was constructed in Figure 2.12A and compared with the MnIDS speciation graph (Fig. 2.12B). A comparable behaviour was observed between CE and speciation results. From the speciation profile of MnIDS, it is evident that a complete complexation is obtained between pH 8 and 10. Some other hydroxides of the metal also exist but at a lower concentrations.

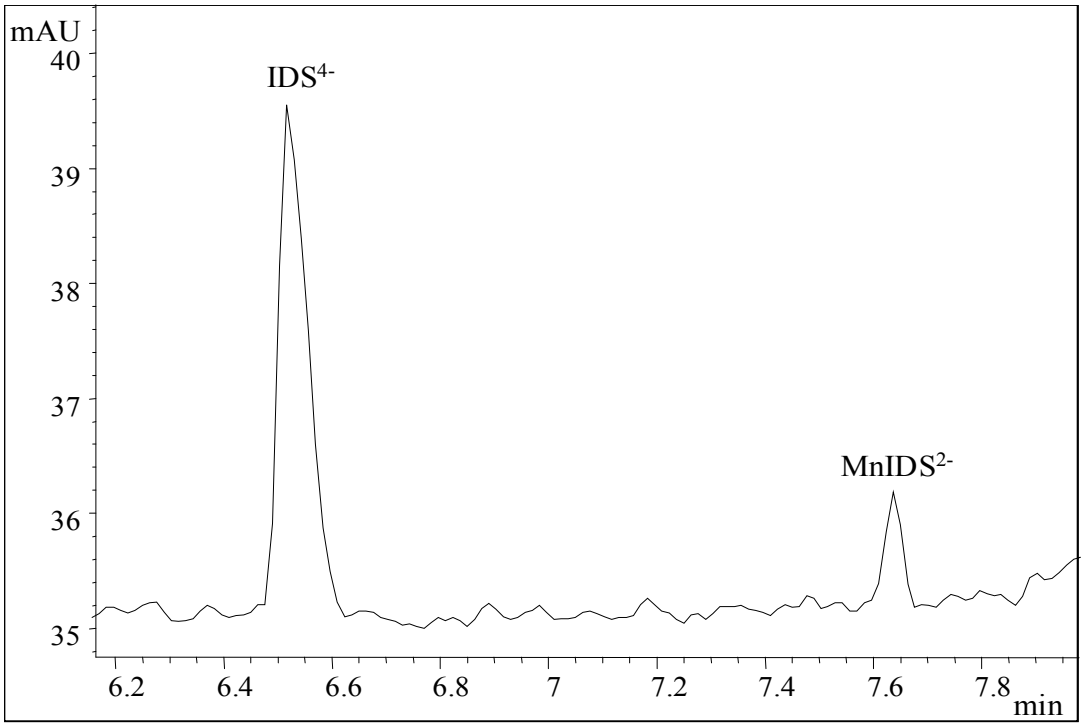

Figure 2.11A: Electropherogram of MnIDS monitored at 200 nm. Conditions same as in Fig. 2.1A.

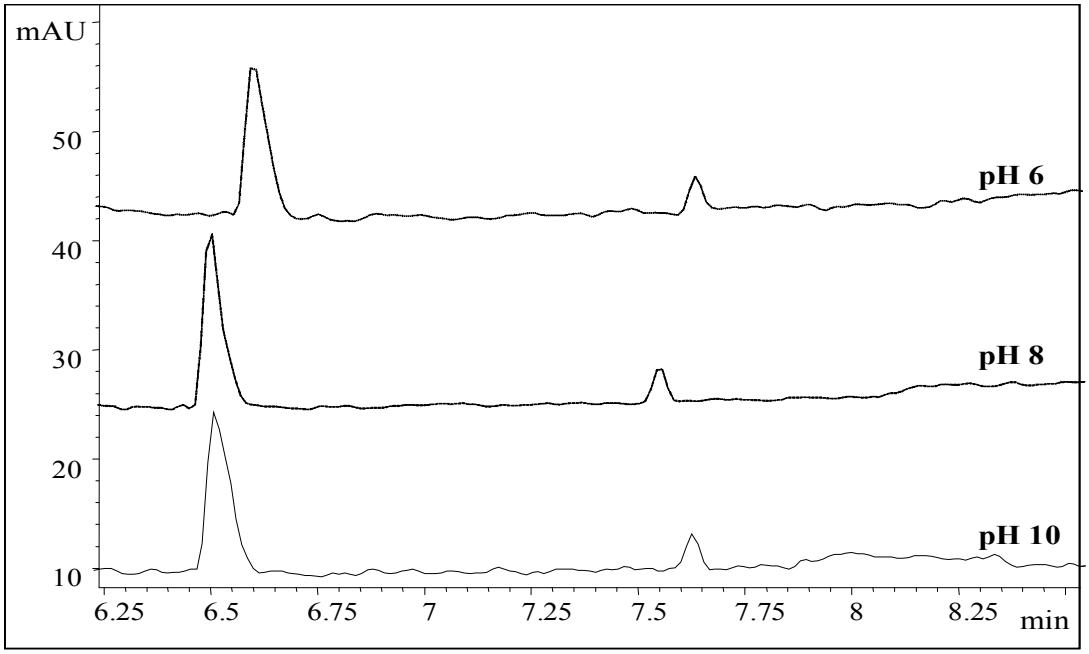

Figure 2.11B: Electropherograms (stacked) of MnIDS monitored at various pH levels. For peak identification and conditions please refer to Fig. 2.11A.

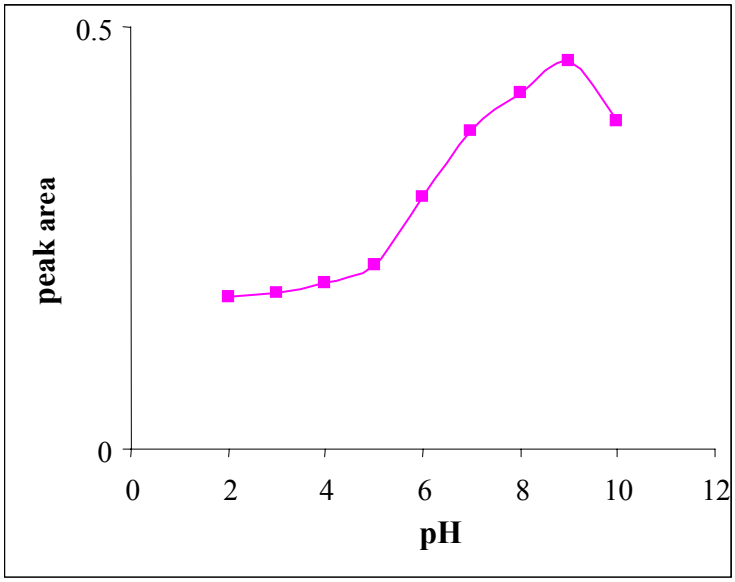

Figure 2.12A: A graph of MnIDS peak area as a function of pH. Conditions same as in Fig. 2.3A.

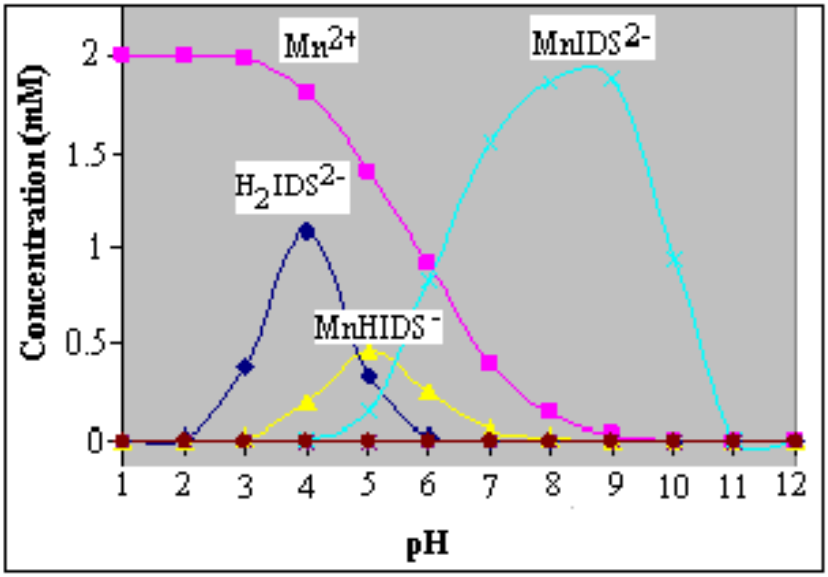

Figure 2.12B: Speciation profile of MnIDS as function of pH; T = 25 ºC, I = 0.1 M.

PbIDS

The electropherogram that illustrate the analysis of $PbIDS^{2-}$ at pH 10 is shown in Figure 2.13A. At pH 10, peaks are due to IDS^{4-}, $PbIDS^{2-}$ and an unknown compound. Figure 2.13B gives the electropherograms of PbIDS at various pH levels. A stable behaviour was observed for the PbIDS peak between pH 5 and 9 (Fig. 2.14A). According to Carbonaro and Stone [3], if metal-ligand complexes exhibit a dissociation half life of 1s, complete dissociation will occur within 10 s ($t_{rxn} << t_{CE}$). Two analyte zones, corresponding to the free ligand peak and free metal peak will result. For a dissociation half-life of 1h, the metal-ligand complex migrates as an intact entity ($t_{rxn} >> t_{CE}$). This results in free ligand and metal-ligand peaks. This behaviour was observed in the case when an excess of ligand was used to complex a metal ion.

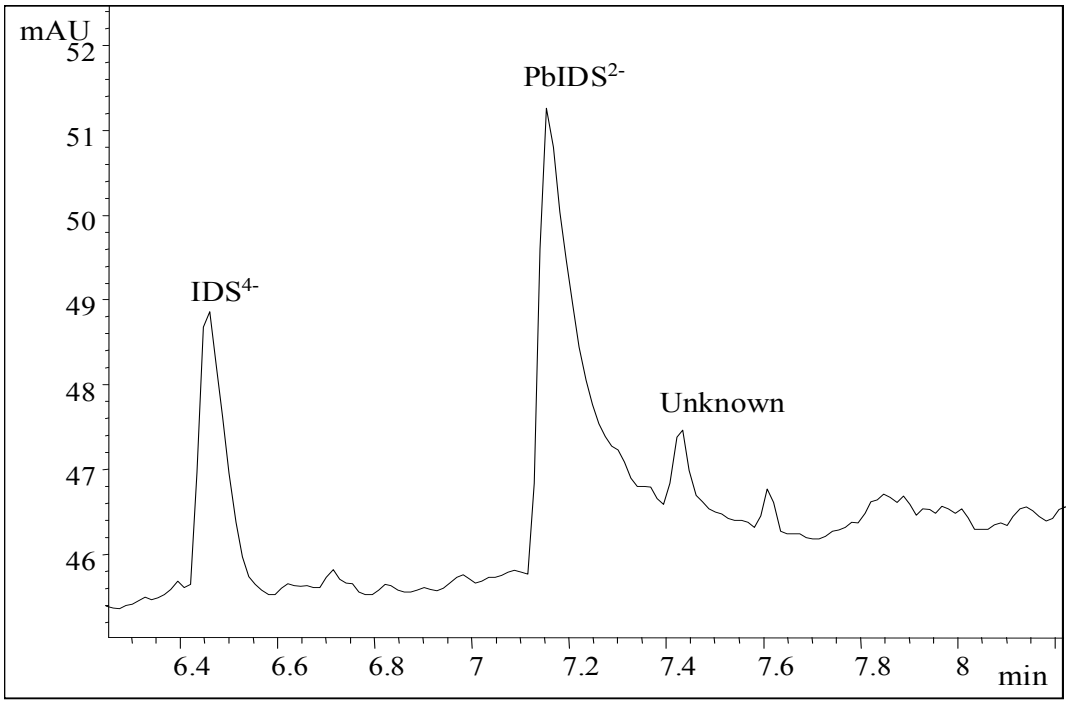

Figure 2.13A: Electropherogram of PbIDS monitored at 200 nm. Conditions same as in Fig. 2.1A.

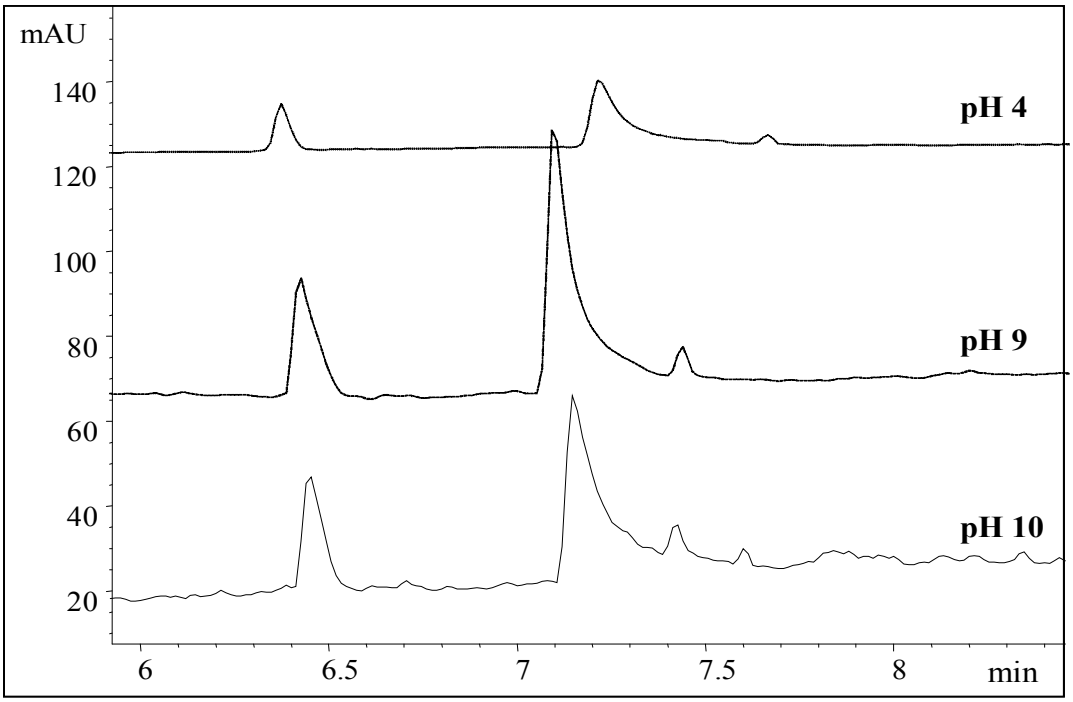

Figure 2.13B: Electropherograms (stacked) of PbIDS monitored at various pH levels. For peak identification and conditions please refer to Fig. 2.13A.

A similar behaviour was observed for other metal-IDS complexes of Cr, Cu, Cd and Zn. A plot of pH vs corrected peak areas for the PbIDS complex was constructed to predict the effect of pH on the equilibrium between metal-ligand complexes. The obtained CE results were comparable with the speciation data. This data fit well with the CE data, which showed an increase in [$PbIDS^{2-}$] at pH 6, illustrated in Figure 2.14B.

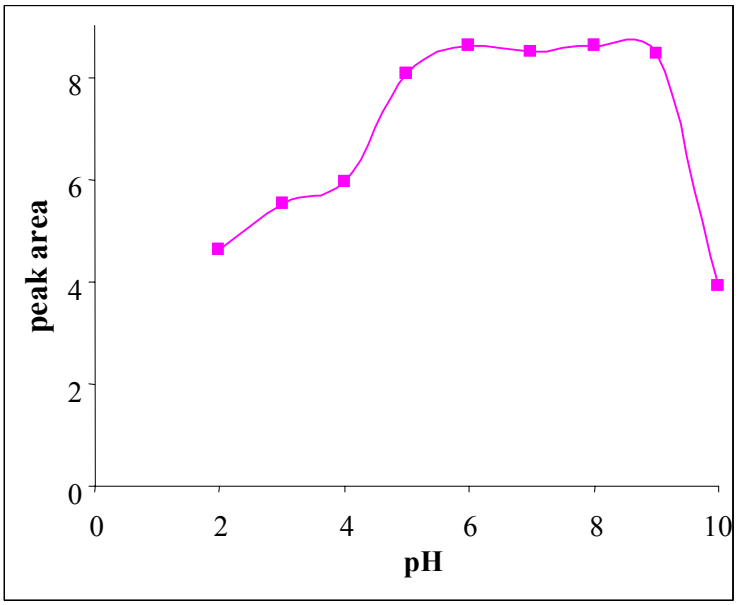

Figure 2.14A: PbIDS peak area as a function of pH. Conditions same as in Fig. 2.3A.

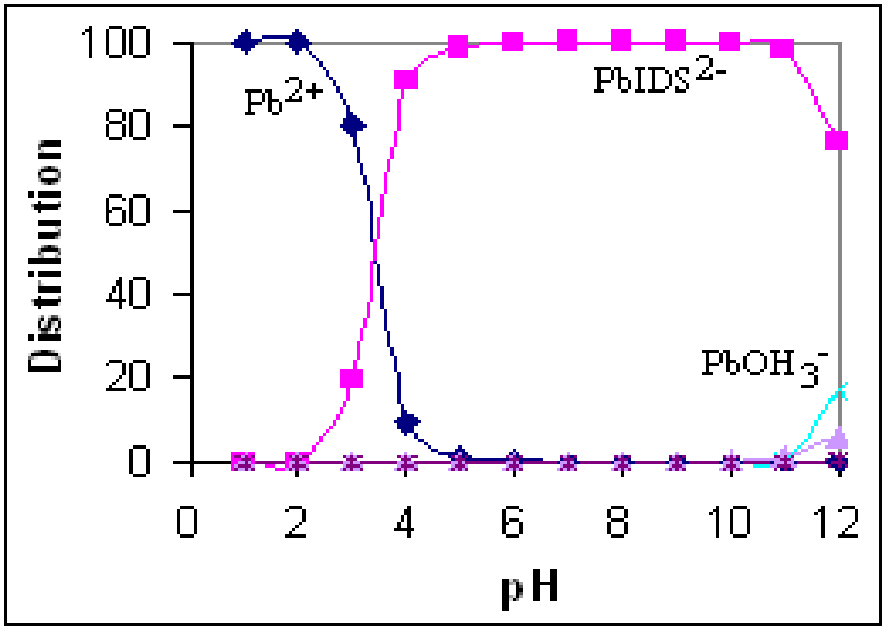

Figure 2.14B: Speciation profile of PbIDS as function of pH; T = 25 ºC, I = 0.1 M.

ZnIDS

The ZnIDS peak is illustrated in Figure 2.15A. A small broad peak was also detected for ZnIDS and a typical graph is given in Figure 2.16A. The results showed a comparable behaviour with the predicted speciation profile observed in Figure 2.16B. An unknown peak was also observed at high pH levels. The ZnIDS speciation curve shows that optimum complexation occurs between pH >≈ 6 and 11, the predominant species being $ZnIDS^{2-}$.

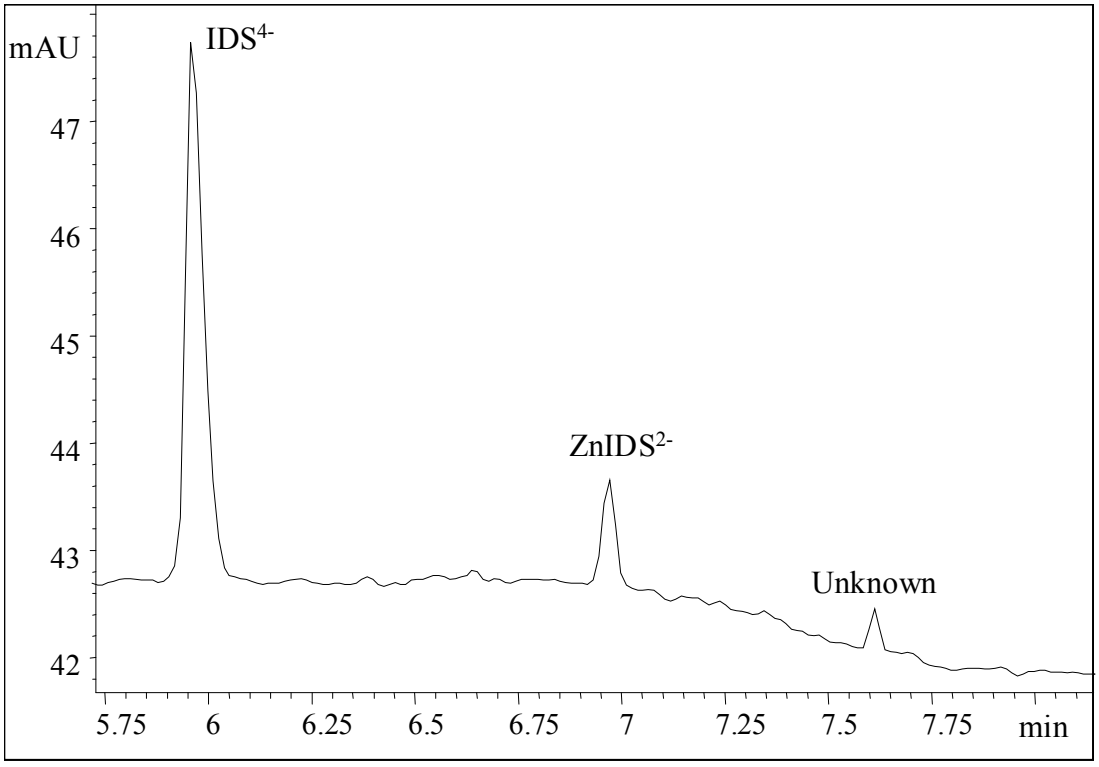

Figure 2.15A: Electropherogram of ZnIDS monitored at 200 nm. Conditions same as in Fig. 2.3A.

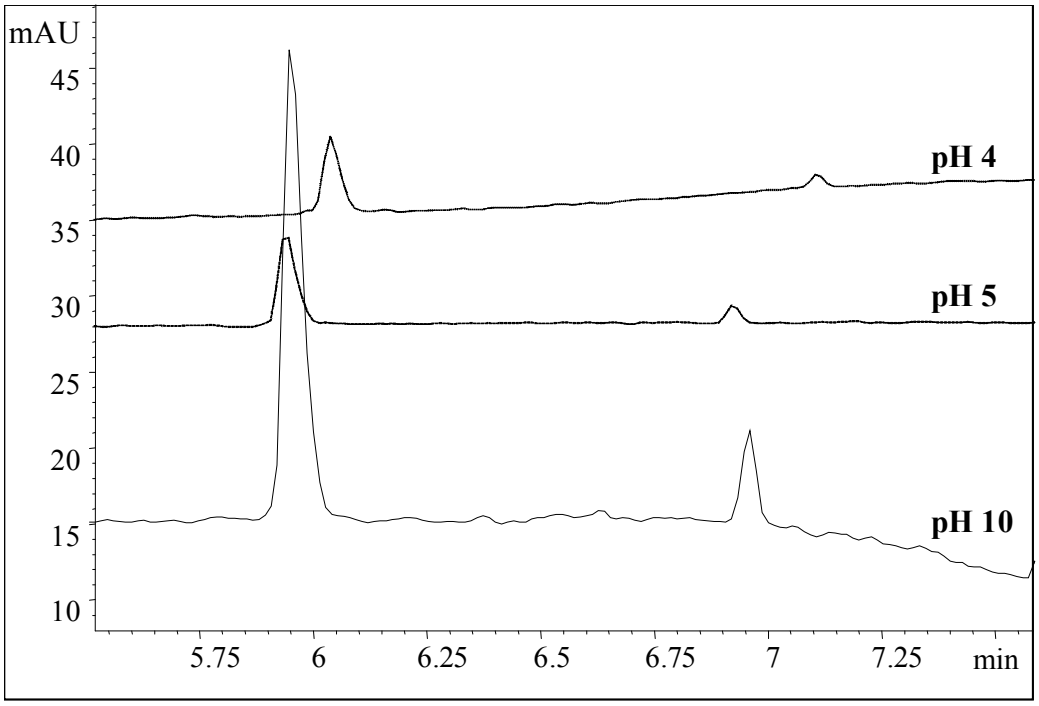

Figure 2.15B: Electropherograms (stacked) of ZnIDS monitored at various pH levels. For peak identification and conditions please refer to Fig. 2.14A.

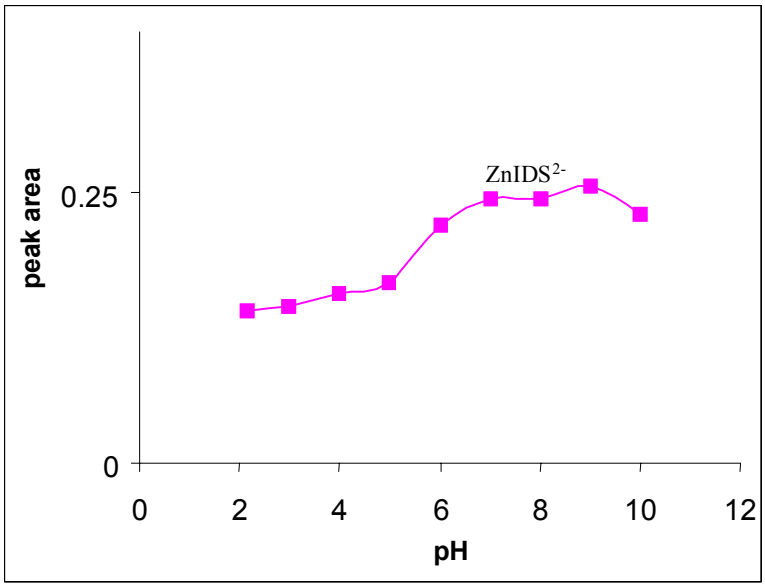

Figure 2.16A: ZnIDS peak area as a function of pH. Conditions same as in Fig. 2.3A.

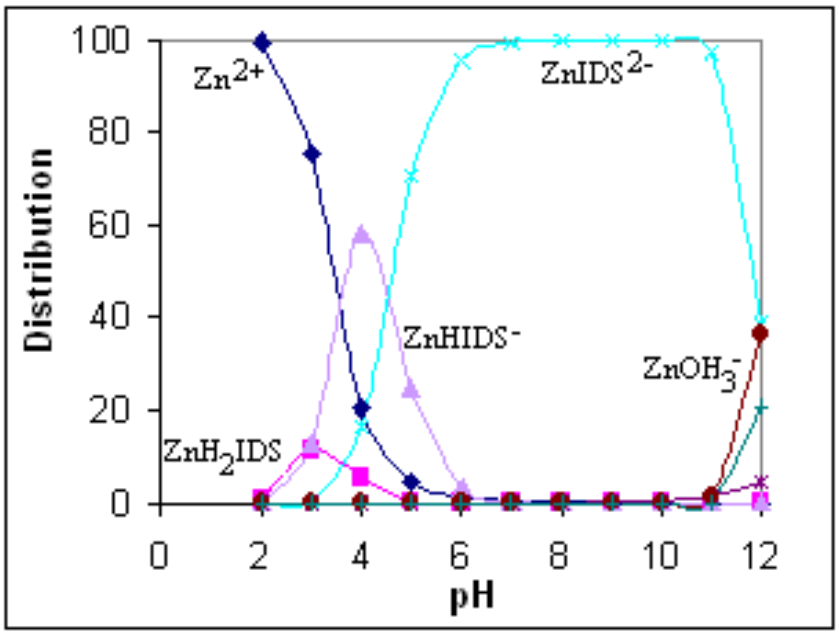

Figure 2.16B: Speciation profile of ZnIDS as function of pH; T = 25 ºC, I = 0.1 M.

2.3.2 Separation of metal-IDS complexes at various IDS concentrations

The selected ML complexes i.e Cu, Pb and Zn were analysed by varying the IDS concentration with constant metal ion concentration of 2 mM. The pH affects the quality of CE separation of ML complexes because their stabilities are strongly pH dependent. At pH levels above 9 most MIDS complexes are stable. The obtained results are discussed below.

CuIDS

The analysis of the CuIDS complex is given in Figure 2.17A. Cu formed a very stable complex with IDS; a sharp peak for this is evident in all the electropherograms. As the concentration of IDS increases a fourth peak is formed, which could be due to $Cu(OH)IDS^-$. This is shown in the speciation graph of CuIDS done by Hyvönen et al. [13]. According to the electropherograms for the CuIDS, Cu forms a stable complex at low IDS concentration. A sharp CuIDS peak appeared within 2 min as shown in Fig. 2.17A and all peaks were separated.

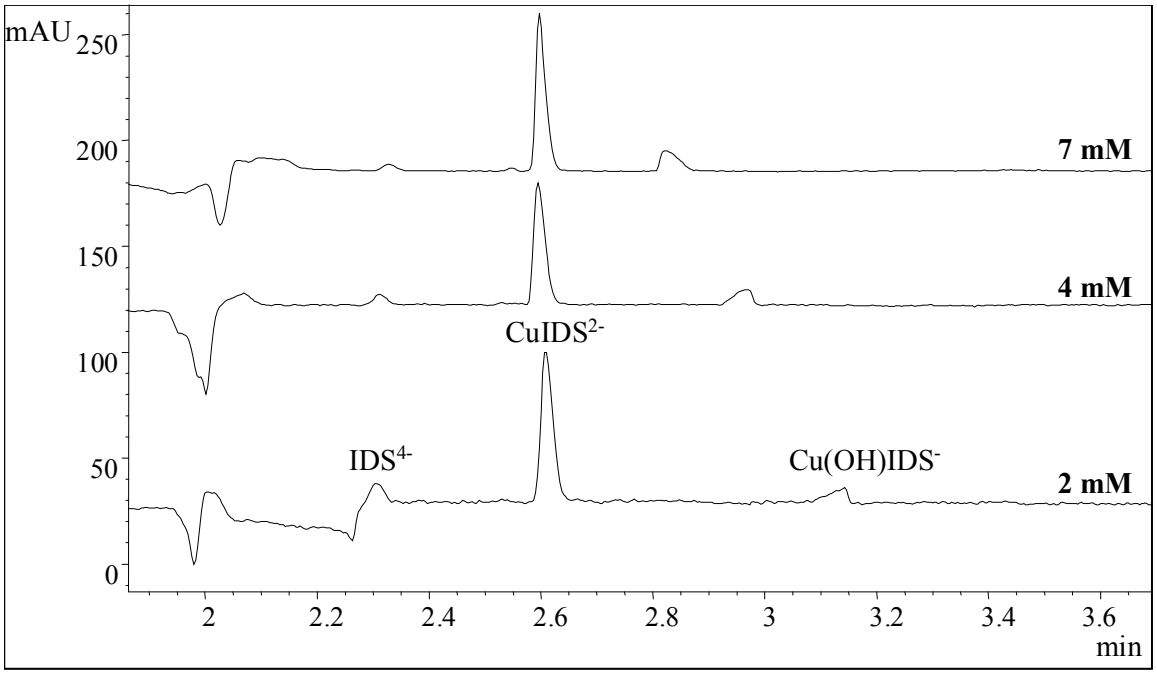

Figure 2.17A: Electropherograms of 2mM Cu^{2+} complexed with IDS at various concentrations. Conditions: 10 mM tetraborate buffer and 0.3 mM CTAB as a modifier at pH 9, applied voltage -20 kV, temperature 25 ºC, hydrodynamic sample injection for 2 s applying 50 mbar pressure, detection at 225 nm.

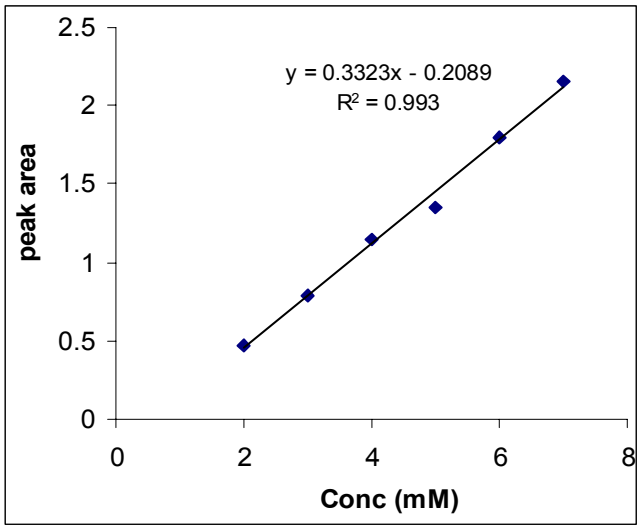

Figure 2.17B: CuIDS peak areas as a function of IDS concentration.

The graph of IDS concentration vs corrected peak area for CuIDS show an increase in CuIDS as the IDS concentration increases. Peak areas increased linearly with IDS concentration increased.

PbIDS

The peak heights for IDS were higher than the PbIDS complex shown in Figure 2.18A. As the concentration of IDS increases, the broad PbIDS peak resolves into two peaks, which result in an unknown peak. There is an increase in PbIDS and unknown peak areas as the IDS concentration increases. The third peak might be due to $Pb(OH)IDS^{3-}$ or $Pb(OH)^{3-}$ as deduced from the modelled speciation profile of PbIDS in Figure 2.14B.

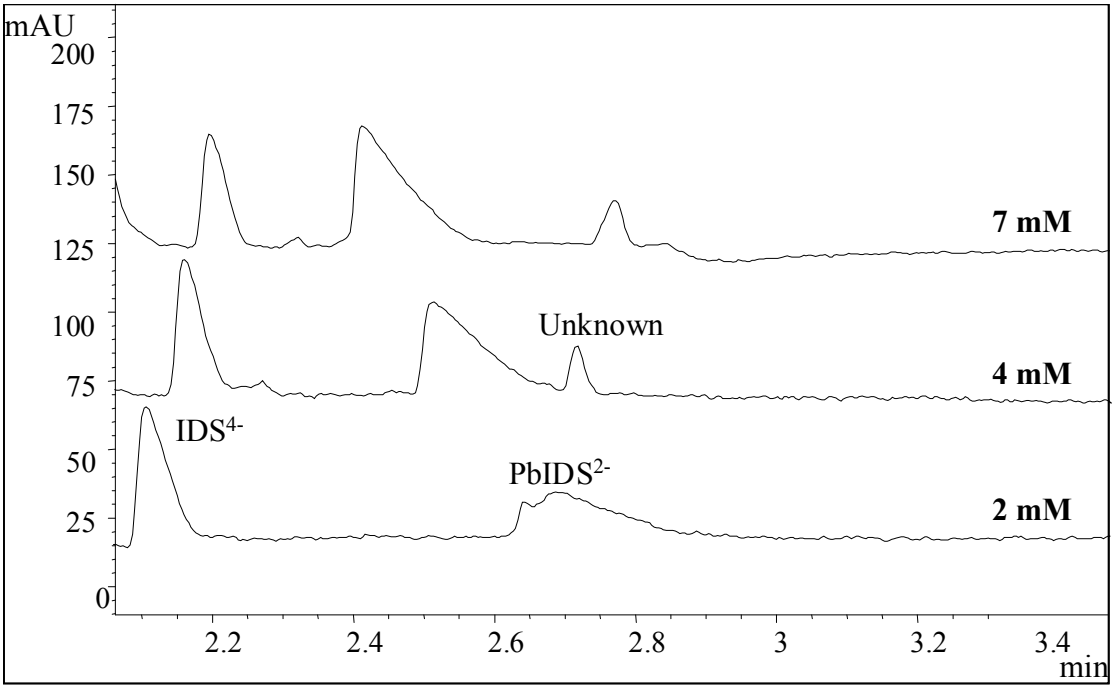

Figure 2.18A: Electropherograms of 2mM Pb^{2+} complexed with IDS at various concentrations. Conditions same as in Fig. 2.17A.

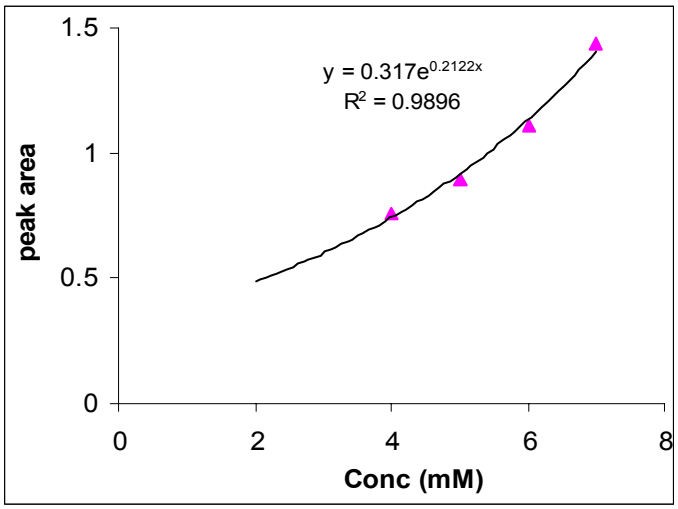

Figure 2.18B: PbIDS peak areas as a function concentration.

ZnIDS

Figure 2.19 illustrates the obtained electropherograms for ZnIDS. When Zn complexes with IDS between 2-4 mM IDS, no ZnIDS peak was observed. The complex starts to form at 5 mM IDS, resulting in a small peak. From the graph of ZnIDS, it seems that as the IDS concentration increases the ZnIDS peak also increases.

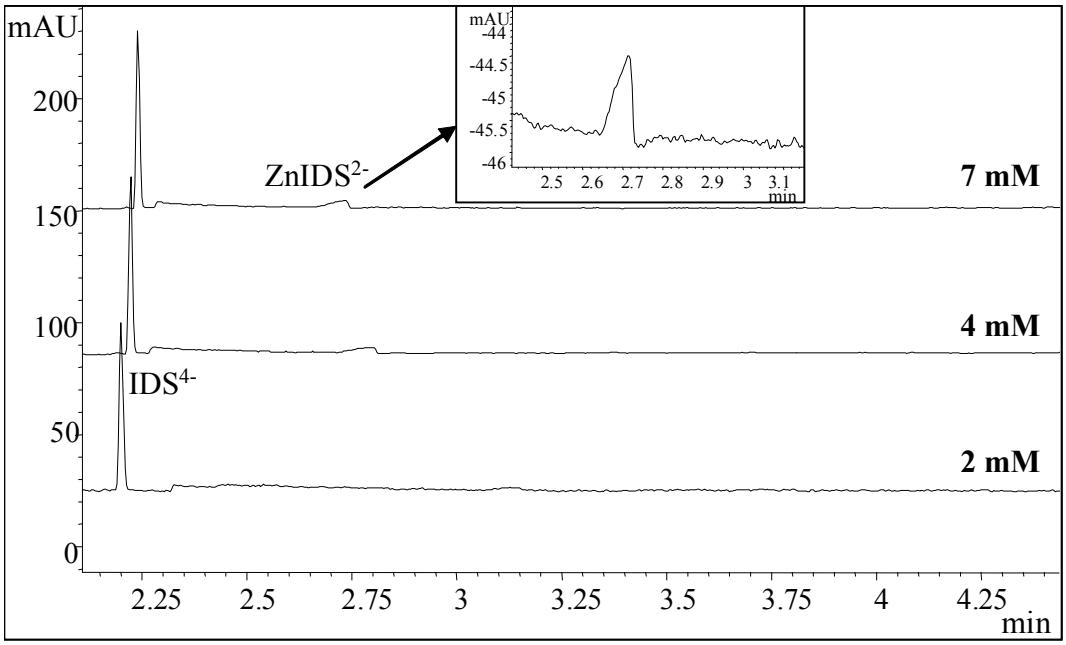

Figure 2.19A: Electropherograms of 2mM Zn^{2+} complexed with IDS at various concentrations. Conditions same as in Fig. 2.17A.

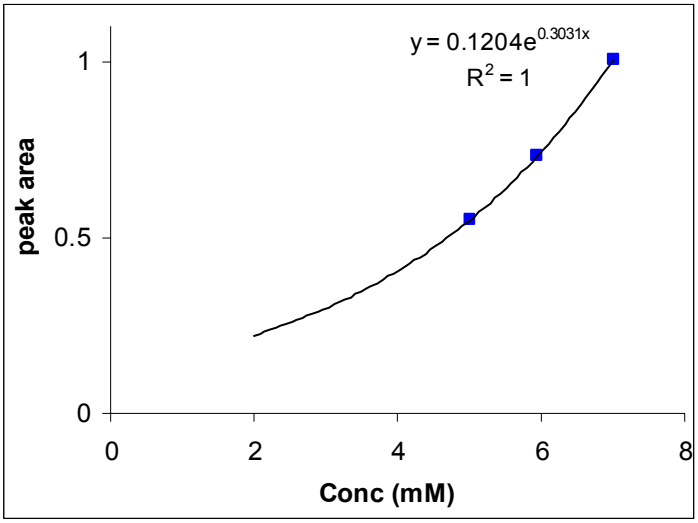

Figure 2.19B: ZnIDS peak areas as a function of concentration.

2.4 Conclusion

This work demonstrates that CE provides a fast and efficient separation of the cations as UV-absorbing chelates with IDS. It was shown that it is possible to separate the metal-ligand chelates at various pH levels using CE. All MIDS complexes formed a reasonably stable complexes compared to the FeIDS complex. Sharp peaks were observed for CuIDS and PbIDS while other MIDS complexes showed small broad peaks. The small broad peaks are attributed to the lability and weakly formation of MIDS complexes during the CE analysis, while sharp peaks are due to strong formation of CuIDS and PbIDS complexes. Short analysis times were also achieved and the results were reproducible for all complexes.

The Joint Expert Speciation System (JESS) simulation program was used as a computer model to calculate the equilibrium distribution of IDS and MIDS complexes as a function of pH. From the species distribution diagrams of all MIDS complexes studied, it was observed that an optimum complexation occurs at pH >4. The lability of the complexes is one of the main factors explaining the discrepancies between theory and experimental results. Better results might be obtainable under pure equilibrium conditions that is with metal in sample and buffer and with the same buffer as sample diluent The speciation data attained by CE can assist in answering many questions about the transformations of metal ligand complexes for e.g. in industrial processes or environmental media.

The resolution of CuIDS, PbIDS and ZnIDS complexes were studied at different IDS concentrations. CuIDS and PbIDS formed relatively inert complexes as compared to the ZnIDS complex. Unknown peaks were also observed in the electropherograms of CuIDS and PbIDS. It is suggested that the peaks might be due to hydroxy species of MIDS. The peaks were not confirmed because the standard samples of hydroxide MIDS complexes were not available.

Bibliography

[1] Kuban P, Kuban V, ***J Chromatogr A***, 1999, 836, 75-80.

[2] Caliaro G.A, Herbots C.A, ***J Pharm. Biomed.Anal***, 2001, 26, 427-434.

[3] Carbonaro R.F and Stone A.T, ***Anal Chem***, 2005, 77(1), 155-164.

[4] Laamanen P-L, Mali A, Matilainen R, ***Anal Bioanal Chem***, 2005, 381, 1264-1271.

[5] Harvey S.D, ***J Chromatogr A***, 1996, 746, 333-340.

[6] Padarauskas A, Schwedt G, ***J Chromatogr A***, 1997, 773, 351-360.

[7] Templeton D M, Ariese F, Cornelis R, Danielsson L G, Muntau H, van Leeuwen H P, Lobinski R, ***Pure Appl. Chem***, 2000, 72, 1453-1470.

[8] Chen Z, Megharaj M, Naidu R, ***Microchemical journal***, 2007, 86, 94-101.

[9] Bayer: Imminodisuccinate, Iminodisuccic acid sodium salt, Product literature from www.bayer.com, 2001.

[10] May. P. M, ***Talanta***, 1991, 38(12), 1409-1417.

[11] May. P. M, ***Talanta***, 1991, 38(12), 1419-1426.

[12] May. P. M, ***Talanta***, 1991, 40(6), 819-825.

[13] Hyvönen H, Orama M, Saarinen H, Aksela R, ***Green Chemistry***, 2003, 5, 410-414.

[14] Martell A.E, Smith R.M, NIST Standard Reference Database 46 Version 8, Gaithersburg, MD USA, 2004.

[2]Chapter 3

Dissociation profiles of metal-aminocarboxylate complexes in aqueous media at different pH levels

3.1 Introduction

In this chapter, the behaviour of four complexing agents, namely DTPA, S,S-EDDS, IDS and R,S-IDS with various metal ions (Cd^{2+}, Cr^{3+}, Cu^{2+}, Fe^{3+}, Pb^{2+} and Zn^{2+}) were investigated at pH 7 and 9. CE was utilized for the separation of metal-ligand complexes at various time intervals. When using DTPA and EDDS, complexation of metals took place as one-step reaction forming stable chelates encapsulating the metal ion which have high stability constants (Table 2.1). The structures of the ligands are given in Figure 1.2.

3.2 Experimental Details

3.2.1 Instrumentation

All separations were performed with an HP CE instrument as reported before in Chapter 2, section 2.2.1. The separation potential of -25 kV was applied during all separations. Samples were introduced by hydrodynamic injection mode (50 mbar, 3 s). All samples were detected within 200-245 nm range. The pH of solutions was measured with a Jenway 4330 pH meter. All experiments were conducted at 25 °C.

3.2.2 Reagents and solutions

The solutions were prepared using deionized water with a resistivity of 18 MΩ cm (Millipore system) and were used throughout. Metal-ligand complexes were prepared by mixing metal stock solutions with a ligand. The working electrolyte was prepared daily from 20 mM sodium tetraborate ($Na_2B_4O_7.10H_20$) buffer and 0.2 mM CTAB used as a

[2] Part of the work described in this chapter has been presented as a poster at the 29th International Symposium on Capillary Chromatography, Pallazo Dei Congressi, Riva del Garda, Italy, 29 May- 2 June 2006, L M Katata and A. M Crouch.

surfactant. The pH was adjusted by the addition of 0.1 M NaOH or HCl. Samples analysed were in a 1:1, 1:2 and 1:4 metal to ligand ratio (L = DTPA, EDDS, IDS, R,S-IDS). The electrolytes were filtered through a 0.45 μm membrane filter prior to use.

3.3 Results and Discussion

3.3.1 Metal-ligand complexes at pH 9

The metal-ligand complexes were prepared in different molar ratios depending on the stability of the complex. Stability constants for the chelating agents complexed with various metal ions are given in Table 2.1. The results obtained by CE are described below.

CE analysis of CuIDS

The CuIDS complex was monitored for 70 hours and CE was used to study the possible changes that occur during the analysis. A solution consisting of 20 mM tetraborate and 0.2 mM CTAB at pH 9 was used as the running buffer. 1 mM CuIDS was transferred to the CE auto-sampler and repeatedly injected and analysed using direct UV detection at 225 nm. Figure 3.1A illustrates the electropherograms of CuIDS at various time intervals and a graph is represented in Figure 3.1B.

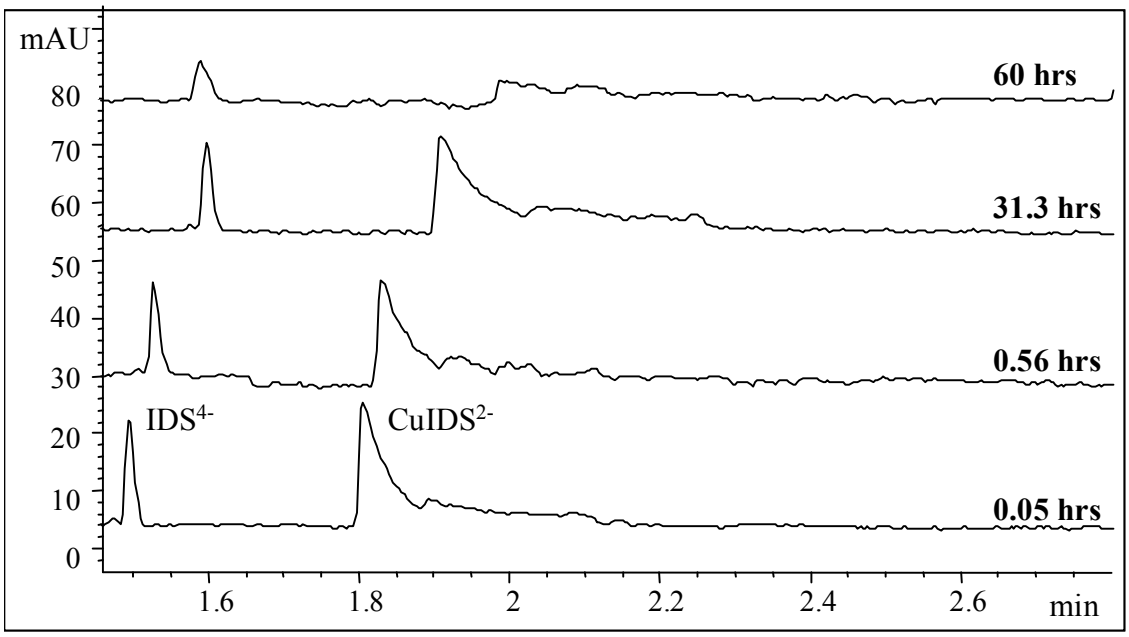

Figure 3.1A: Electropherograms of 1 mM CuIDS monitored at various time intervals (hours). Conditions: 20 mM tetraborate buffer and 0.2 mM CTAB as a modifier at pH 9, applied voltage -25 kV, temperature 25 ºC, hydrodynamic sample injection for 2 s applying 50 mbar pressure, detection at 225 nm.

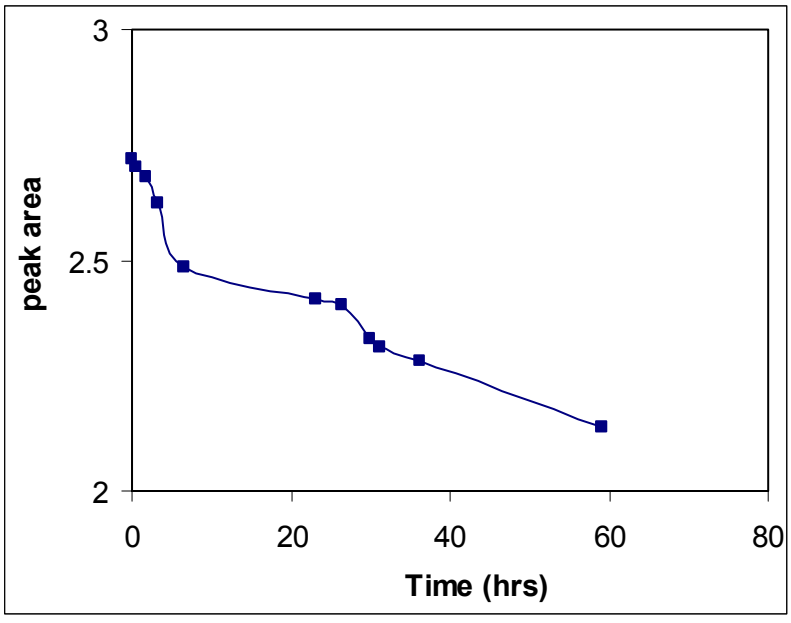

Figure 3.1B: CuIDS peak area as a function of time at pH 9.

The graph shows a steady decrease in the CuIDS concentration and there was also formation of a small unknown peak at the beginning of the analysis, which might be due to $Cu(OH)IDS^{3-}$. According to the speciation profile of CuIDS at high pH levels, the complex is very stable and also some formation of hydroxy species is observed. Speciation studies of $CuIDS^{4-}$ indicated that aqueous solutions buffered at a high pH of BGE yield 95% $[CuIDS]^{2-}$ and 5% $[Cu(OH)IDS]^{3-}$. Vasilév et al [1] determined the stability constants of Cu^{2+} with IDS in a 1:1 ratio by potentiometry and identified formation of the following complexes CuH_2IDS, $CuHIDS^{-}$ and $CuIDS^{2-}$. These results are in agreement with the work done by Hyvönen et al [2], but in their case they also obtained the presence of hydroxyl species of CuIDS complex, i.e. $Cu(OH)IDS^{3-}$. The structures of possible CuIDS complexes present in aqueous media are given in Figure 3.2.

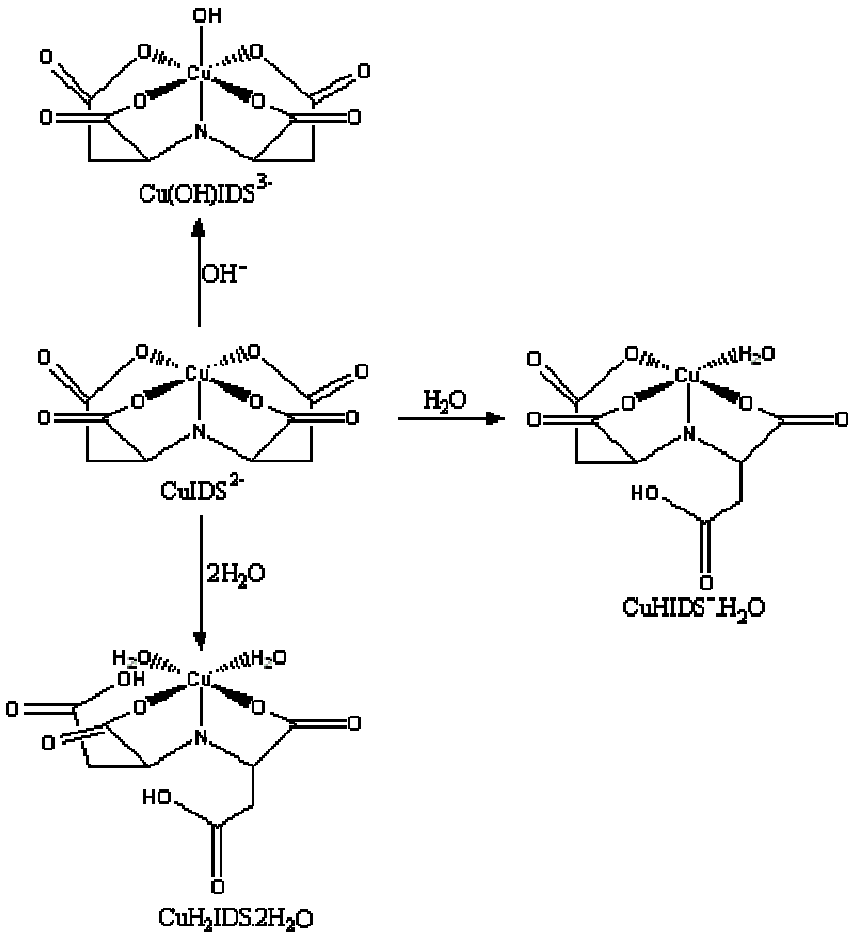

Figure 3.2: Possible structures of CuIDS complexes in aqueous media.

A similar time-dependent study was investigated for the CuIDS complex but in this study the pH was changed to 7. The effect of pH on these complexes is discussed as follows. 1 mM CuIDS complex was monitored for 61 hours and the results are given in Figure 3.3. A sharp peak was seen for CuIDS and the peak areas also decreased with time at pH 7. After 34 min there was a formation of a small broad unknown peak which might be due to $CuHIDS^-$. CuIDS complex showed a stable behaviour at this pH as compared to pH 9.

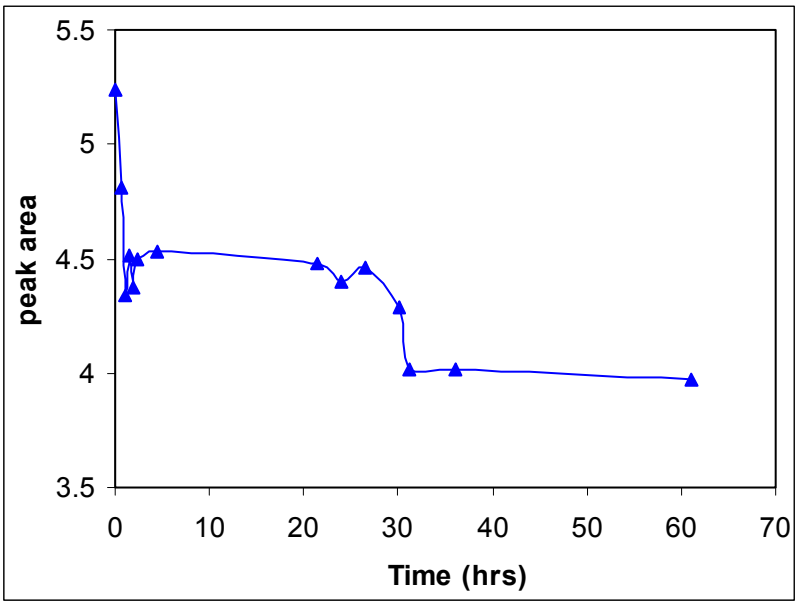

Figure 3.3: CuIDS peak area as a function of time at pH 7.

CE analysis of CuR,S-IDS

R,S-IDS is an isomer of the IDS ligand. A Cu^{2+} metal ion was complexed with the isomer to form a CuR,S-IDS complex. Figure 3.4A shows the electropherogram of 2 mM CuR,S-IDS at pH 9. Two peaks were observed, i.e. NO_3^- and CuR,S-IDS when copper complexed with R,S-IDS. The CuR,S-IDS peak was stable for some time compared to CuIDS, and decreased as time progressed to 72 hours. This is evident in graph of the corrected peak area of CuR,S-IDS complex given. The shape of CuR,S-IDS peaks changed as a function of time and diminished in size. This is due to the lability of the complex during the time analysis.

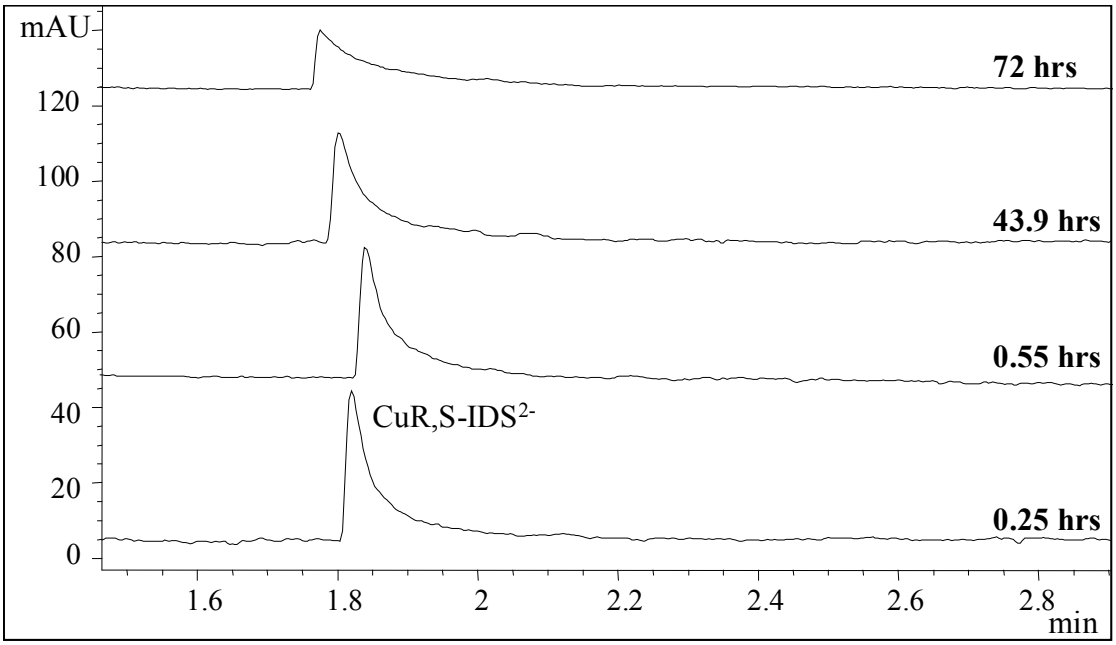

Figure 3.4A: Electropherograms of 2 mM CuR,S-IDS monitored at various time intervals (hours). Conditions same as in Fig. 3.1A.

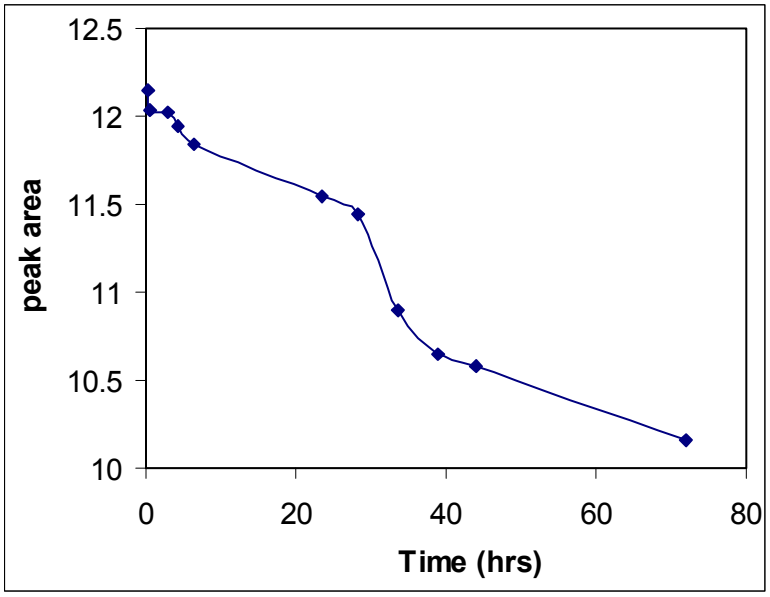

Figure 3.4B: CuR,S-IDS peak area as a function of time at pH 9.

A 2mM CuR,S-IDS peak at pH 7 was sharper than the CuR,S-IDS peak at pH 9 and three peaks were observed due to NO_3^-, CuR,S-IDS and thiourea (EOF marker). The peak areas of the complex decreased with time for a period of 61.45 hrs as seen in Figure 3.5. There was formation of a small unknown peak at 30.65 hrs and its peak areas were stable throughout.

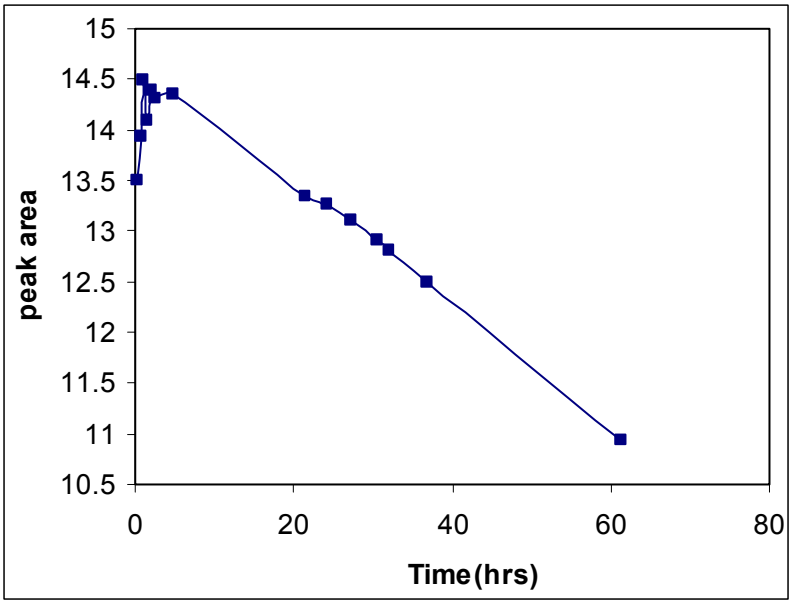

Figure 3.5: CuR,S-IDS peak area as a function of time at pH 7.

CE analysis of CuEDDS

The time-dependent analysis of 2 mM CuEDDS was monitored at pH 9. Electropherograms and a graph of the complex are depicted in Figure 3.6A and B. CuEDDS was found to decrease with time over a period of 45 hours. The following complexes were assumed to form: CuH_2EDDS, $CuHEDDS^-$, $CuEDDS^{2-}$, $Cu(OH)EDDS^{3-}$,depending on the metal to ligand ratio in the aqueous solution. There are some structural variations but in all the MEDDS complexes, the central metal atom is coordinated by two imine nitrogen atoms and by one oxygen atom from each of the four carboxylate groups of the ligand. This can clearly be seen in Figure 3.7.

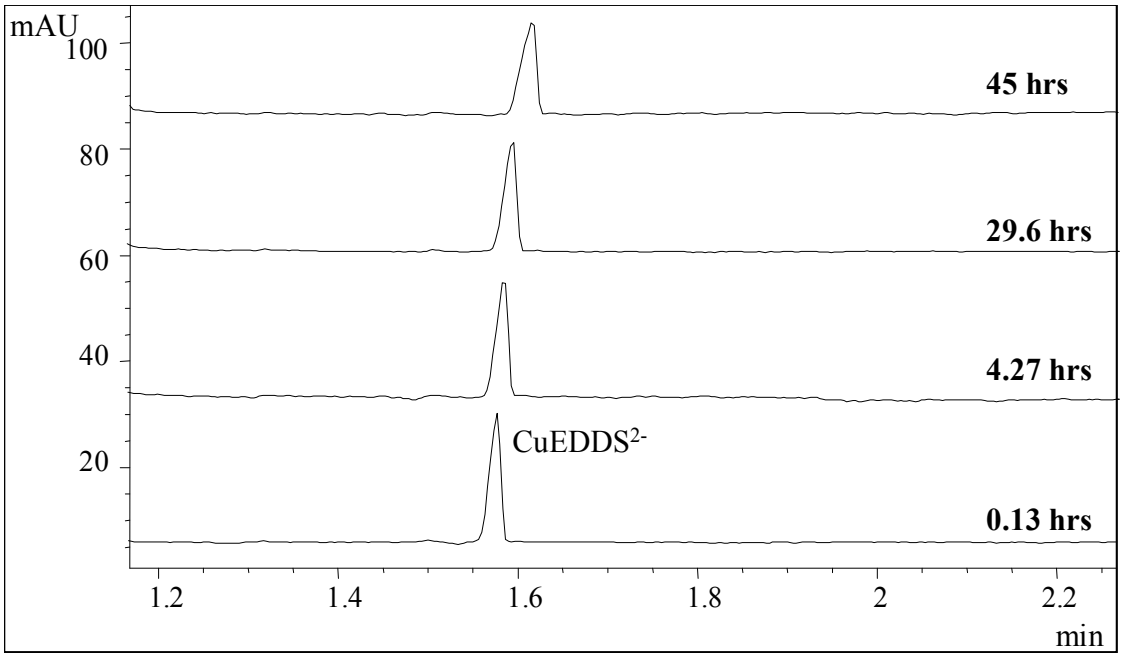

Figure 3.6A: Electropherograms of 2 mM CuEDDS monitored at various time intervals (hours) a. 0.13, b. 4.27, c. 29.6, d. 45. Conditions same as in Fig. 3.1A.

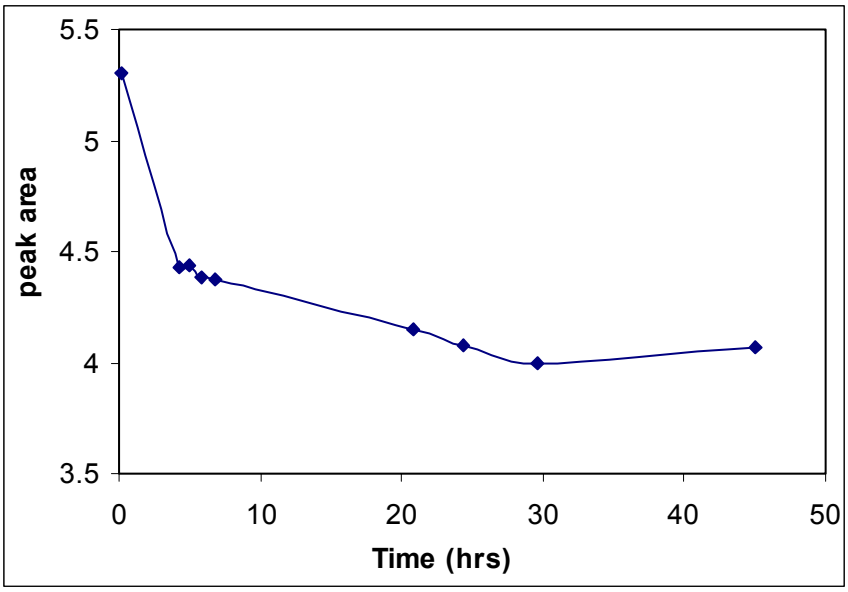

Figure 3.6B: CuEDDS peak area as a function of time at pH 9.

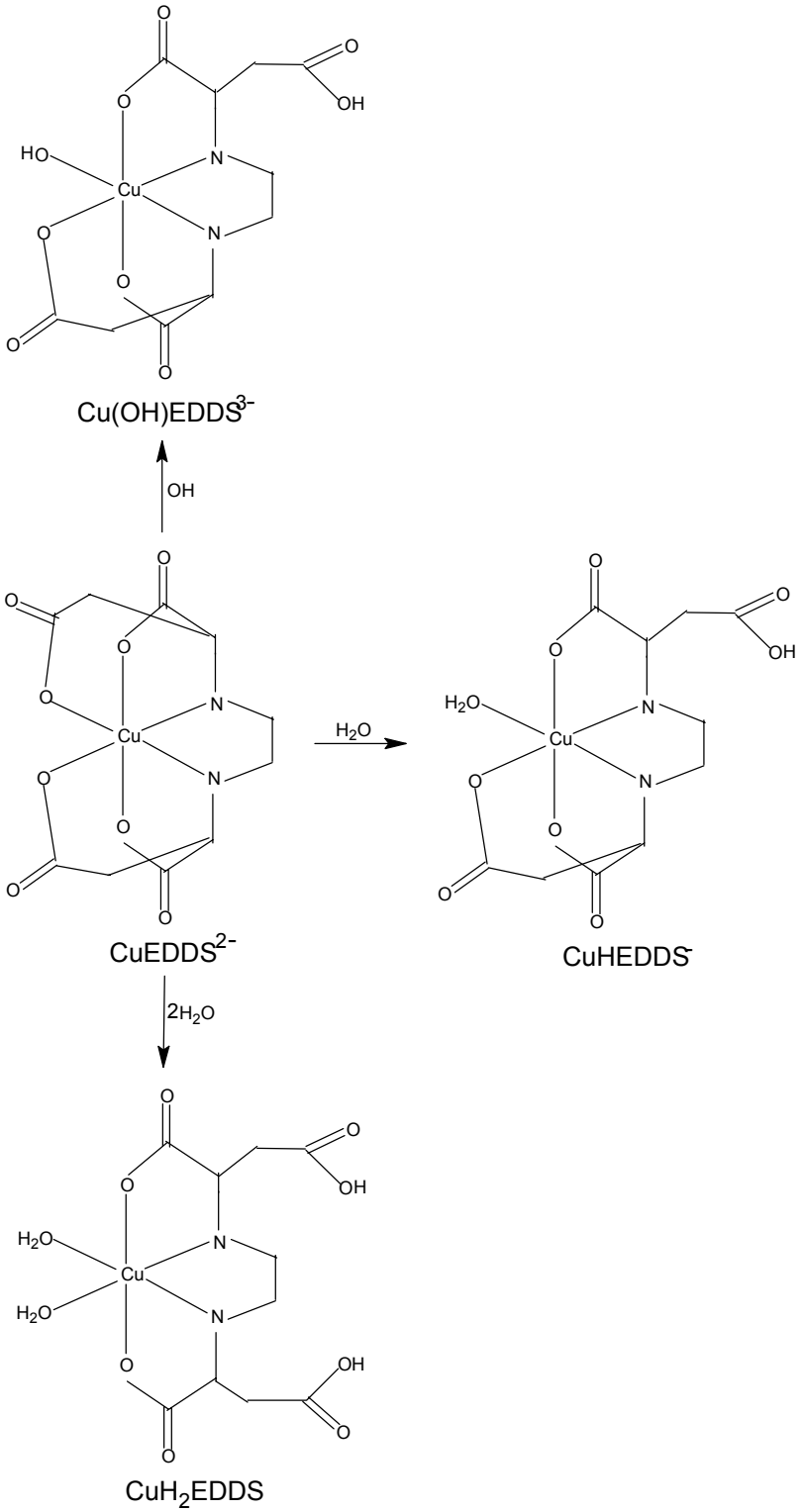

Figure 3.7: Possible structures of CuEDDS complexes in aqueous media.

A relatively sharp peak of CuEDDS was observed at pH 7. Figure 3.8 shows a graph of the peak areas of the CuEDDS complex. The results illustrated a stable behaviour of the complex peak over a period of 51 hrs. There was a formation of a small new peak at 46.25 hrs. The analysis revealed differences in the peak shape and size of CuEDDS from the one seen at pH 9.

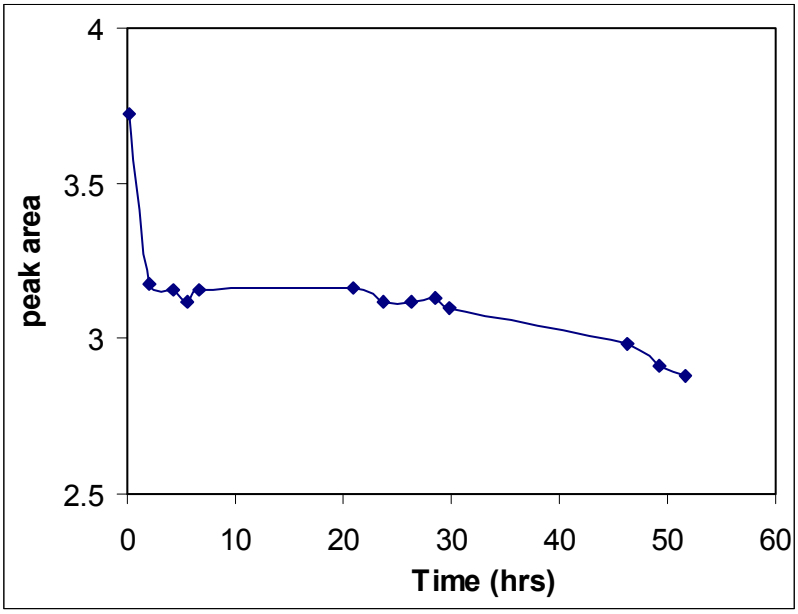

Figure 3.8: CuEDDS peak area as a function of time at pH 7.

CE analysis of CuDTPA

Figure 3.9A shows the electropherograms of 2 mM CuDTPA complex and a graph, where the corrected peak areas were plotted vs the time intervals. This is because DTPA forms inert complexes with most metal ions. There was an increase in the peak areas of CuDTPA complex and an upward trend of the curve was observed. The most likely species to be present in aqueous media between pH 1-10 are CuH_3DTPA, CuH_2DTPA, $CuHDTPA^{2-}$ and $CuDTPA^{3-}$. The structure of $CuDTPA^{3-}$ is given in Figure 3.10. Its speciation profile shows that it is present between pH 6-10. According to Xie and Tremaine [3], CuDTPA complexes reflect the efficient wrapping of the charged ligand around the metal ion and do not contain coordinated water. The time study revealed

CuDTPA as a stable complex at pH 9 over a period of 50 hours and a sharp peak was observed.

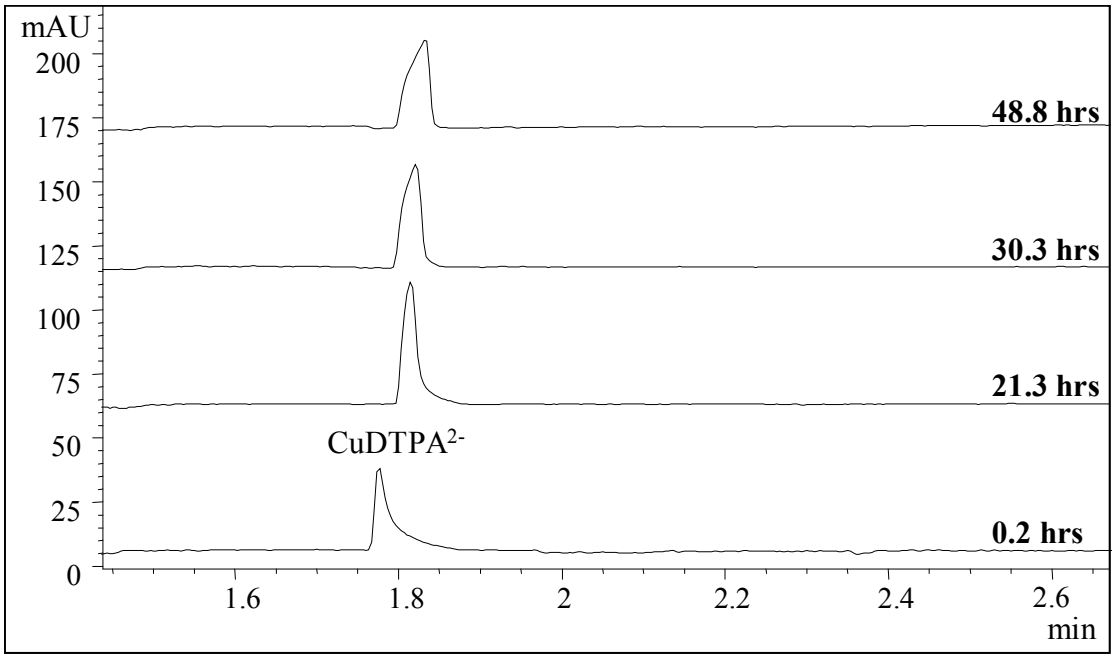

Figure 3.9A: Electropherograms of 2 mM CuDTPA monitored at various time intervals (hours). Conditions same as in Fig. 3.1A.

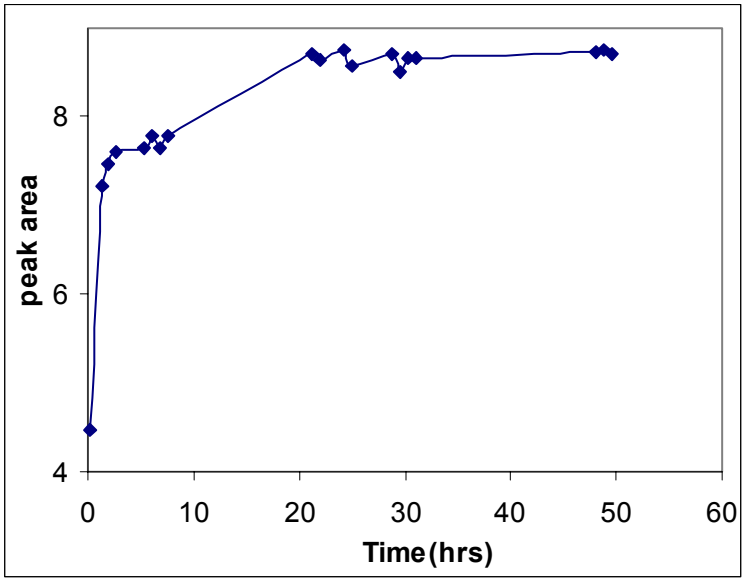

Figure 3.9B: CuDTPA peak area as a function of time at pH 9.

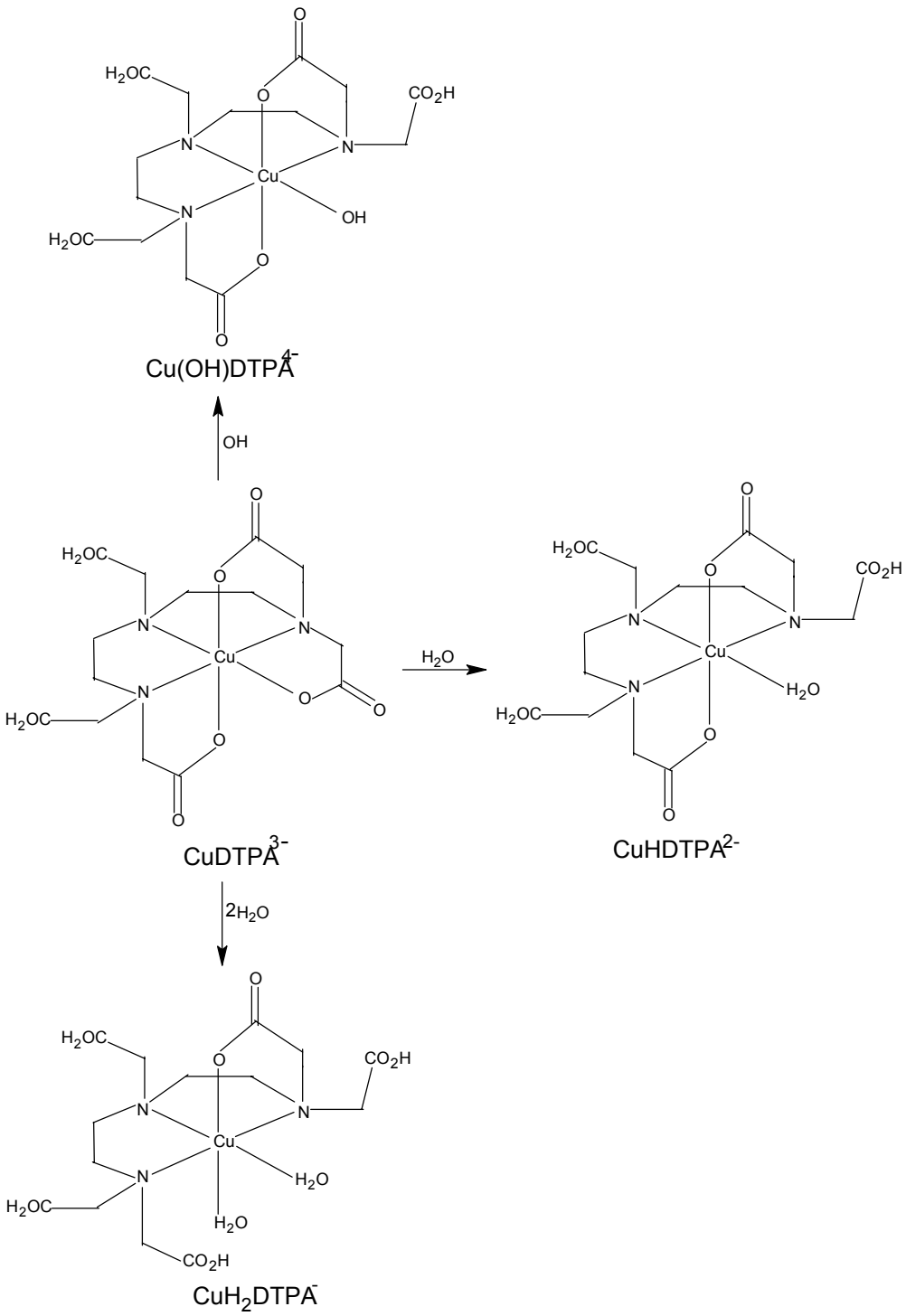

Figure 3.10: Possible structures of CuDTPA complexes in aqueous media.

A different behaviour was observed when the pH was decreased 7. CuDTPA exhibited a relatively sharp tailing peak and its peak areas decreased when monitored over a period

of 49 hours (Fig 3.11). The formation of a new unknown peak at was seen at 28 hours and speciation studies suggest the formation of protonated species. The complex seems to be stable and predominant at pH 9 as compared to pH 7.

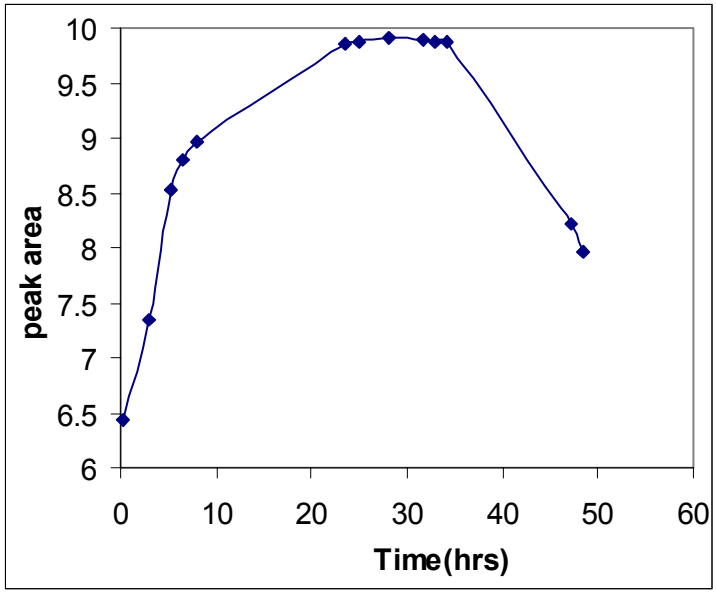

Figure 3.11: CuDTPA peak area as a function of time at pH 7.

3.3.1.2 Determinations of various metal-ligand complexes by CE

A similar approach was taken in all subsequent determinations of other metal ligand complexes such as CdL, PbL, ZnL, CrL, FeL and MnL at pH 9 and 7. The results obtained by CE are discussed briefly in the text.

Time analysis study of IDS complexed with Cd, Pb, Zn, Cr, Fe and Mn

The electropherograms of CdIDS, CrIDS and MnIDS at different time intervals showed a small broad peak for MIDS complexes. Many unknown peaks were also observed. There was a decrease in the corrected peak areas of CdIDS, CrIDS and MnIDS as time progressed. A stable behaviour was seen in the case of PbIDS complex when monitored for 52 hours. No peaks were observed for FeIDS and ZnIDS at pH 9. This is because they

complex less with IDS and also at high pH levels they form hydroxyl species thus making it difficult for analysis. Their rate constants are given in Table 3.2 (see supplementary information).

Time analysis study of R,S-IDS complexed with Cd, Pb, Zn, Cr, Fe and Mn

Complexes for CdR,S-IDS, FeR,S-IDS, MnR,S-IDS and ZnR,S-IDS did not show any ML peaks when studied for more than 50 hours by CE. This could be due to their low stability and labile behaviour when complexed with R,S-IDS at high pH. CrR,S-IDS and PbR,S-IDS exhibited small and unknown peaks over a period of 52 hours. Their peak areas revealed a downward trend during the period of study indicating the degradation of ML complexes.

Time analysis study of EDDS complexed with Cd, Pb, Zn, Cr, Fe and Mn

A small sharp peak was evident for the analysis of PbEDDS and ZnEDDS complexes. The complexes were stable for a period of 51 hours. While CdEDDS, CrEDDS and FeEDDS showed small peaks and decreased as function of time. MnEDDS displayed upward stable trend behaviour for the first 48 hours when analyzed for 50 hours. The supplementary information illustrates the rate constant for various MEDDS complexes.

Time analysis study of DTPA complexed with Cd, Pb, Zn, Cr, Fe and Mn

The PbDTPA complex showed a similar behaviour to CuDTPA as a stable upward curve was seen for its peak areas throughout the study. This demonstrates that Cu and Pb ions are indeed stable when complexed with DTPA at high pH levels. FeDTPA and MnDTPA were monitored for 50 hours. The complexes illustrated a stable behaviour within 45 hours and decreased after 48 hours. A decrease with time was observed for CdDTPA, CrDTPA and ZnDTPA. Unknown peaks were also seen in their electropherograms.

Time analysis study of L (IDS, R,S-IDS, EDDS and DTPA) complexed with Cd, Pb, Zn, Cr, Fe and Mn at pH 7

CdEDDS and CdIDS peaks could only be detected within 9 hours of the time period of 50 hours. Whereas CdDTPA showed a decrease in its peak areas as time progressed and no peaks were observed for CdR,S-IDS. PbL and ZnL decreased as time progressed during the analysis. This shows the instability of PbL and ZnL complexes at pH 7 as compared to pH 9. For example PbIDS and PbR,S-IDS could only be seen within 5 hours of the analysis time. In the case of CrL, FeIDS, FeR,S-IDS, MnEDDS and MnDTPA, there was also a decrease in its peak areas over a period of time. FeDDS and FeDTPA showed an upward trend and stable behaviour when monitored for 50 hours at pH 7. A very small peak was evident for MnIDS and it was very difficult to analyse the complex while peaks for MnR,S-IDS were not seen.

3.3.2 Kinetic data of Cu-ligand complexes.

The kinetic behaviour of CuL complexes was also investigated from the obtained electropherograms. A metal ion (M) and ligand (L) interact to form a reaction that is capable of proceeding to 1:1 metal-ligand (ML) complex. The general reaction could be expressed as shown in the scheme below (charges are omitted). A reaction will either follow a first or second order reaction depending on the type of metal ion and ligand. ML complexes tend to dissociate into hydrides and hydroxy complexes at various pH levels i.e. in acidic or alkaline media. In acidic medium ML tends to favour protonated ML complexes and at alkaline media hydroxy species are evident. Therefore MLH, MLH_2 and MLOH are assumed to be in rapid equilibrium with ML but in this study they were not always observed.

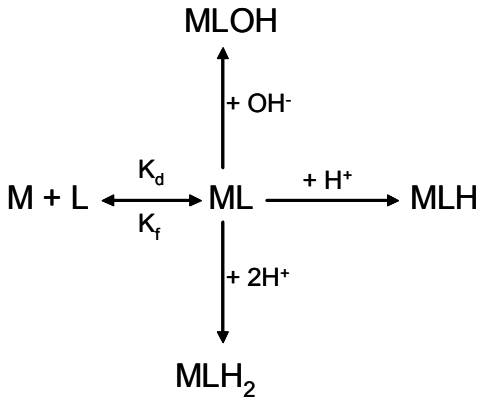

Scheme 3.1: General reaction of ML complexes

The reaction rate is defined as $Rate = \frac{k_d}{k_f}$, where k_d is the dissociation constant and k_f is the formation constant. Therefore, the kinetic dissociation rate of reaction can be expressed as given in equation 3.1,

$$Rate = \frac{\Delta[ML]}{\Delta t} = k[ML]^n \qquad [3.1]$$

where $[ML]$ is the concentration of ML complex in solution, t is the reaction time, k is the rate constant and n is either 1 or 2 for a first or second order reaction. The general derivation is as follows:

$$\frac{d[ML]}{dt} = k[ML]^n, \qquad [3.2]$$

once n is known, apply the appropriate equation that is ,

$$\frac{d[ML]}{dt} = k[ML],$$

for first order and we then rearrange this to give

$$\frac{d[ML]}{[ML]} = kdt, \qquad [3.3]$$

then integrate from time = 0 to time = t,

$$\int_{[ML]_0}^{[ML]_t} \frac{d[ML]}{[ML]} = k\int_0^t dt, \qquad [3.4]$$

rearrange to give

$$\ln \frac{[ML]_t}{[ML]_0} = kt \text{ or } \log \frac{[ML]_t}{[ML]_0} = \frac{kt}{2.303} \qquad [3.5]$$

$[ML]_t$ is the concentration at time t and $[ML]_0$ is the initial concentration of $[ML]$ that is the concentration at t = 0.

The rate constants of CuL complexes were determined by first and second order kinetics and their values are given in Table 3.1. Two graphs were plotted, i.e. log [area] vs time and 1/[area] vs time to determine the most linear graph for CuEDDS complex at pH 9. Figure 3.12 illustrate a plot of 2 mM CuEDDS and the rate of dissociation is the value of the slope. A first order reaction with corresponding rate constant for individual complexes was obtained from a linear relationship between log [area] and time. For a second order a plot 1/ [area] against time was used. At pH 9 values of the rates of dissociation of the complexes were found to decrease in the order of CuDTPA > CuIDS> CuEDDS > CuR,S-IDS. Rates of CuDTPA and CuIDS were higher than k_{CuEDDS} and $k_{CuR,S-IDS}$ indicating that they dissociate faster. This was also in agreement with the obtained CE results as both complexes showed an increase in peak areas at the beginning of the time study. The results from the time analysis experiments showed a complicated behaviour for CuDTPA at high pH.

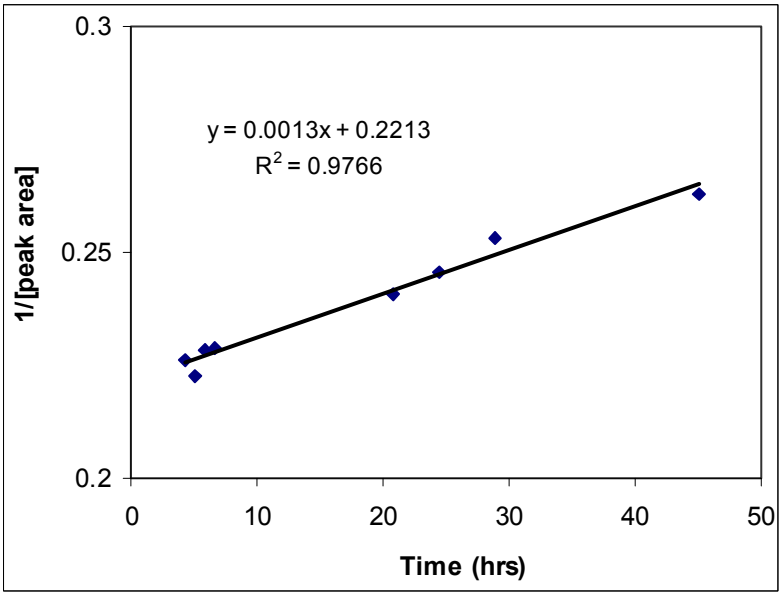

Figure 3.12: CuEDDS 1/[peak area] as a function time at pH 7.

Table 3.1: Rate constants of CuL complexes at pH 9 and 7.

Complex type	pH	1st order rate constant (s^{-1})	2nd order rate constant mol/(L.s)
CuIDS	9		1.9×10^{-3}
	7		7.0×10^{-4}
CuR,S-IDS	9		2.0×10^{-4}
	7	1.7×10^{-3}	
CuEDDS	9		1.3×10^{-3}
	7		8.0×10^{-4}
CuDTPA	9	2.5×10^{-3}	
	7		4.0×10^{-4}

3.4 Conclusion

The results obtained show the importance of the use of a method like CE for the time analysis study of chelating agents with metals. This is because CE is non intrusive on the equilibrium of metal ligand complexes and it is also possible to monitor the equilibrium species over a longer period of time. New peaks were observed in some ML complexes when the pH was changed from pH 9 to 7. Sharp peaks were seen for CuL, FeDTPA and FeEDDS at both pH levels, while small broad peaks were observed for FeIDS, CrL and MnL complexes. CuDTPA and CuEDDS complexes showed a great stability over time and this agreed well with the literature in terms of the inertness of the complex. It was difficult to assign peaks for some ML complexes, for e.g. in the case of CrL complexes. This problem can be resolved by using CE-MS as an analysis tool.

The rates of dissociation for various complexes based on CE results were determined. Higher rates were observed for CuDTPA and CuIDS as compared to CuEDDS and CuR,S-IDS at pH 9. The results also showed a strong pH dependence of all the

investigated metal ligand complexes. The information obtained will also give an idea of the eventual fate and behaviour of various complexes in aqueous media.

Bibliography

[1] Vasilèv V.P, Katrovtseva A.V, Bychkova S.A, Tukumova N.V, ***Russian Journal of Inorganic Chemistry***, 1998, 43, 731-732.

[2] Hyvönen H, Orama M, Saarinen H, Aksela R, ***Green Chemistry***, 2003, 5, 410-414.

[3] Xie W.W, Tremaine P.R, ***Journal of Solution Chemistry***, 1999, 28, 291-325.

Supplementary information

Table 3.2: Rate constants of ML complexes at pH 9 and 7.

Complex type	pH	1st rate constant	2nd rate constant
CdIDS	9		3.4×10^{-3}
	7		6.19×10^{-2}
CdR,S-IDS	9	ND	
	7		6.0×10^{-4}
CdEDDS	9		1.48×10^{-2}
	7		8.0×10^{-4}
CdDTPA	9		4.0×10^{-4}
	7	1.66×10^{-2}	
CrIDS	9		1.0×10^{-2}
	7		3.0×10^{-3}
CrR,S-IDS	9		6.0×10^{-4}
	7	2.9×10^{-3}	
CrEDDS	9	2.2×10^{-2}	
	7		
CrDTPA	9	4.7×10^{-3}	
	7		5.0×10^{-4}
FeIDS	9	ND	
	7		7.0×10^{-4}
FeR,S-IDS	9	ND	
	7		1.6×10^{-3}
FeEDDS	9	6.6×10^{-3}	
	7		5.0×10^{-4}

FeDTPA	9		1.0×10^{-4}
	7		2.0×10^{-4}
MnIDS	9		7.8×10^{-3}
	7	ND	
MnR,S-IDS	9	ND	
	7	1.7×10^{-3}	
MnEDDS	9		1.6×10^{-3}
	7		5.3×10^{-3}
MnDTPA	9		9.0×10^{-5}
	7		3.1×10^{-3}
PbIDS	9		2.0×10^{-4}
	7	1.7×10^{-3}	
PbR,S-IDS	9		6.0×10^{-4}
	7	1.0×10^{-1}	
PbEDDS	9		1.3×10^{-3}
	7	1.92×10^{-2}	
PbDTPA	9	2.3×10^{-3}	
	7		1.86×10^{-2}
ZnIDS	9	ND	
	7	4.5×10^{-3}	
ZnR,S-IDS	9	ND	
	7	1.3×10^{-3}	
ZnEDDS	9		9.0×10^{-4}
	7		7.0×10^{-3}
ZnDTPA	9		1.0×10^{-4}
	7		2.43×10^{-2}

ND – Not detected.

Chapter 4

Influence of metal catalysed redox processes on speciation of metal complexes

4.1 Introduction

Capillary electrophoresis was utilized with direct UV detection for the separation of Cu^{2+}, Cr^{3+}, Fe^{3+}, Mn^{2+} and Pb^{2+} metal ions complexed with chelating agents, namely iminodisuccinic acid (IDS), ethylenediaminedisuccinic acid (EDDS) and ethylenediaminetetraacetic acid (EDTA). The effect of background electrolyte parameters such as electrolyte nature, pH and concentration on the electrophoretic behaviour of metal complexes was investigated and discussed. A mixture of two of Good's buffers i.e. 2-(N-morpholino)ethanesulfonic acid monohydrate (MES) and 3-morpholino-2-hydroxypropanesulfonicacid (MOPSO) was selected as the running buffer because of the non-complexing effects opposed to tetraborate buffer. All metal complexes were determined within 5 minutes, when –25 kV was applied across 50 μm i.d. × 50 cm long narrow fused silica capillary. A clear resolution was seen for metal-EDTA complexes compared to metal-EDDS and metal-IDS complexes.

4.2 Experimental Details

4.2.1 Instrumentation

All separations were performed with an HP CE instrument as reported before in chapter 2 section 2.2.1. Absorbances were monitored at 215 and 235 nm for the detection of analytes. The pH of solutions was measured with a Jenway 4330 pH meter. All experiments were conducted at 25 °C.

4.2.2 Reagents and solutions

Deionised water passed through a MilliQ water purification system with a resistivity of 18 MΩ·cm was used throughout the experiments. All chemicals were of analytical reagent grade. Baypure CX 100 (IDS) was a gift from Bayer, S,S-Ethylenediamine-N,N'-disuccinic acid trisoduim salt solution (EDDS) was purchased from Fluka (Buchs, Switzerland), Ethylenediaminetetraacetic acid disoduim salt dehydrate (EDTA) and all metal nitrate stock standard solutions were obtained from Sigma-Aldrich (Steinheim, Germany). 2-(N-morpholino)ethanesulfonic acid monohydrate (MES), 3-morpholino-2-hydroxypropanesulfonicacid (MOPSO) and tetradecyltrimethylammonium bromide (TTAB) were purchased from Sigma-Aldrich (Steinheim, Germany). 0.1M of HCl and NaOH were used to adjust the pH of buffers and samples. Metal-ligand complexes were prepared by mixing metal stock solutions with a ligand. The background electrolytes were prepared daily from various buffers and their compositions are mentioned in the text. TTAB was used as an EOF modifier and thiourea as a neutral marker for CE analysis. The electrolyte and samples were sonicated and filtered through a 0.45-µm membrane filter prior to use.

4.2.3 Procedure for Electrophoresis

The bare fused silica capillary was rinsed with 0.1 M NaOH for 10 minutes, then with deionized water for another 10 minutes and equilibrated with the appropriate buffer solution for a further 10 minutes. Between each injection the capillary was filled with the buffer solution by flushing the entire capillary for 5 minutes. The sample solution was introduced into the anodic end of the capillary by hydrodynamic injection (50 mbar, 2 s). A voltage of –25 kV was then applied for separation.

4.3 Results and Discussion

This work examined the use of CE for the analysis of five mixed metal complexes of IDS, EDDS and EDTA using various background electrolyte (BGE) buffer systems. Speciation profiles of most metal-ligand (ML) complexes studied showed stability in the

pH range of 4-9 [1, 2], therefore the chosen pH levels for this work was within this range. The best separations were observed when a 5 mM of ligand was added to the BGE for either MES or MOPSO buffers. The addition of TTAB reverses the direction of EOF [3] so that there is a flow towards the detector and these results in shorter migration times for negatively charged complexes. TTAB has an added advantage of occupying reactive silanol sites within the capillary that may be occupied by metal ions or free chelating agents under investigation. The obtained CE results are discussed below.

4.3.1 Separation of MIDS (M = Cu^{2+}, Cr^{3+}, Fe^{3+}, Mn^{2+} and Pb^{2+}) complexes

IDS is a medium strength chelating agent for metal ion (shown in Table 2.1) as compared to EDDS and EDTA. The separation of metal-IDS by CE is based on differences in their own electrophoretic mobilities of the analytes. These complexes have similar structure and size and as a consequence very similar electrophoretic mobilities [4]. The separation of a mixture of metal chelates is often difficult especially for equally charged metal ions that form complexes with the same stoichiometry. In this case, there is only a small difference in the ratio of charge to radius, which results in nearly identical electrophoretic mobilities of the complexes [4]. Separation selectivity of these complexes is normally very poor in the CE mode [5].

Initially, tetraborate buffer at pH 9 was employed in an attempt to separate a mixture of metal-IDS complexes. The CE results exhibited broad peaks and most of the complexes co-migrated. Methanol was added to the running buffer in order to improve the separation selectivity but poor separation were also observed. Another set of buffers recommended by Good as non-complexing, i.e. MES and MOPSO were further investigated [6]. These buffers have been used extensively in studying the speciation of metal ions in natural waters [7, 8]. Electroanalytical studies by Soares et al showed that MES, MOPS and MOPSO are suitable pH buffers for the determination of metal ions as they do not complex with the metals [9].

Figure 4.1 illustrates an electropherogram of a mixture of metal-IDS complexes that consisted of 0.5 mM Cr^{3+}, Mn^{2+}; 0.25 mM Pb^{2+}; 0.1 mM Cu^{2+}, Fe^{3+} with 3 mM IDS was

analysed using 5 mM IDS in 25 mM MES and 0.25 mM TTAB at pH 6.5 as the running buffer. The addition of the ligand in the running buffer improved the separation of the ML complexes because an excess of ligand promotes equilibrium of various metal ions in the sample. This improvement was also observed by Kubáň [10] et al. These peaks were assigned as IDS, MnIDS, Pb/CrIDS and Cu/FeIDS complexes, respectively. Pb and Cr comigrated and this was also observed for Cu and Fe when determined by CE.

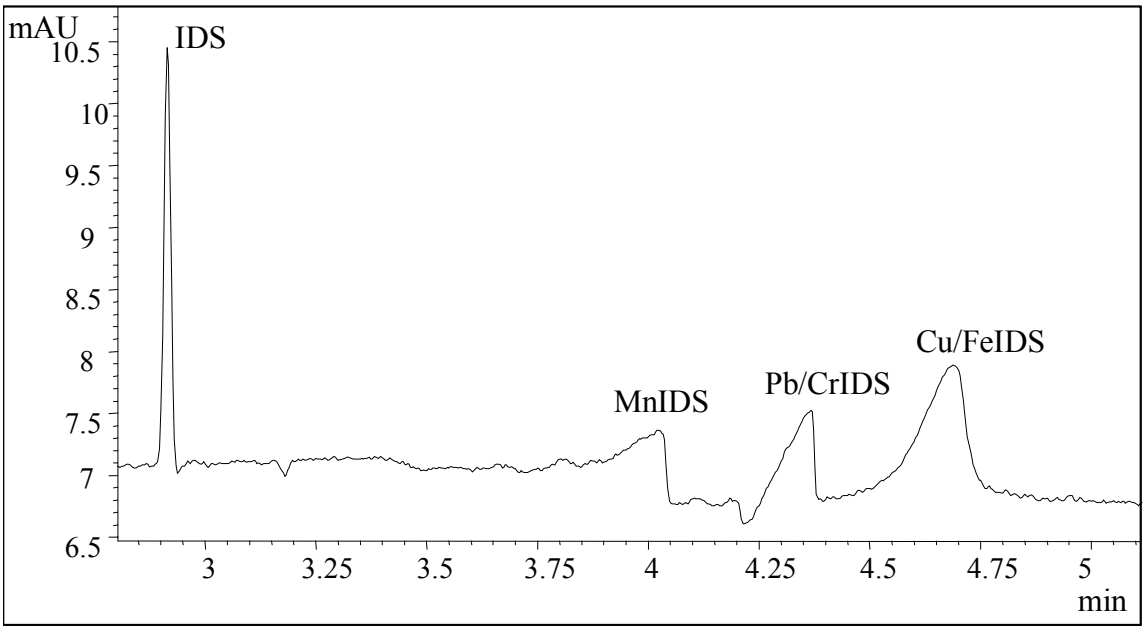

Figure 4.1: A typical electropherogram of five metal-IDS chelates at 235 nm. Conditions: 5mM IDS in 25mM MES and 0.25mM TTAB at pH 6.5 used as buffer, applied voltage -25 kV, temperature 25 ºC, hydrodynamic sample injection for 2 s applying 50 mbar pressure.

Competing influence of metals on metal-IDS complexes

A mixture of metal-IDS complexes was further spiked by different concentrations of individual standards. The electropherograms of a mixture spiked with Fe^{3+} standard is given in Figure 4.2. The addition of Fe^{3+} resulted in the increase of Cu/FeIDS peak while the MnIDS peak slightly increased. The increase in the Cu/FeIDS corrected peak areas might be due to the fact that Fe complex has a higher stability constant than CuIDS. A

change in PbIDS peak was not significant. This is observed in a plot of concentration versus corrected peak area of the MIDS mixture. Therefore Fe^{3+} will exchange or compete with Cu^{2+} for the ligand in the solution mixture as compared to other metal ions thus increasing its concentration. The exchange reactions could be explained as an exchange reaction of Fe^{3+} with CuIDS and can be described by the following equation:

$$Fe^{3+} + CuIDS^{2-} \Leftrightarrow FeIDS^{-} + Cu(OH)_2$$

The extent of exchange can be related to the metal ion IDS stability constants as listed in Table 2.1. FeIDS has a higher stability constant value than CuIDS and may also have the fast ligand exchange reaction with Cu.

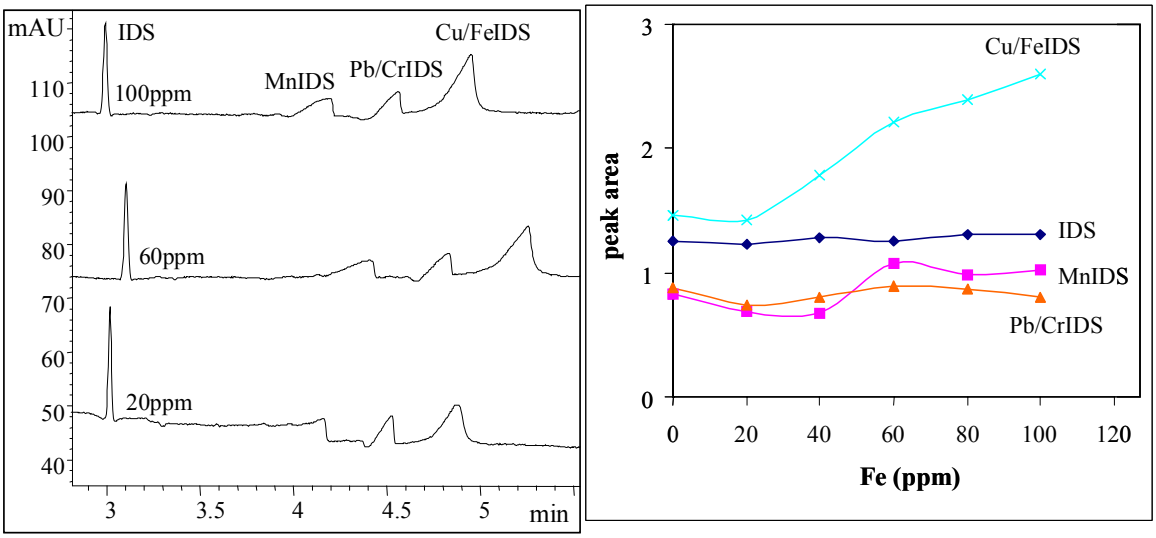

Figure 4.2: Electropherograms of five metal-IDS chelates spiked with Fe^{3+} and a graph of peak area as a function of Fe^{3+} concentration at 235 nm. Conditions same as in Fig. 4.1.

When Mn^{2+} was added to the mixture, there was a slight increase in the peak height of MnIDS complex. This is due to the competition of metal ions present in the mixture for IDS ligand, as seen in Figure 4.3. A plot of the corrected peak area is also shown in the figure and it is quite clear that a great change is not observed when Mn^{2+} is added to the mixture as compared to Fe^{3+}.

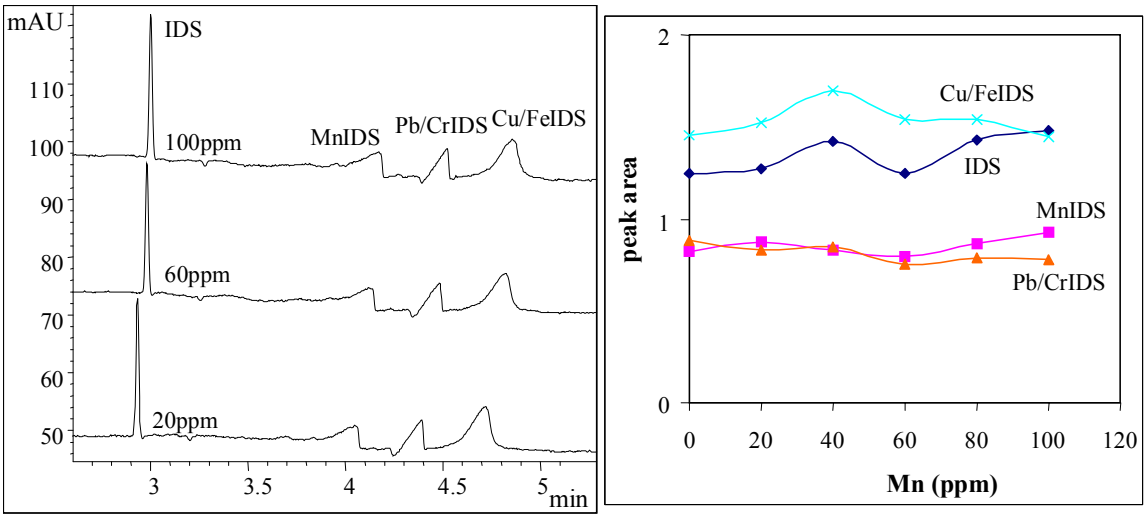

Figure 4.3: Electropherograms of five metal-IDS chelates spiked with Mn^{2+} and a graph of peak area as a function of Mn^{2+} concentration at 235 nm. Conditions same as in Fig. 4.1.

4.3.2 Separation of MEDDS (M = Cu^{2+}, Cr^{3+}, Fe^{3+}, Mn^{2+} and Pb^{2+}) complexes

In the case of MEDDS complexes, a preliminary investigation involved the use of tetraborate at pH 8.5 as the BGE for the separation. No separation was observed because all MEDDS complexes migrated closely and resulted as one peak. Figure 4.4 shows a simultaneous separation of MEDDS complexes attained in less than 3 minutes when using 5mM EDDS in 25mM MOPSO and 0.25mM TTAB at pH 7. CrEDDS and Cu/FeEDDS peaks managed to separate, though it was not possible to separate Cu-and FeEDDS as they comigrated. The order of elution was MnEDDS > PbEDDS > CrEDDS > CuEDDS = FeEDDS and did not follow the Irving-Williams order but followed their size to charge ratio and also their stability. The metalEDDS complexes with the lowest log K values migrated first as compared with Cu and Fe which are larger.

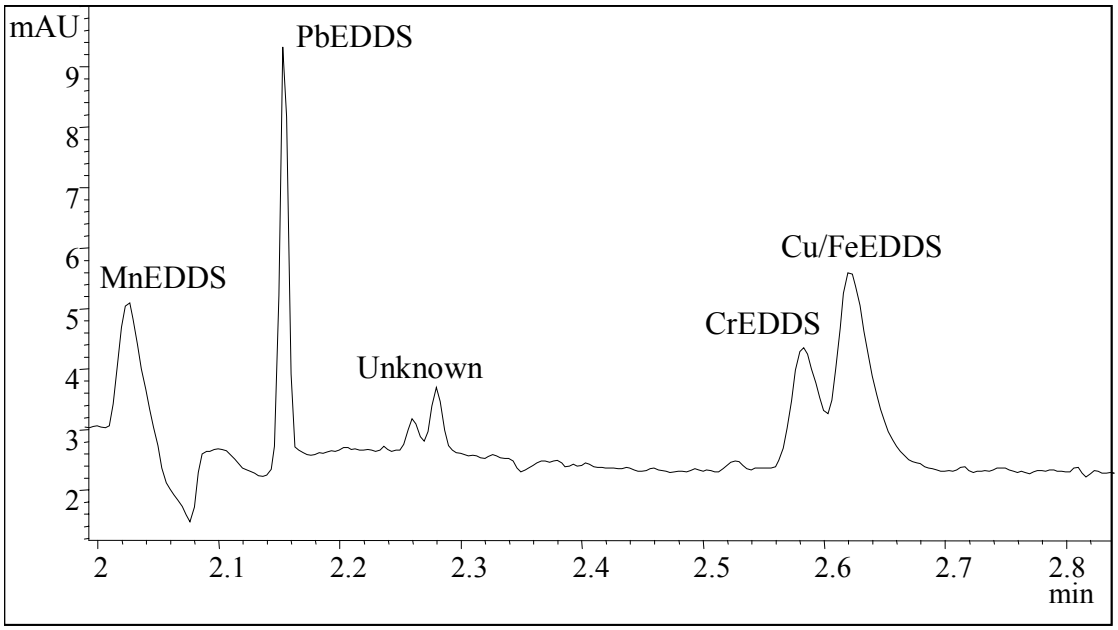

Figure 4.4: A typical electropherogram of five metal-EDDS chelates at 215 nm. Conditions: 5mM EDDS in 25mM MOPSO and 0.25mM TTAB at pH 7 used as buffer. Other conditions same as in Fig 4.1.

Competing influence of metals on metal-EDDS complexes

A clear increase in the peak height of Cu/FeEDDS is observed in the electropherograms when Cu^{2+} standard was added into the sample mixture (Figure 4.5). The other metal-EDDS peaks remained almost stable throughout the addition of Cu^{2+} standard. Therefore this suggests that Cu is stable in the mixture as compared to other metal ions. It is not clear at this stage as to what effect Cu^{2+} addition has on the FeEDDS complex since they both co-migrated and eluted at the same time. A slight replacement of Fe^{3+} by Cu^{2+} might have occured, when concentration of Cu^{2+} was much higher than Fe.

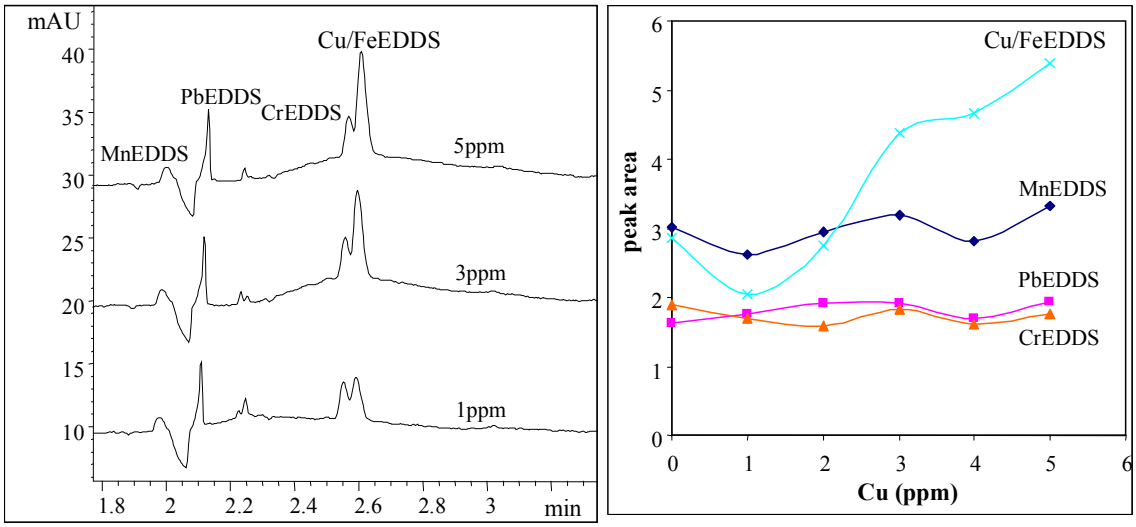

Figure 4.5: Electropherograms of five metal-EDDS chelates spiked with Cu^{2+} and a graph of peak area as a function of Cu^{2+} concentration at 235 nm. Conditions same as in Fig. 4.4.

Figure 4.6 illustrates a stacked electropherograms of a mixture of metal-EDDS complexes spiked with different concentrations of Pb^{2+} standard. An interesting behaviour was observed for the Cu/FeEDDS peak, i.e. there was a larger increase in its peak area while a slight increase was seen for PbEDDS. This might be due to Pb^{2+} reducing Cu^{2+} to Cu^{1+} in the CuEDDS complex, thus increasing its peak areas in the aqueous media at this pH. The electrochemical redox results from the previous work done in our group also support this and it is given in Table 4.1. These findings indicate that because PbEDDS has a much larger reduction potential than CuEDDS, it will always have a greater tendency to reduce it in the aqueous mixture.

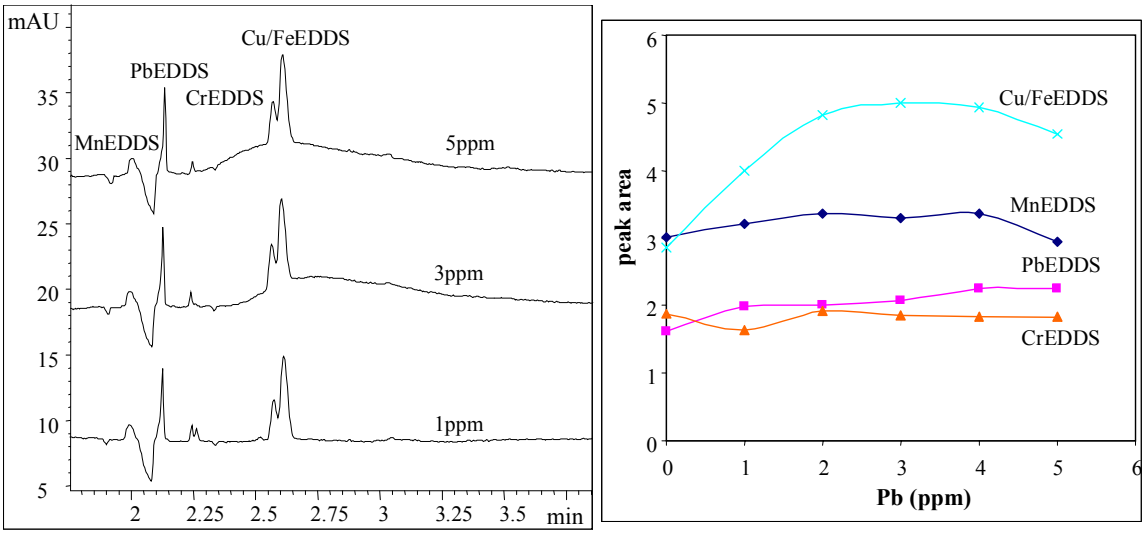

Figure 4.6: Electropherograms of five metal-EDDS chelates spiked with Pb^{2+} and a graph of peak area as a function of Pb^{2+} concentration at 235 nm. Conditions same as in Fig. 4.4.

Table 4.1: Reduction potentials determined by Cyclic Voltammetry of the ML complexes [1, 2].

Complex	Reduction potential (V)
CuEDTA	-0.50
PbEDTA	-1.50
ZnEDTA	-1.10
CdEDTA	-1.00
FeEDTA	0.12
CuEDDS	-0.60
PbEDDS	-1.60
ZnEDDS	-1.00
CdEDDS	-1.00
CdIDS	-1.47
CuIDS	-1.28
PbIDS	-1.34
ZnIDS	-1.53

4.3.3 Separation of MEDTA (M = Cu^{2+}, Cr^{3+}, Fe^{3+}, Mn^{2+} and Pb^{2+}) complexes

The separation of five metal complexes of EDTA is demonstrated in Figure 4.7 and a good resolution is observed. Chelates were resolved using 5 mM EDTA in 25mM MES and 0.25mM TTAB at pH 6.5 as the carrier electrolyte, and MEDTA complexes exhibited single sharp peak. Analyte identity was established by analysing the individual MEDTA complexes. The order of separation of a mixture of MEDTA complexes observed in this work was similar to that observed by Baraj et al [11], that is CuEDTA > PbEDTA > MnEDTA > CrEDTA > FeEDTA. Although their work was carried out using acetate and TTAB as a carrier electrolyte at pH 5.5. Baraj also experienced problems in separating Cu and PbEDTA complexes, but in the present work the two were resolved without increasing the total length of the capillary.

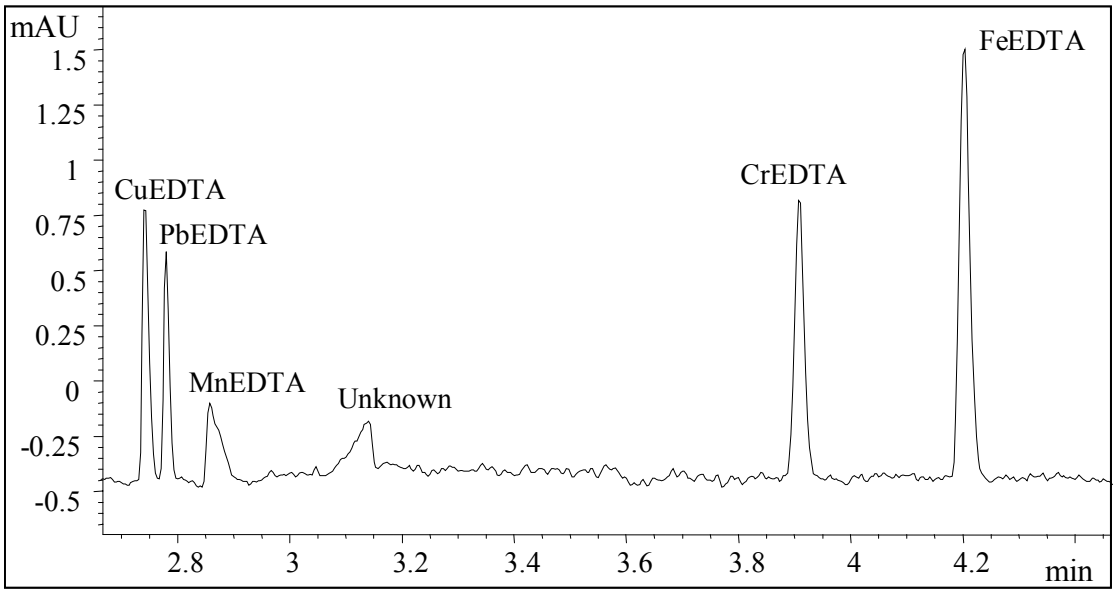

Figure 4.7: A typical electropherogram of five metal-EDTA chelates at 235 nm.
Conditions: 5mM EDTA in 25mM MES and 0.25mM TTAB at pH 6.5 used as buffer. Other conditions same as in Fig 4.1.

Competing influence of metals on metal-EDTA complexes

An increase in the peak height of CuEDTA complex was observed when various concentrations of Cu^{2+} standard solutions were added to the mixture as shown in Figure 4.8. A graph of corrected peak area vs concentrations of Cu^{2+} standard was plotted and a great increase of the peak areas was observed in CuEDTA and slightly in FeEDTA as the concentration of Cu increased. As a result of a competition between the ligand and the metal ions, the most stable metal-ligand complex will always be favoured in a mixture. This observation was based on the pH, concentration of metal and ligand, and also temperature. These results were expected because in natural waters EDTA is present almost exclusively in the form of metal complexes. Therefore, remobilization of metals is sometimes a metal-metal-EDTA exchange reaction [12]. A stable behaviour was observed for Mn, Cr and PbEDTA complexes, respectively.

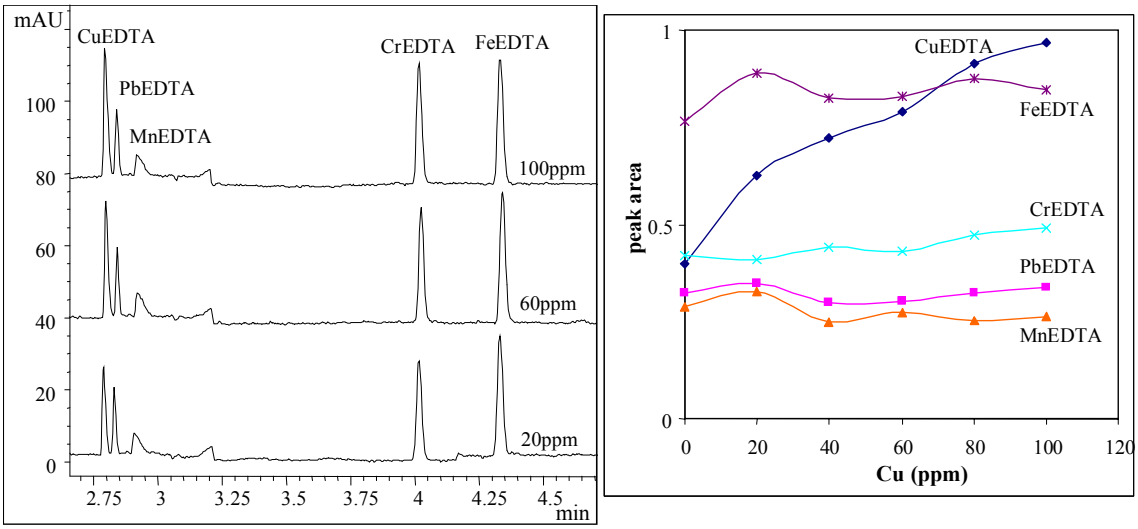

Figure 4.8: Electropherograms of five metal-EDTA chelates spiked with Cu^{2+} and a graph of peak area as a function of Cu^{2+} concentration at 215 nm. Conditions same as in Fig. 4.7.

Upon the addition of Pb^{2+} standard solution in the mixture, a gradual increase in the PbEDTA complex is observed. The complexes that also show an increase is FeEDTA and

CrEDTA. This indicates that Pb^{2+} has a tendency of reducing Fe^{3+} to Fe^{2+} as EDTA complex, thus an increase in its peak area (Fig. 4.9). The reduction takes place due to a difference in the stability constants of metal-EDTA complexes as well as the reactivity of the complexes.

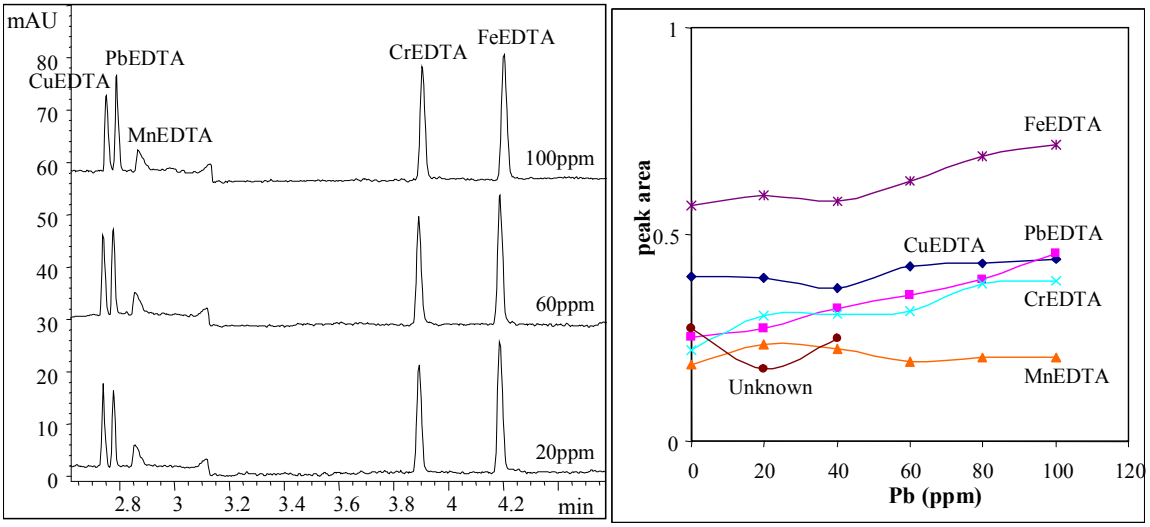

Figure 4.9: Electropherograms of five metal-EDTA chelates spiked with Pb^{2+} and a graph of peak area as a function of Pb^{2+} concentration at 215 nm. Conditions same as in Fig. 4.7.

A new peak for Fe^{2+}EDTA is not shown in the electropherogram because its migration time is the same if not very close as Fe^{3+}EDTA. This was proved by injecting individual Fe^{2+}/Fe^{3+}EDTA complexes and followed by injecting a mixture of both (Fig. 4.10). One peak was seen when the mixture of Fe^{2+}/Fe^{3+}EDTA was injected for CE analysis. However, under these conditions, injection of the Fe^{2+}/Fe^{3+}EDTA mixture resulted in a single sharp peak. The similar pattern was also observed by Schäffer et al [13]. They managed to separate the two peaks by selective separation only i.e. complexing Fe^{2+} with O-phenanthroline (O-phen) and Fe^{3+} with EDTA.

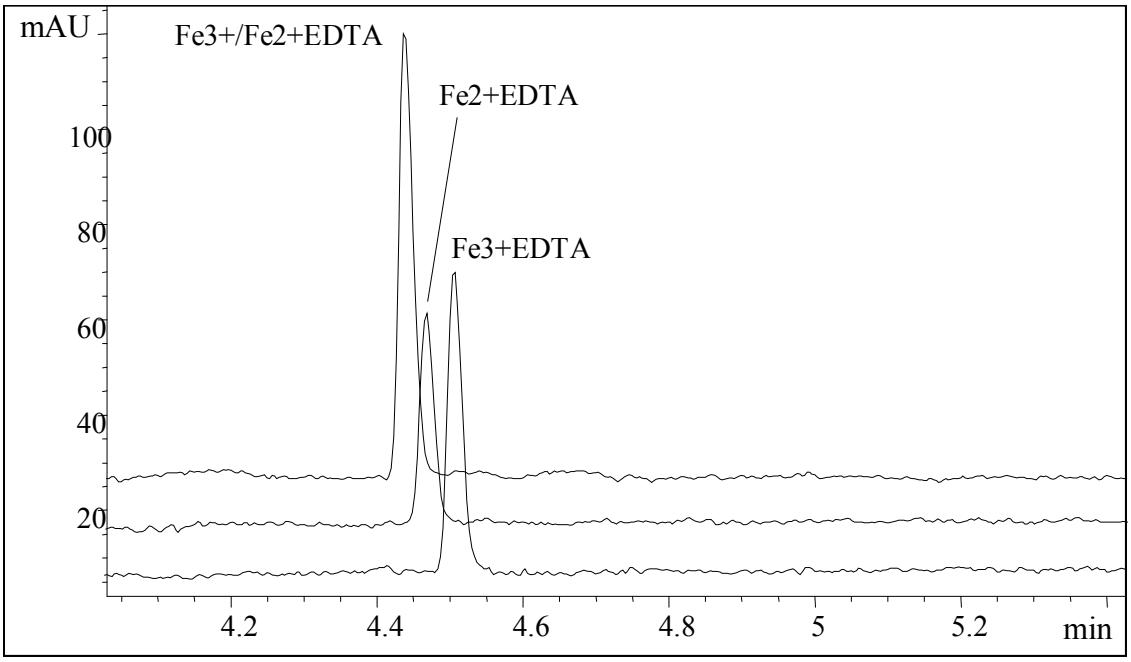

Figure 4.10: Electropherograms Fe^{2+}/Fe^{3+}EDTA individually and as a mixture. Conditions same as in Fig. 4.7.

The complexing agents O-phen and EDTA, involved in the developed method react selectively with Fe^{2+} and Fe^{3+} to form positively and negatively charged species, respectively. They also mentioned that Fe^{2+} and Fe^{3+} complexes can only be separated if one complex is positive and the other is negative.

4.4 Conclusion

This work demonstrated that it is possible to separate the metal-ligand complexes of readily biodegradable ligands utilizing capillary electrophoresis. CE also provided fast and fairly efficient separations for all ML complexes studied. MEDTA complexes showed better separations as compared to MEDDS and MIDS complexes. A longer capillary can be used for resolving Cu and Fe peaks of IDS and EDDS complexes which could not be separated. The importance of the selection of the background electrolyte in the analysis of metal-ligand complexes was also illustrated. Buffers with weak complex

properties (i.e. MES and MOPSO) are recommended for the separation of mixtures of metal complexes to avoid the competition of metal ions with buffers and the ligands used.

There influence of one metal complex on the presence of another was illustrated. This will depend on their relative redox potentials as listed in Table 4.1. The work also showed that the addition of a standard metal ion in a mixture of ML complexes does not necessarily mean that an increase in the ML complex will also increase. For instance in the case of where Pb is added in the mixture, it will either oxidize or reduce other ML complexes instead of simple exchange reactions.

Bibliography

[1] Khotseng L.E, PhD thesis, University of Stellenbosch, South Africa, 2004

[2] Katata L.M, MSc thesis, University of Stellenbosch, South Africa, 2001.

[3] Padarauskas A, Schwedt G, ***J. Chromatogr. A***, 1997, 773, 351-360.

[4] Inoue M.B, Inoue M, Muñoz I.C, Bruck M.A, Quintus F, ***Inorganic Chimica. Acta***, 1993, 209, 29.

[5] Gouin S.G, Gestin J.-F, Joly K, Loussouarn A, Reliquet A, Meslin J.-C, Deniaud D, ***Tetrahedron***, 2002, 58, 1131.

[6] Good N.E, Winget G.D, Winter W, Connolly T.N, Izawa S, Singh R.M, ***Biochemistry***, 1966, 5, 467.

[7] Xue H, Sigg L, ***Aquat.Geochem***, 1999, 5, 313.

[8] Rozan T.F, Benoit G, Marsh H, Chin Y.-P, ***Environ.Sci.Technol***, 1999, 33, 1766.

[9] Soares H.V.M, Conde P.L, Almeida A.N, Vasconcelos M.T, ***Anal. Chim. Acta***, 1999, 394, 325.

[10] Kubáň P, Kubáň V, ***J. Chromatogr. A***, 1999, 836, 75-80.

[11] Baraj B, Martinez M, Sastre A, Aguilar M, ***J. Chromatogr. A***, 1995, 695, 103-112.

[12] Gulzar S, Fatima N, Maqsood Z.T, ***J.Saudi.Chem.Soc***, 2005, 9 (1), 113.

Chapter 5

The effect of various electrophoretic flow modifiers and counter anions on the separation efficiency of APCAs (EDTA, EDDS and IDS) by CE

5.1 Introduction

The effect of various cationic electroosmotic flow (EOF) modifiers are represented in scheme 1 on the separation of aminopolycarboxylic acids (APCAs) as Cu(II) complexes was studied by capillary electrophoresis (CE) with on-column UV detection at 235 nm. Cu(II) was complexed with ethylenediaminetetraacetic acid (EDTA), *S*,*S* - ethylenediaminedisuccinic acid (EDDS) and iminodisuccinic acid (IDS) to form anionic complexes and analysis were achieved by reversing the EOF in the capillary. The behaviour of various modifiers was compared and the best results were observed when 0.3 mM of tetradecyltrimethylammonium bromide (TTAB) and cetyltrimethylammonium bromide (CTAB) was added to 40 mM tetraborate buffer (pH 6.00 with NaOH) in order to reverse the EOF in the fused silica capillary (50 cm × 50µm i.d) at an applied voltage of -25 kV. This resulted in short analysis time and better peak shapes. Reproducibility in migration times for TTAB and CTAB was 1.6 and 1.2 (R.S.D %). The effect of different counteranions in the EOF modifiers on the separation was also examined. It was also found that the counter anions of EOF modifiers used influences the separation parameters such as migration times, resolution and efficiency. It is hereby recommended that more attention should be paid to the selection of the counteranions.

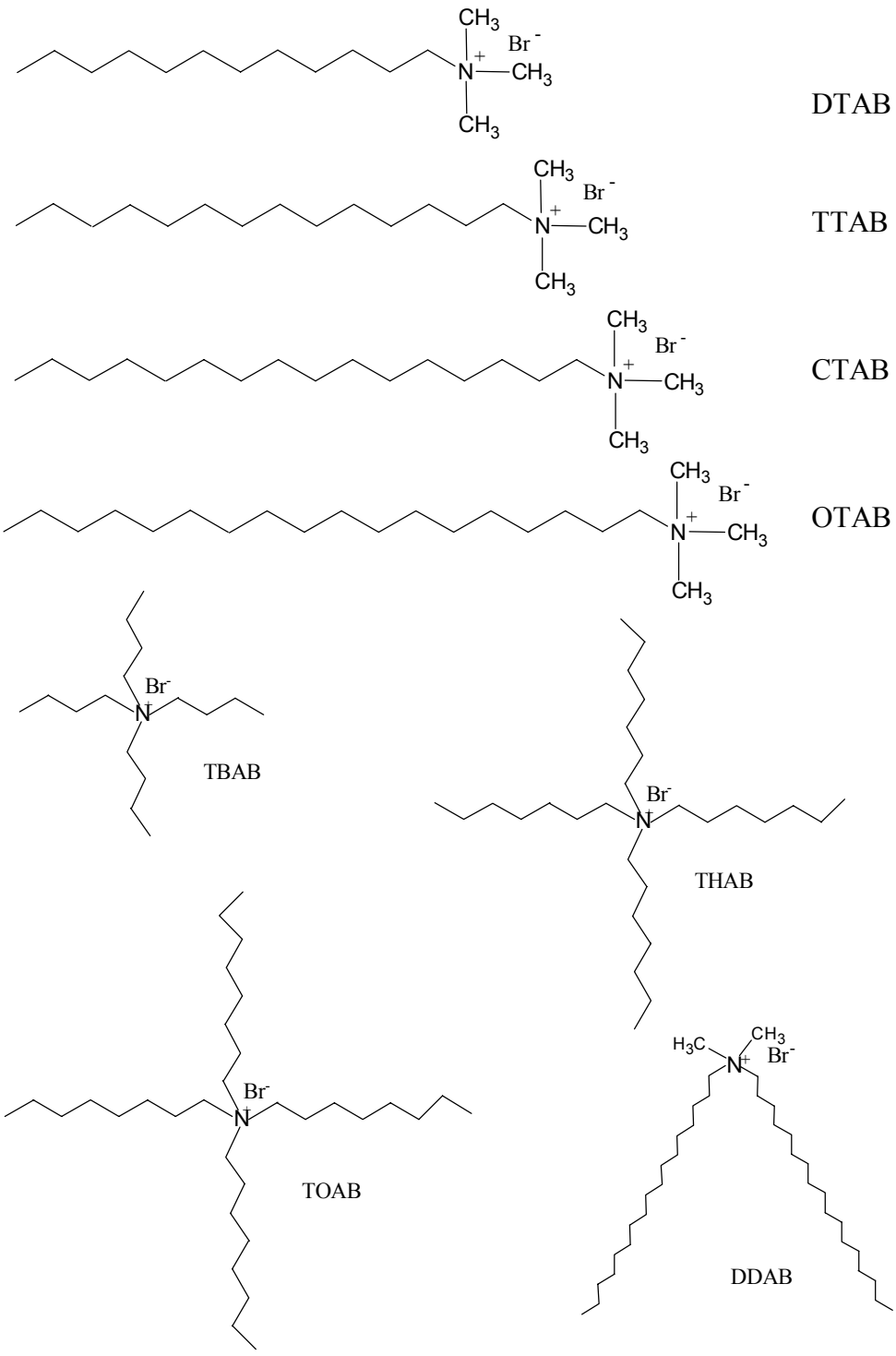

Scheme 5.1: Molecular structures of various cationic EOF modifiers used in the study

5.2 Experimental Details

5.2.1 Materials and reagents

Deionized water was prepared by passing distilled water through a Millipore (Bedford, MA, USA) Milli Q water purification system. All reagents were of analytical reagent grade unless stated otherwise. Copper(II) and Iron(III) nitrate standard solution, Dodecyltrimethylammonium bromide (DTAB), Octadecyltrimethylammonium bromide (OTAB), Tetraoctylammonium bromide (TOAB), Tetraheptylammonium bromide (THAB), Tetrabutylammonium bromide (TBAB), Cetyltrimethylammonium bromide(CTAB), tetradecyltrimethylammonium bromide (TTAB), Cetyltrimethylammonium chloride (CTAC), Hexadecyltrimethylammonium hydrogen sulfate (CTAHS), Tetradecyltrimethylammonium chloride (TTAC), Tetradecyltrimethylammonium hydrogen sulfate (TTAHS), Dimethyldioctadecylammonium bromide (DDABr), EDTA, 2-(N-morpholino)ethanesulfonic acid monohydrate (MES) and 3-morpholino-2-hydroxypropane-sulfonicacid (MOPSO) are obtained from Sigma–Aldrich (Steinheim, Germany). S,S′-EDDS, and Baypure CX 100 (IDS) were procured from Fluka (Buchs, Switzerland) and Bayer (Leverkusen, Germany), respectively. Disodium tetraborate decahydrate from Merck (Darmstadt, Germany) was used.

5.2.2 Instrumentation

5.2.2.1 Capillary Electrophoresis

All separations were performed with an HP CE instrument as reported before in chapter 2 section 2.2.1. The capillary cassette temperature was adjusted to 25 °C with air cooling. A separation potential of −25 kV was applied during all separations and samples were introduced by applying a 50 mbar pressure for 2 s. Absorbances at 225, 235 and 245 nm were monitored for the detection of analytes. The pH measurements were carried out with combined conductivity/pH meter (Jenway, UK) model 3880 equipped with a combined glass calomel electrode, which was calibrated using standard buffer solutions (Sigma–

Aldrich, Steinheim, Germany) of pH 4.0, 7.0 and 9.2 before measuring the pH of the solutions. 40 mM tetraborate buffer was prepared daily and used as the background electrolyte. Various surfactants and ionic liquids were used as EOF modifiers, while thiourea was used as a neutral marker for CE analysis. The electrolyte and samples were sonicated and filtered through a 0.45 μm PVDF membrane filter (Sigma–Aldrich, Steinheim, Germany) prior to use. 0.1 M of HCl and NaOH were used to adjust the pH of buffers and samples. All experiments were conducted at 25 °C.

The new bare fused silica capillary was rinsed with 0.1 M NaOH for 10 min, then with deionized water for another 10 min and equilibrated with the buffer solution for a further 10 min. In between each injection the capillary was filled with the buffer solution by flushing the entire capillary for 5 min. The sample solution was introduced into the anodic end of the capillary by hydrodynamic injection. A voltage of −25 kV was then applied for separation. After every fourth sample, the capillary was conditioned by flushing it with 0.1 M NaOH (5 min), ultra pure water (10 min) and BGE for 10 min to ensure that the capillary was in good condition throughout the sequence.

5.2.3 Analytical procedure

The standards were prepared from stock solutions of EDDS (20 mM), EDTA (20 mM), IDS (20 mM) and $Cu(NO_3)_2$ (10 mM) dissolved in background electrolyte (BGE) which consisted of 40 mM tetraborate buffer and various EOF modifier. Metal complex solutions were prepared by mixing the desired proportions of metal and appropriate complexing agents and diluting with the buffer. The pH of the sample was then adjusted to the same level as the electrolyte used. The buffer and samples were filtered through a 0.45 μm PVDF membrane filter. It was then directly injected into the CE system for analysis.

5.2.4 Calculations

Separation of CE parameters, i.e. resolution (Rs), efficiency (N) and migration times (t_m) were monitored and compared. Efficiency in terms of the number of the theoretical plates was found directly from an electropherogram using the following equation:

$$N = 5.54\left(\frac{t_m}{w_{1/2}}\right)^2$$

where t_m is the analyte migration time and $w_{1/2}$ is the peak width at half height. The resolution of two components in CE is determined in the same manner as in HPLC:

$$R_s = \frac{2(t_2 - t_1)}{w_1 + w_2}$$

where t_1 and t_2 are the migration times of first and second components and w_1 and w_2 are the baseline widths of peaks 1 and 2 respectively.

5.3 Results and Discussion

A brief theory of the use of surfactants as one way in controlling electroosmotic flow in CE is discussed briefly below. When a fused silica capillary is filled with the buffer, the surface silanol (SiOH) groups are ionized to negatively charged silanoate (SiO^-) groups catalyzed by the OH^- ions in the solution. The positive counter ions in liquid phase will compensate the negative charge of the wall so that an electrical double layer is created at the interface between solid wall and the liquid phase. An electric potential difference across the double layer is created and called the zeta potential. Under the external applied voltage along the capillary, the positive counter ions attracted to the negative capillary wall will move toward the cathode and form the electroosmotic flow (EOF). The EOF has a substantial influence on the time the analytes reside in the capillary.

Surfactants are molecules possessing both a hydrophilic and hydrophobic regions on their molecule. Interactions between surfactants and the surface of the fused silica CE capillary

are essential for control of electroosmotic flow (EOF). A schematic illustration of hemimicelles formation on the capillary wall is shown in Figure 5.1. Surfactants can play an important role in separations at concentrations below critical micelle concentration by acting as solubilizing agents for hydrophobic solutes or by functioning as ion-pairing reagents or as capillary surface modifiers. Cationic surfactants such as CTAB first adsorbs individually by electrostatic interactions and then begins to associate into hemimicelles forming a double layer on the surface of the fused silica by Van der Waals attraction [1], thereby reversing or slowing the direction of the EOF from anode to cathode when a negative potential is applied. The control of EOF is very important for improving the separation and shortening the analysis time of anions in CE.

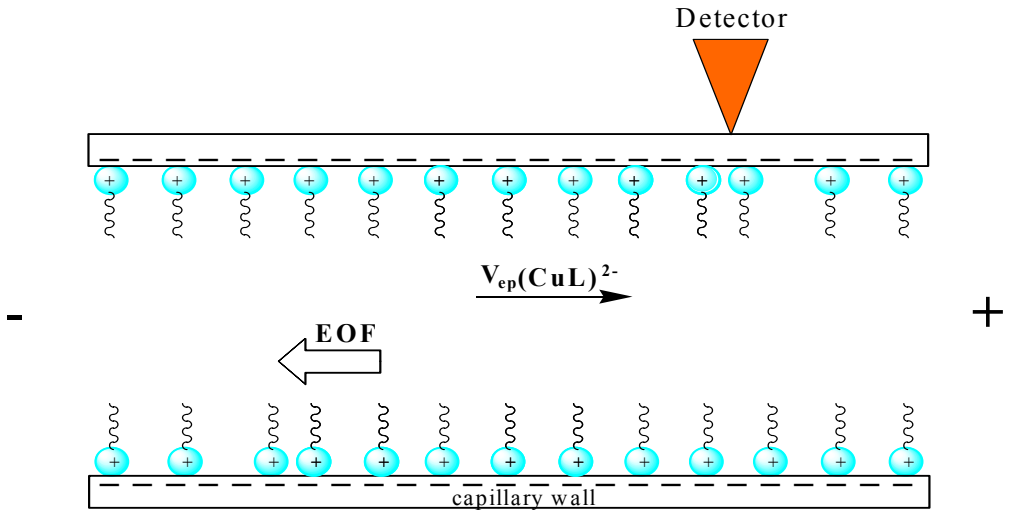

Figure 5.1: Schematic illustration of the adsorption of cationic EOF modifier on the capillary wall forming a hemimicelle layer.

5.3.1 Comparison of various cationic EOF modifiers

A mixture of 2-(N-morpholino)ethanesulfonic acid monohydrate (MES) and 3-morpholino-2-hydroxypropane-sulfonicacid (MOPSO) as a BGE was originally used for the separation of a mixture of APCAs (EDTA, EDDS and IDS) as Cu(II) or Fe(III) complexes at pH 5.5 using various EOF modifiers. On the basis of the previous studies

which was concerned the determination of Fe(III) complexes of IDS, EDDS and EDTA [2], the results obtained were not favourable as broad peaks and noisy backgrounds were observed for other modifiers, except for TTAB. The tetraborate as BGE was then further investigated for the analysis at various concentrations. Tetraborate buffer concentration was varied between 60 and 10 mM concentration at pH 6. Good separations were observed when 40 mM tetraborate as BGE was used and hence chosen for the separation of Cu(II) complexed with APCAs. In the case of Fe(III), EDTA and EDDS coeluted as one peak. Therefore, Cu(II) was chosen as the metal ion to complex APCAs used in our study. Poor resolution and peak shapes were seen at higher and lower tetraborate buffer concentration. The pH was also varied between 7 and 5 at a fixed buffer concentration of 40 mM tetraborate and 0.25 mM TTAB. At high pH levels above 6.5 resolution was poor for EDTA and EDDS complexes, while at low pH's no peaks were observed for CuL (L = EDTA, EDDS and IDS) complexes. Higher resolution peaks were seen when the pH was 6.

Eight cationic EOF modifiers i.e. DTAB, TTAB, CTAB, OTAB, TBAB, THAB, TOAB and DDABr were selected to study their effect on migration times, resolution and efficiency of CuL complexes. Low concentrations of all modifiers were varied over the range of 0.3-0.8 mM for all except for TBAB, THAB, TOAB and DDABr (varied between 0.03-0.08 mM). The concentration range studied for each modifier was selected in order to obtain the best efficiency of the separation i.e. short analysis time and good resolution. The concentration of the BGE was kept constant at 40 mM and pH level of 6 established earlier. The electrophoretic currents varied from -97 and - 140 μA. A detection wavelength of 235 nm was chosen for all measurements. The best separations were obtained at 0.3 mM and 0.03 mM concentration for the various modifiers. As the concentration increased the resolution was poor for TTAB, CTAB and OTAB even though the peaks were sharper. Figure 5.2 illustrates a typical CE electropherograms for CuL complexes when DTAB, TTAB, CTAB, OTAB and DDABr were utilised as EOF modifiers. A clear separation was seen for the obtained results except for OTAB. In the case of three ionic liquids used in this study i.e. TBAB, THAB and TOAB, the CE results obtained were not reproducible. Ionic liquids, sometimes referred to as molten salts, are

ionic substances with melting points at or close to room temperature. Ionic liquids consist of cations and anions and in distinction to an ionic solution they are only composed of ions. This is due to the bulkiness of the modifiers, thereby making it impossible to adsorb strongly on the capillary wall. The similar results were also observed by Galceran et al [3] when they compared different EOF modifiers for the analysis of inorganic anions. They found that the tetrabutylammonium (TBA^+) increased the EOF due to its bulky nature which prevented effective adsorption onto the capillary wall.

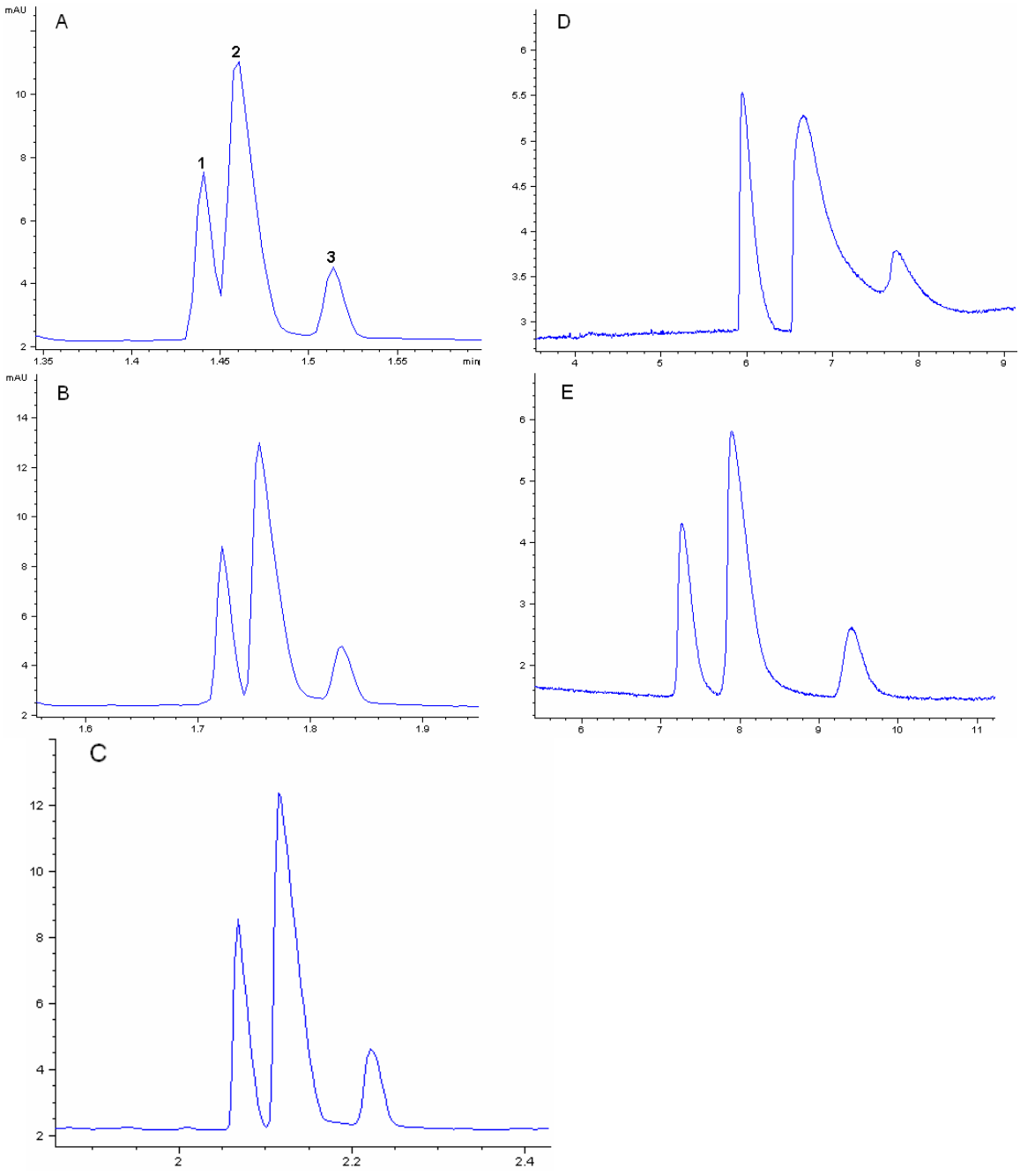

Figure 5.2: Electropherograms of CuL complexes (L = EDTA, EDDS and IDS) using various EOF modifiers. 3 mM IDS, 1 mM EDTA, EDDS, 6 mM Cu(II) was used as the sample. Peaks: (1) CuEDTA, (2) CuEDDS and (3) CuIDS. A. 0.3 mM OTAB, B. 0.3 mM CTAB, C. 0.3 mM TTAB, D. 0.03 mM DDAB, E. 0.3 mM DTAB. Conditions: 40 mM

tetraborate buffer and modifier at pH 6, applied voltage -25 kV, temperature 25 ºC, hydrodynamic sample injection for 2 s applying 50 mbar pressure, detection at 235 nm.

The strength of the dispersion interaction between the surfactant tails is dependent on the chain length, the longer the chain the stronger the interaction. Therefore it is expected that OTAB favours the assembly of the bilayer more effectively than DTAB, TTAB and CTAB, in this order slowing or reversing the EOF leading to faster migration times. This behaviour is clearly seen in Figure 5.2. Table 5.1 shows the obtained migration times of various EOF modifiers. The shortest migration time was obtained in OTAB, while the longest was in DTAB. This was expected, as shorter alkyl chains are less hydrophobic than longer ones and they form a less stable bilayer inside the capillary. Shorter and smaller ammonium bromides can roll over and do not form a balanced layer to assist the EOF reversal and separation of anionic analytes.

Table 5.1: The migration times of CuL complexes using various cationic EOF modifiers.

EOF Modifier	Migration times (min)		
	CuEDTA	CuEDDS	CuIDS
DTAB	7.26 (2.2)	7.88 (2.1)	9.42 (2.1)
TTAB	2.07 (1.4)	2.12 (1.0)	2.22 (1.6)
CTAB	1.72 (0.8)	1.75 (1.2)	1.83 (1.0)
OTAB	1.44 (0.4)	1.46 (0.4)	1.51 (0.6)
DDAB	5.94 (1.5)	6.64 (1.5)	7.73 (1.3)

Values in parenthesis are relative standard deviations (injected 4 times). Conditions: 40 mM tetraborate buffer and modifier at pH 6, applied voltage -25 kV, temperature 25ºC, hydrodynamic sample injection for 2s applying 50 mbar pressure, detection at 235 nm.

Overall, DTAB and DDAB gave the best resolution values for adjacent peaks, while CTAB gave the worst values (Table 5.2). This indicates that differences in resolution exist which means that a type of modifier affects selectivity under the present

experimental conditions. Two peaks (i.e. CuEDTA and CuEDDS), which coeluted in OTAB, were clearly resolved in DTAB and DDAB. It is worth noting that although DTAB gave the best resolved separation, the t_m values were longer than all modifiers. Long periods of time are normally not ideal or acceptable in routine analysis. Analysis of CuL complexes revealed that the order of resolution as DTAB > DDAB > OTAB > CTAB > TTAB. DDAB and DTAB both suffered from poor efficiency.

Table 5.2: Comparison of the number of theoretical plate and resolution of the adjacent peaks of CuL complexes using various EOF modifiers.

EOF Modifier	Efficiency		Resolution of adjacent peaks		
	CuEDTA	CuEDDS	CuIDS	***1***	***2***
DTAB	8299	3158	7438	2.42	5.23
TTAB	58 472	26 174	49 115	1.92	3.83
CTAB	75 799	24 795	45 196	1.00	2.05
OTAB	50 587	39 257	41 219	1.23	3.09
DDAB	8269	2901	12 764	3.15	4.84
TTAC	25 219	7739	10 499	2.89	4.09
TTAHS	5612	3809	960	0.52	0.62
CTAC	19 767	5304	15 592	3.44	5.83
CTAHS	60 452	22 582	26 451	2.25	1.75
DDAC	13 000	3549	12 764	2.96	5.09

1, 2 represent CuEDTA-CuEDDS and CuEDDS-CuIDS of adjacent peaks. Conditions: 40 mM tetraborate buffer and modifier at pH 6, applied voltage -25 kV, temperature 25ºC, hydrodynamic sample injection for 2s applying 50 mbar pressure, detection at 235 nm.

Efficiency is a function of the electroosmotic velocity, therefore controlling the EOF will be beneficial in maximizing efficiency and could lead to superior separations. The number of theoretical plates obtained by using the various modifiers is illustrated in Table

5.2. The results indicated that when TTAB, CTAB and OTAB were used good efficiencies were obtained, however there was some loss of resolution. This is evident from comparing the Figure 5.2 B, C and D. DTAB and DDABr did not give sharp peaks and the theoretical plates numbers were low. In this work, broad tailing peaks resulting in poor efficiency for CuL were observed when DDABr was utilised. This was in contrast to the work done by Laamanen et al [4], where a double-chained ionic surfactants gave better or comparable results as TTAB for the separation of Cu(II) complexes of eight APCAs. Melanson et al [5] also studied the behaviour of single-chained surfactants which form spherical aggregates at the silica surfaces and double-chained surfactants that form bilayer inside the capillary. According to Melanson et al double-chained surfactants may form a stable bilayer inside the capillary and allow a more stable environment for the separation of analytes than common single-chained EOF modifiers.

5.3.2 Effect of the surfactant counter anion on CuL complexes

The nature of the anionic counterion in solution has a strong effect on the magnitude of the reversed EOF observed. Lucy and Underhill [6] illustrated that studies on the fundamental properties of EOF in bare silica capillaries (in the absence of cationic surfactant) have demonstrated that adsorption of counter ions onto the fixed ionic sites of the capillary wall can alter the magnitude of the flow. They then postulated that a similar adsorption mechanism can be used to explain the effect of counter anions on EOF reversed by the adsorption of cationic surfactants. The proposed adsorption behaviour is:

$$X^- + \overline{(CTAB)}^+ E^- \xleftrightarrow{K_{wall}} \overline{(CTAB)}^+ X^- + E^-$$

where X^- is the counter anion in solution $\overline{(CTAB)}$ is the cationic surfactants adsorbed onto the capillary wall and E^- is the anionic portion of the double layer. If this hypothesis is valid, then there should exist an inverse relationship between EOF observed and the magnitude of the equilibrium constant, K_{wall}. As the adsorption of the counter ion increases in strength, the magnitude of the reversal EOF decreases. The buffer cation will compete with the surfactant for the cation exchange sites on the capillary surface.

5.3.2.1 The comparison of TTAC, TTAB and TTAHS on CuL complexes

The use of cationic quaternary alkylammonium bromides as EOF modifiers is very popular in CE. However in many published material, they are used as bromide salts, without taking into consideration the effect of the other counter anions of the modifier. In this study the effect of the counter anions of three surfactants i.e. TTA^+ in the Cl^-, Br^- and HSO_4^- forms was also investigated. Figure 5.3 illustrates the separation of CuL complexes using 0.3 mM of TTAC and TTAHS as EOF modifiers in 40 mM tetraborate buffer at pH 6. The obtained results showed tailing peaks for CuEDDS and CuIDS when TTAC (Figure 5.3A) was used compared to sharp peaks for TTAB (Figure 5.2B).

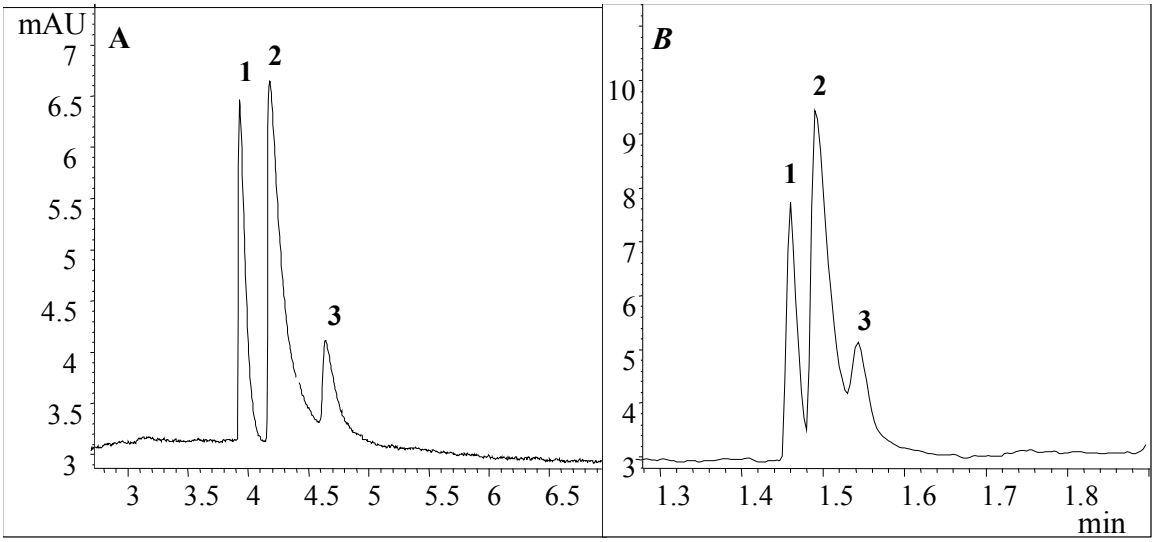

Figure 5.3: Typical electropherograms of CuL complexes using 0.3 mM (A) TTAC and (B) TTAHS. For peak identification and other conditions please refer Fig. 5.2.

The faster elution of CuL complexes was seen when TTAHS was utilised, although the resolution was poor. This is because HSO_4^- is a bigger anion as compared to Cl^- and Br^- and it slows down the EOF. In terms of the migration of CuL complexes the order of migration times follows TTAHS > TTAB > TTAC. We suggest that dynamic modification is not based only on the interactions with silanol groups on the capillary wall but can also depend on the counter anion of surfactants.

Improved resolution for complexes was obtained when TTAC was used and the values are given in Table 5.2. The values given indicate that the EOF is fast resulting in slower elution of CuL complexes. Whereas when TTAHS was used, complexes suffered from poor resolution and efficiency but their migration times were fast. The efficiency values were high for TTAB and low for TTAHS. The results in Table 5.2 show that the use of TTAB is preferable as opposed to TTAC and TTAHS. While the migration time was shorter using TTAHS, the resolution was better with TTAB and TTAC. Little attention has been paid to the effects of surfactant counter anions when separating analytes. The size of the counter anion on the surfactant is shown to influence the separation of CuL complexes. It was realized that differences were observed in resolution, migration times and efficiency of Cu(II)L complexes using various counter anions.

5.3.2.2 The comparison of CTAC, CTAB and CTAHS on CuL complexes

Figure 5.4 illustrates the electropherograms of CuL complexes and a good separation was observed when CTAC, CTAB and CTAHS were used as EOF modifiers. All peaks for CuL complexes were resolved and this was not the case when TTA^+ with various counter anions was used. This also reiterates that surfactants with longer alkyl chains behave much better than shorter ones.

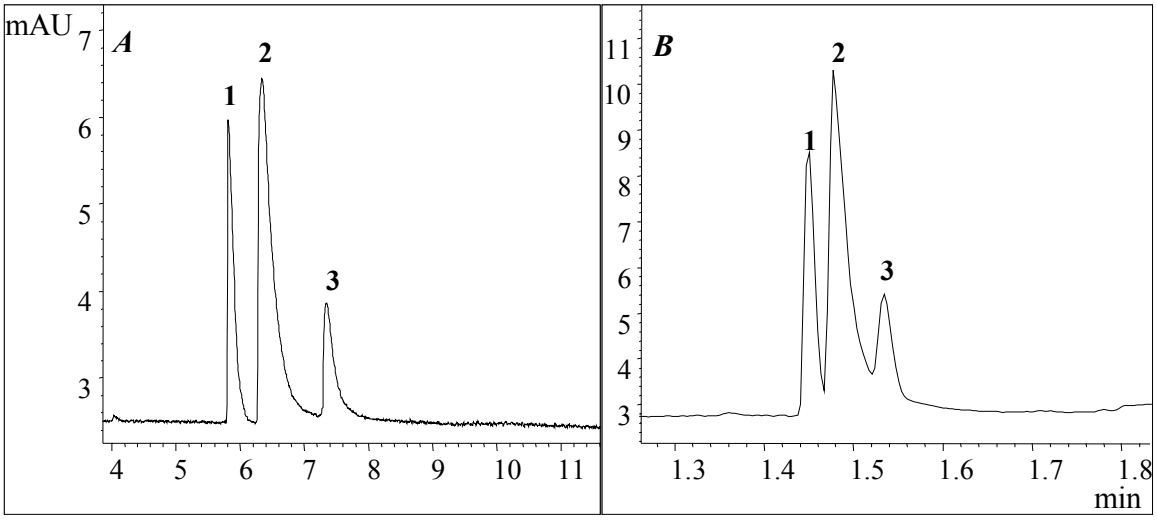

Figure 5.4: Typical electropherograms of CuL complexes using 0.3 mM (A) CTAC and (B) CTAHS. For peak identification and other conditions please refer Fig. 5.2.

A similar migration order was seen earlier in the case of TTA^+ with various counter anions. The slowest t_m is due to CTAC and CTAHS is the fastest. There is a major difference between the migration times of Cl^- and that of Br^- and HSO_4^-.

All modifiers showed a clear separation. This is seen in Fig. 5.2C and Figure 5.4. CTAC showed higher resolution (Table 5.2) due to its small counter anion. The obtained results also show the importance of the nature of the counter anions of the EOF modifiers. The smaller the size of the counter anion the faster the EOF thereby slowing down the mobility of analytes in a reversed EOF mode. The efficiencies with various EOF modifiers in BGE were compared to each other (Table 5.2). The highest values were obtained with CTAB and CTAHS for all CuL complexes except for CuEDDS in CTAB. CTAC gave the lowest efficiencies for all CuL complexes.

5.3.2.3 The comparison of DDAC, DDAB on CuL complexes

DDA^+ was only available in the two forms of counter anions i.e. Br^- and Cl^-. The results for DDAC were much better than DDAB and this is demonstrated in Figure 5.5. DDAC

provided sharper and more symmetrical peaks as opposed to broad tailing peaks observed from DDAB.

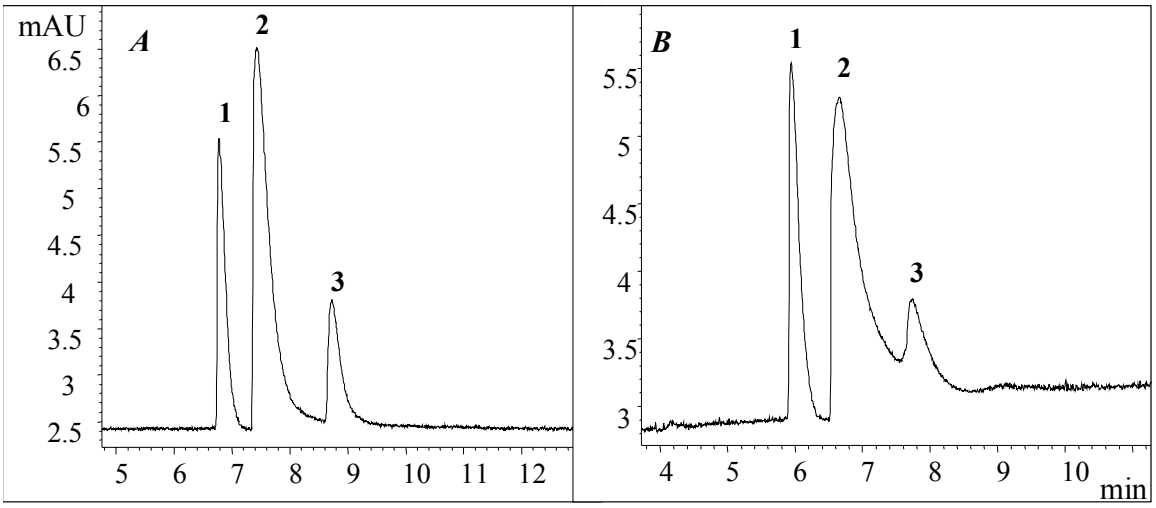

Figure 5.5: Typical electropherograms of CuL complexes using 0.3 mM (A) DDAC and (B) DDAB. For peak identification and other conditions please refer Fig. 5.2.

A comparison of t_m using various modifiers reveals that t_m is lower when DDAB is utilized. Although the difference between Br^- and Cl^- anions was not that much as compared to TTA^+ and CTA^+ with different counter anions. The resolution for adjacent peaks is excellent for both DDAB and DDAC and values are seen in Table 5.2. The calculated R_s values were comparable between the two EOF modifiers even though DDAB resulted in the peak shapes that were not good. All CuL complexes were resolved satisfactorily.

A remarkable effect on separation efficiency was seen although the separation efficiency was not the highest for CuEDDS in both EOF modifiers. The results in Table 5.2 show that the separation of CuL complexes is strongly affected by the type of counter anion used in the surfactants.

5.4 Conclusion

This work demonstrated the use of CE in studying the behaviour of various EOF modifiers on the separation of APCAs as Cu(II) complexes. CE also provided fast and fairly efficient separations for CuEDTA, CuEDDS and CuIDS complexes when using CTAB and TTAB as EOF modifiers. The length of the alkyl chain of EOF modifiers additive proved to significantly influence the separation process inside the capillary. This was clearly seen when shorter DTAB produced long migration times. The counter anion also plays a major role in the CE separation process. The results of this study illustrate that surfactants and their counter ions influence not only EOF and migration times, but also resolution and efficiency. Therefore, attention should be paid to the selection of the surfactant including its counter ion.

Bibliography

[1] Kaneta T, Tanaka S, Taga M, ***J Chromatogr A***, 1993, 653,313.

[2] Katata L, Nagaraju V, Crouch A.M, ***Anal. Chim. Acta***, 2006, 579, 177-184.

[3] Galceran M.T, Puignou L, Diez M, ***J Chromatogr A***, 1996, 732, 167.

[4] Laamanen P.-L, Busi S, Lahtinen M, Matilainen R, ***J Chromatogr A***, 2005, 1095, 164-171.

[5] Melanson J.E, Baryla N.E, Lucy C.A, ***Anal Chem***, 2000, 72, 4110.

[6] Lucy C.A, Underhill R.S, ***Anal Chem***, 1996, 68, 300.

[3]Chapter 6

Analysis of chelating agents in cosmetics by CE and LC

6.1 Introduction

In this chapter a simple isocratic reversed phase ion pair HPLC method and a capillary electrophoresis method for the simultaneous determination of ethylenediamine tetraacetic acid (EDTA), S,S'-ethylenediaminedisuccinic acid (EDDS) and R,S-iminodisuccinic acid (IDS) complexing agents as their Fe(III) complexes is described. The non biodegradable EDTA is used in combination with biodegradable analogues like EDDS and IDS in many commercial products. The performance of the two methods was evaluated in terms of linearity, limit of detection (LOD), limit of quantitation (LOQ) and reproducibility. The LOD values obtained from HPLC are better when compared with CE. The results obtained by both CE and HPLC were found to be comparable and in good agreement. The methods are applied for determinations in shower creams and foam baths. The products were chosen because the chelating agents are part of the ingredients in cosmetics, and end up in the environment after use.

6.2 Experimental Details

6.2.1 Materials and reagents

All reagents were of analytical reagent grade unless stated otherwise. HPLC grade methanol from BDH (Poole, England) was used. EDTA, tetrabutylammonium hydrogen sulfate, sodium formate, formic acid and iron(III) chloride and nitrate stock standard solutions, 2-(N-morpholino)ethanesulfonic acid monohydrate (MES), 3-morpholino-2-hydroxypropane-sulfonicacid (MOPSO) and tetradecyltrimethylammonium bromide (TTAB) are obtained from Sigma-Aldrich (Steinheim, Germany). S,S'-EDDS, and Baypure CX 100 (R,S-IDS) were procured from Fluka (Buchs, Switzerland) and Bayer

[3] Part of the work described in this chapter has been published in Analytica Chimica Acta, 2006, 579, 177, L Katata, V Nagaraju and A. M Crouch.

(Leverkusen, Germany) respectively. Deionized water was prepared by passing distilled water through a Millipore (Bedford, MA, USA) Milli Q water purification system.

6.2.2 Instrumentation

6.2.2.1 Capillary Electrophoresis

All separations were performed on a Hewlett-Packard^{3D} CE instrument (Agilent Technologies, Waldbronn, Germany) equipped with a diode array UV-visible detector. A bare fused silica capillary (Composite Metal Services Ltd., Worcester, UK) of 50 μm i.d. with the total length of 50 cm and the detection window burned at 8.5 cm from the capillary end. The separation potential of -25 kV was applied during all separations and samples were introduced by applying a 50 mbar pressure for 2 seconds. Absorbances between 200 and 225 nm were monitored for the detection of analytes. Metal-ligand complexes were prepared by mixing a mixture of metal stock solutions with a ligand. 10 mM MES and MOPSO buffer was prepared daily and used as the background electrolyte. TTAB was used as EOF modifier and thiourea as a neutral marker for CE analysis. The electrolyte and samples were sonicated and filtered through a 0.45 μm membrane filter prior to use. 0.1 M of HCl and NaOH were used to adjust the pH of buffers and samples. All experiments were conducted at 25 ºC.

The new bare fused silica capillary was rinsed with 0.1 M NaOH for 10 minutes, then with deionized water for another 10 minutes and equilibrated with the borate buffer solution for a further 10 minutes. Between each injection the capillary was filled with the buffer solution by flushing the entire capillary for 5 minutes. The sample solution was introduced into the anodic end of the capillary by hydrodynamic injection. A voltage of – 25 kV was then applied for separation.

6.2.2.2 Liquid chromatography

A HPLC (Waters, Milford, MA, USA), model 510 pump with a 20 μL loop injector was used. A Waters, Lambda Max model 481 LC spectrophotometer was connected after the

column. All the operations were performed using Waters System Controller model 600E. A reversed-phase Luna 5µ C_{18} (2) (Phenomenex, Torrance, CA, USA) column (25 cm x 4.6 mm id, particle size 5 µm) was used for determination of the three complexing agents. pH measurements were carried out with Combined Conductivity/ pH meter (Jenway, UK) model 3880 equipped with a combined glass calomel electrode, which was calibrated using standard buffer solutions of pH 4.0, 7.0 and 9.2 before measuring the pH of the solutions.

The mobile phase was a methanol:formate buffer (2 mM tetrabutylammonium hydrogen sulfate and 15 mM sodium formate, pH adjusted to 4.0 with formic acid) (10:90 V/V); before delivering into the HPLC system it was filtered through 0.45 µm PTFE filter and degassed using a vacuum. The analysis was carried out under isocratic conditions using a flow rate of 0.8 mL min^{-1} at 24^0C temperature and UV detection at 240 nm.

6.2.3 Analytical procedure

6.2.3.1 CE

The standards were prepared from stock solutions of EDDS (10 mM), EDTA (10 mM), IDS (20mM) and $Fe(NO_3)_3$ (10 mM) dissolved in 10 mM MES and MOPSO buffer. Metal complex solutions were prepared by mixing the desired proportions of Fe and appropriate complexing agents and diluting with a buffer. The samples were prepared as follows: 2 g of shower cream or foam bath was weighed accurately and transferred into 25 mL volumetric flask and diluted with BGE, followed by ultrasonic treatment for 10 minutes. A 2000 µL of concentration of sample was further diluted with BGE in 10 mL volumetric flask. The sample was adjusted to pH 5.5 and then filtered through 0.45 µm PVDF filter. It was directly injected into the CE system for analysis.

6.2.3.2 HPLC

The stock solutions of EDTA (10 mM) and EDDS (10 mM) were prepared in deionized water, whereas IDS (20 mM) was in formate buffer. A10 mM of $Fe(III)Cl_3$ was prepared

in 10 mM HCl. The stock solutions were stored in refrigerator. Metal complex solutions were prepared by mixing the desired proportions of iron and appropriate complexing agents and diluting with deionized water which was previously adjusted to pH 2.5 with dilute HCl. The solutions were kept in refrigerator and left to stand over night to ensure complete complexation.

Samples of shower cream (2g) and foam bath (1g) were accurately weighed and transferred into 100 mL volumetric flasks and dissolved in deionized water and made-up to the volume with the same. The pH of the samples was adjusted to 2.5 with dilute HCl and filtered through Whatman No.2 filter paper and then with 0.45 μm PVDF filter. To the sample solution 10 mM of iron solution was added and made up to the known volume with deionized water which was previously adjusted to pH 2.5 with dilute HCl. The solutions were kept in refrigerator and left to stand over night to ensure complete complexation and injected in to the chromatograph.

6.3 Results and Discussion

6.3.1 Method development

6.3.1.1 High performance liquid chromatography

A number of HPLC methods were available for determination of EDTA and a few were reported for EDDS and IDS. Most of the reported methods used reversed-phase, ion-pair chromatography and determined the complexing agents as either iron or copper complexes. The initial method development was started by using methanol and tetrabutylammonium bromide (TBA) at different concentrations, ratios and at different pH levels with a Luna C_{18} (2) column to separate the three complexes of EDTA, EDDS and IDS. EDTA and EDDS were successfully separated in the pH range of 4.0-5.0, when methanol is at 15% and TBA 85%, but the IDS was eluted as a broad peak. Then, TBA in acetate buffer and methanol as an organic modifier were tried. IDS was not retained on the column at any pH and concentration of TBA. It was also observed that the EDDS peak was splitting at pH 4.0 to 5.0 and this is due to speciation of EDDS at various pH

levels. Cokesa et al [15] used 12.5% (v/v) methanol in formate buffer (15 mM sodium formate, 5 mM formic acid and 2 mM tetrabutylammonium hydrogen sulfate) to separate the stereo isomers of IDS as Cu (II) complexes in biodegradation studies. The published method was confined only to the separation of the isomers of IDS complexes. The same method was applied in the present studies and optimized to separate the EDTA, EDDS and IDS as their Fe (III) complexes.

Figure 6.1 shows the chromatogram of a standard mixture of Fe(III) complexes of EDTA, IDS and EDDS. The three complexes were well separated from each other and identified by injecting them individually and comparing the retention times. The mobile phase used was methanol:formate buffer (2 mM tetrabutylammonium hydrogen sulfate and 15 mM sodium formate, pH adjusted to 4.0 with formic acid) (10:90 v/v). The separation and resolution were found to be pH dependent. The effect of pH on the separation of the complexes in the range 3.0-5.0 on the mobile phase was studied (Fig. 6.2A). pH values between 3.5-4.2 were found to be the optimum, but at pH 4.0 the three peaks with good resolution and baseline separation were obtained. Although from the Fig. 6.2A, the pH 3.0 looks ideal but it was observed that the EDTA peak is broad with severe peak tailing. Methanol was used as an organic solvent modifier to improve the separation. The effect of percentage of methanol on retention of the complexes was studied (Fig. 6.2B). The chromatographic separation was also found to be dependent on the concentration of methanol and found to be optimum at 10% (v/v) because peaks were well separated at this concentration. The influence of tetrabutylammonium hydrogen sulfate (TBAHS) and sodium formate on retention of these complexes were studied (Fig. 6.2C). It can be seen from Fig. 6.2C that concentrations of TBAHS of between 2.0 and 5.0 mM was found to be ideal. A concentration of 2.0 mM was selected for the analysis. A sodium formate concentration of 15 mM was found to be ideal for the separation of EDTA, IDS and EDDS complexes (Fig. 6.2D). The chromatographic data including retention time (t_R), relative retention time (RRT), retention factor (k'), tailing factor (T_f) and relative response factors (RRF) are given in Table 6.1. It can be seen from the Table 6.1 that the elution order of the complexes are EDTA, IDS and EDDS and the response of the EDTA

is high when compared with the IDS and EDDS. It should be noted that certain points of FeIDS complex are missing because it could not be detected at those points.

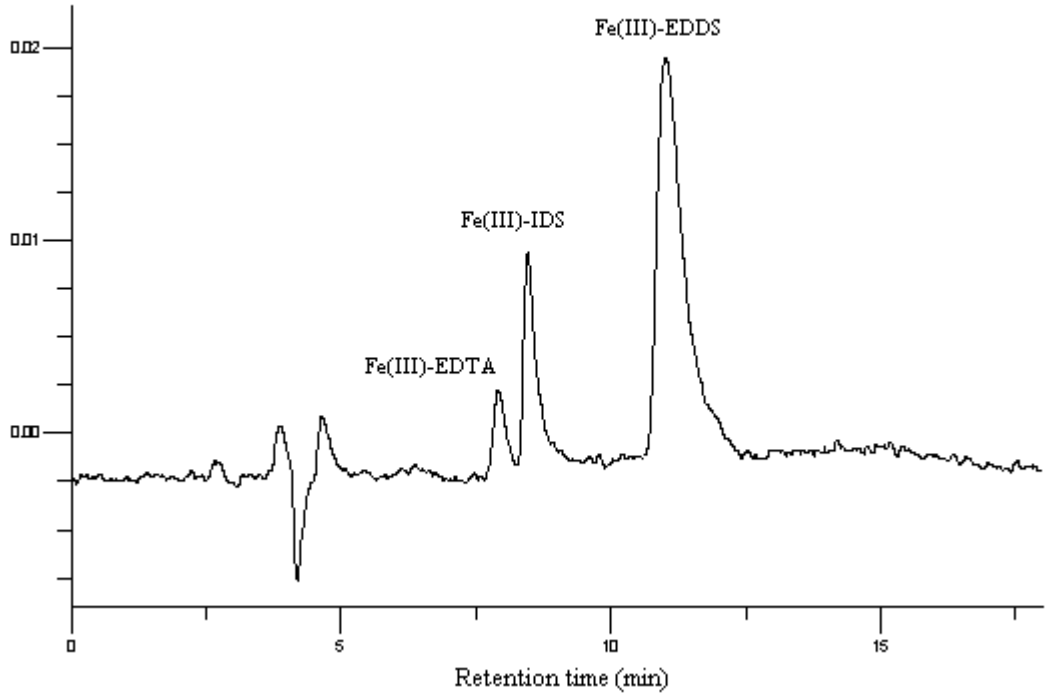

Figure 6.1: A typical chromatogram of a standard mixture containing Fe(III) complexes of EDTA (0.3 µM), IDS (10 µM) and EDDS (15 µM).

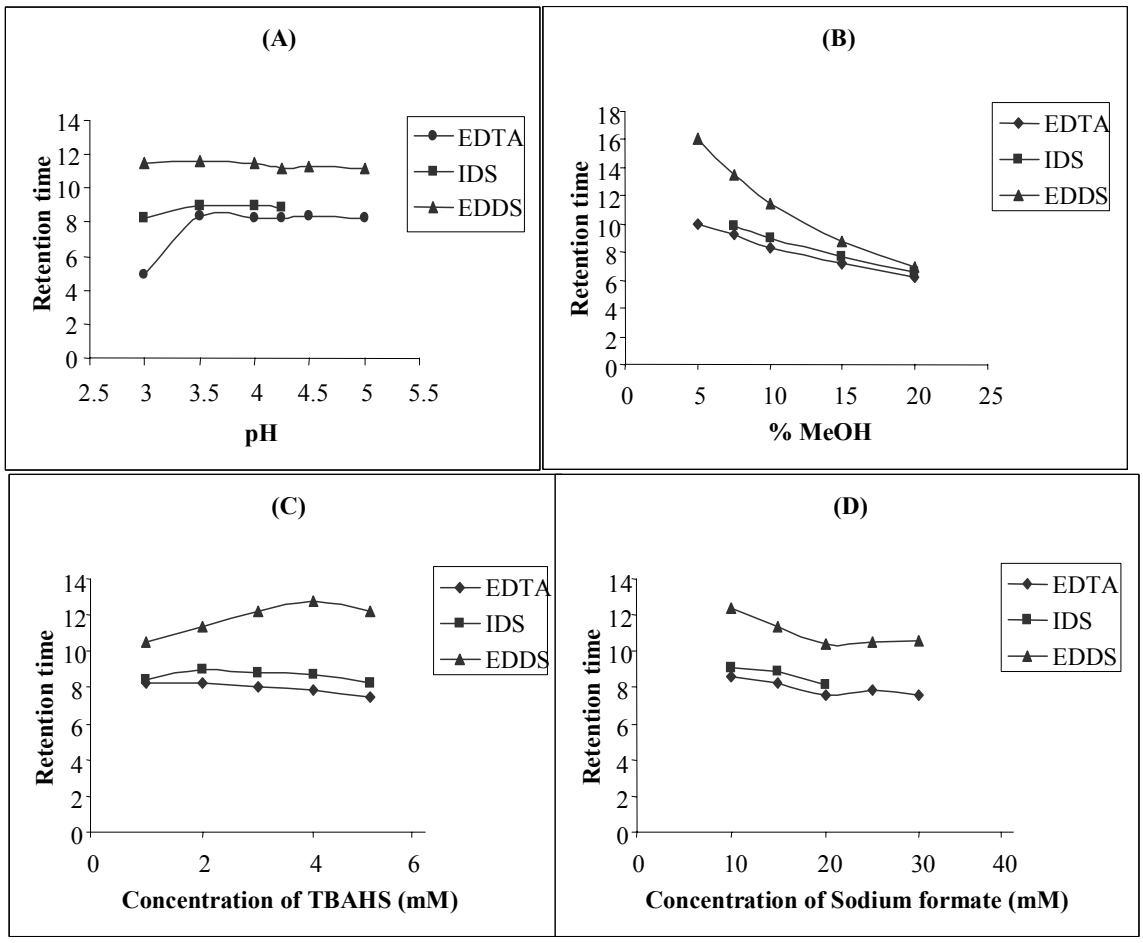

Figure 6.2: Effect of (A) pH, (B) % methanol, (C) concentration of TBAHS and (D) concentration of sodium formate on retention of Fe(III) complexes of EDTA, IDS and EDDS.

Table 6.1: Retention and response data of Fe(III) complexes of EDTA, IDS and EDDS by HPLC.

Complex	t_R	RRT	k'	T_f	RRF
Fe(III)-EDTA	8.10	1.00	2.86	1.10	1.00
Fe(III)-IDS	8.67	1.07	3.10	1.23	0.10
Fe(III)-EDDS	11.37	1.40	4.41	1.42	0.20

6.3.1.2 Capillary Electrophoresis

The initial analysis of a mixture of Fe(III) complexed with three chelating agents namely IDS, EDDS and EDTA, was investigated using various background electrolytes (BGEs). 25 mM MES and MOPSO buffer with 0.25 mM TTAB as an EOF modifier at pH 5.5 was found to be suitable for the separation of a mixture of the three ligands. The best experimental conditions for the separation were established by varying the buffer concentration. The concentration of the BGE was varied from 8.5 mM to 35 mM and the resolution and migration times were both affected. The results obtained (Fig. 6.3A) showed that the concentration of BGE plays an important role in the separation of the mixture of Fe with IDS, EDDS and EDTA. The peaks were sharper at lower buffer concentrations and the FeEDDS and FeEDTA peaks were well resolved. Therefore, a 10 mM MES and MOPSO buffer at pH 5.5 was selected as optimal. The effect of pH was also investigated within the pH range of 4.5-6.5 at a fixed buffer concentration of 10 mM MES and MOPSO. It was found that when the pH was raised, the resolution decreased while the analysis time was fast. The FeIDS peak was smaller and broader at high and lower pH. At pH 6.5, FeEDDS and FeEDTA complexes migrated together and were eluted as one peak. Based on the results in Fig. 6.3B, pH 5.5 was chosen as the optimized pH.

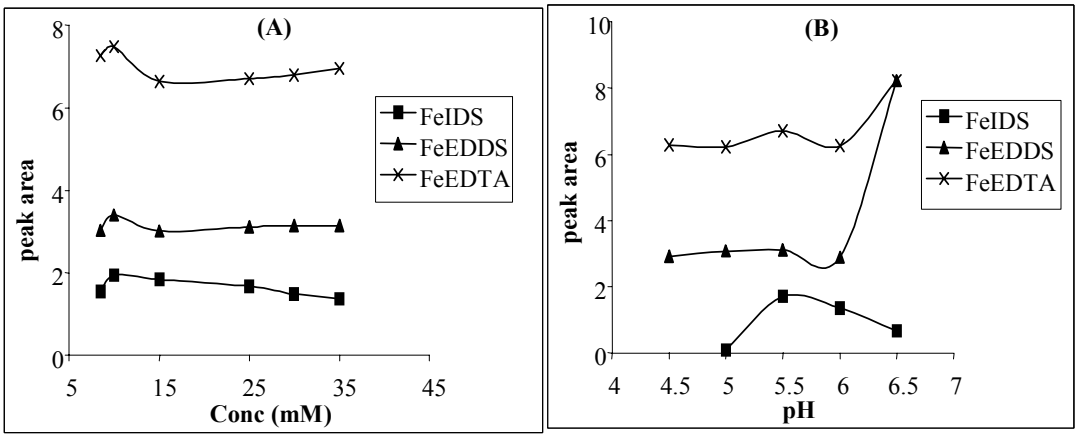

Figure 6.3: Effect of concentration of buffer (MES and MOPSO) and pH on the peak areas of Fe(III) complexes of IDS, EDDS and EDTA.

The electropherogram of a mixture of 1 mM FeIDS, FeEDDS and FeEDTA complexes separated in less than 4 minutes is shown in Fig. 6.4. The CE results exhibited good peaks and the migration order was as follows i.e. FeIDS < FeEDDS < FeEDTA. This elution order closely follows the log K values of the complexes which are 16.1, 22.0 and 27.2 for FeIDS, FeEDDS and FeEDTA respectively. The elution order and time analyses were different from those obtained by HPLC method because the separation is governed by the different molecular sizes and hydrophobicities.

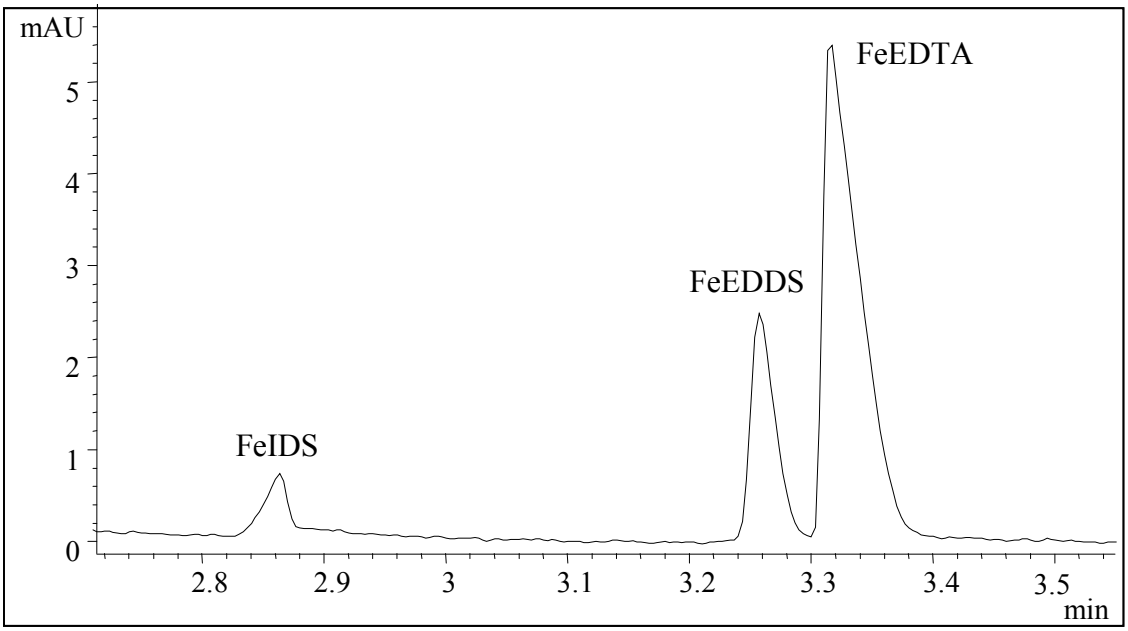

Figure 6.4: A typical electropherogram of Fe(III) complexed with 1 mM of each chelating agent. Conditions: 10 mM MES and MOPSO buffer with 0.25 mM TTAB, applied voltage -25 kV, temperature 25 ºC, hydrodynamic sample injection for 2 s applying 50 mbar pressure, detection at 225 nm.

6.3.2 Method validation

Standard mixtures containing known amounts of Fe(III) complexes of EDTA, IDS and EDDS were prepared and analyzed by HPLC and CE. The accuracy of the methods was checked by the standard addition technique. It was found that the additions were reflected in their peak areas and percent recovery is in the range 80-104%. The repeatability of the optimized method was determined by injecting standard mixture five times into HPLC and CE. The relative standard deviations (RSD %) were calculated for peak areas and retention times for HPLC. In the case of CE the corrected peak area and migration times were used. The repeatability of HPLC peak areas was relatively poor because manual injection was used for this technique. The data was given in Table 6.2. Calibration graphs (concentration vs peak area) were constructed at six concentration levels using HPLC and CE for the three complexes. Three independent determinations were carried out at each

concentration level. Good linearity and reproducibility was found during the experiments. Table 6.3 gives the linearity equation, mass range and correlation coefficients. The limit of detection (LOD) and limit of quntitation (LOQ) were calculated based on 3 and 10 times noise level respectively.

Table 6.2: Repeatability of the HPLC and CE methods

Complex	Relative standard deviation (%)			
	Peak area		Retention/migration time	
	HPLC	CE	HPLC	CE
Fe(III)-IDS	1.58	0.57	1.25	0.21
Fe(III)-EDDS	1.76	0.78	1.52	0.80
Fe(III)-EDTA	1.84	0.54	1.43	0.81

Table 6.3: Linear regression data of Fe(III)-EDTA, Fe(III)-IDS and Fe(III)-EDDS

Complex	Range (μM)	Linear regression	Correlation coefficient (r)	LOD (μM)	LOQ (μM)
By HPLC					
Fe(III)-EDTA	0.3-2.0	15.596x + 2575.5	0.9974	0.1	0.25
Fe(III)-IDS	10.0-40.0	3510.3x – 4464.9	0.9906	5.0	10.0
Fe(III)-EDDS	5.0-20.0	5327.3x + 17009	0.9811	0.4	1.0
By CE					
Fe(III)-IDS	1000-3500	1.0735x – 0.1835	0.9982	300.0	900.0
Fe(III)-EDDS	200-700	2.87x – 0.0103	0.9961	50.0	150.0
Fe(III)-EDTA	200-700	6.0219x + 0.0549	0.9995	25.0	75.0

6.3.3 Analysis of cosmetics

The optimized ion-pair chromatographic and CE methods were applied to the determination of EDTA, IDS and EDDS in cosmetics. Different batches of two different brands of cosmetics which were having EDTA and IDS as one of the ingredients in their composition were procured from the local supermarket. The brand which contains EDTA is a foam bath and IDS is in the commercial shower cream. Due to the non availability of cosmetics containing EDDS in South Africa, the EDDS was determined by spiking to the other two brands. As described in the Experimental section the samples were prepared and injected into the HPLC and CE. Figures 6.5 and 6.6 give the chromatograms of samples of shower cream and foam bath respectively. It could be seen from the Figures 6.5 and 6.6 the IDS and EDTA were clearly separated and no interference with any peak was observed. Figures 6.7 and 6.8 give the electropherograms of samples of shower cream and foam bath respectively. An unknown peak was observed at the migration time around 3.2 min in both the products and it is not interfering with IDS and EDTA. The summarized results are presented in Table 6.4. To know the applicability of the methods to EDDS in cosmetics and also to check the accuracy of the methods, known amounts of EDTA, IDS and EDDS were spiked to the samples and the recoveries were calculated. Figs. 6.9 and 6.10 show the chromatogram and electropherogram spiked with EDTA, IDS and EDDS to the cosmetics. A significant in migration times between Figs 6.4 and 6.10 were seen due to analysis of complexes in various matrices. Table 6.5 gives the results of recoveries. It could be seen from Table 6.5 that the three complexes were successfully determined by using the present CE and HPLC methods.

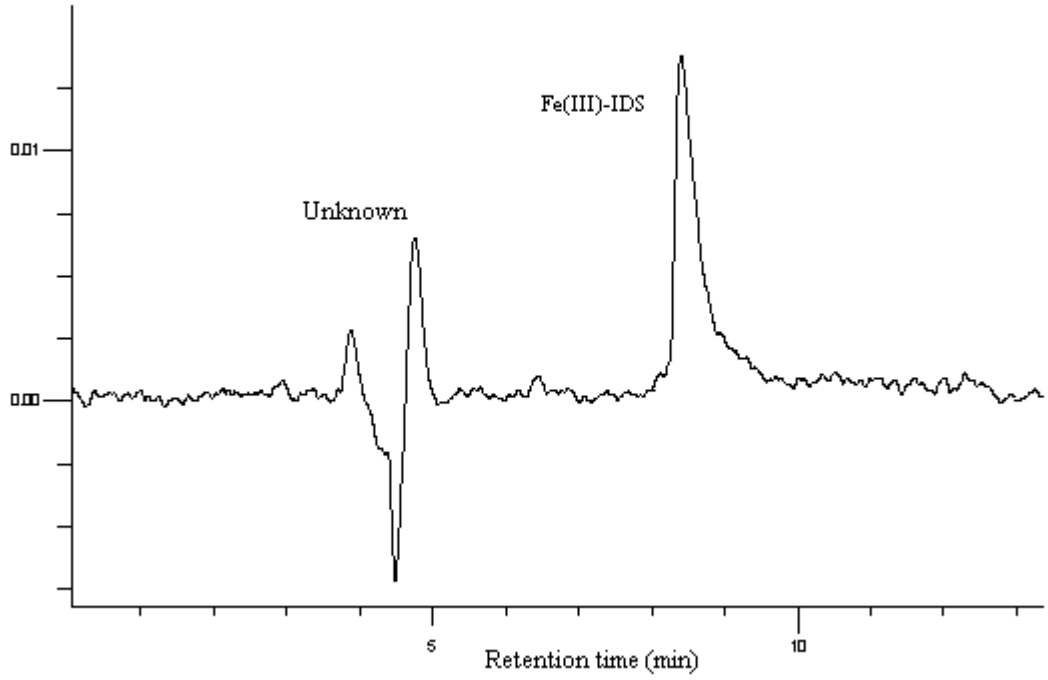

Figure 6.5: A typical chromatogram of a sample of shower cream determined by the HPLC method. Conditions: column C18, mobile phase methanol-formate buffer (20 mM tetrabutylammonium hydrogen sulfate, 15 mM sodium formate adjusted to pH 4 with formic acid) (10:90, v/v), detector UV at 240 nm.

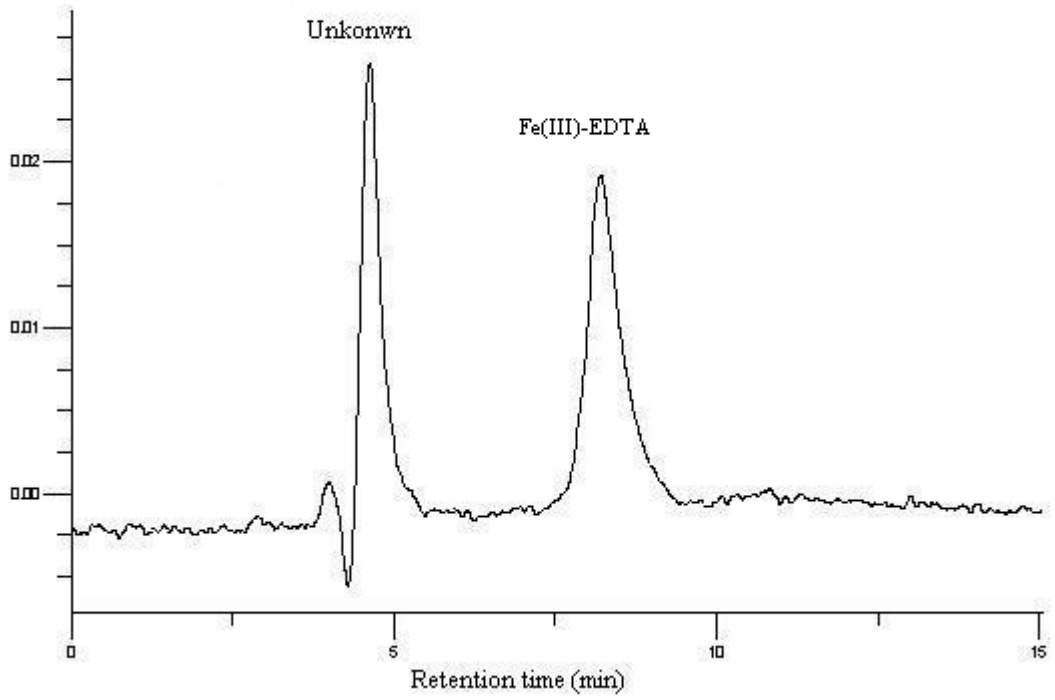

Figure 6.6: A typical chromatogram of a sample of foam bath analyzed by the present HPLC method. Conditions same as Fig. 6.5.

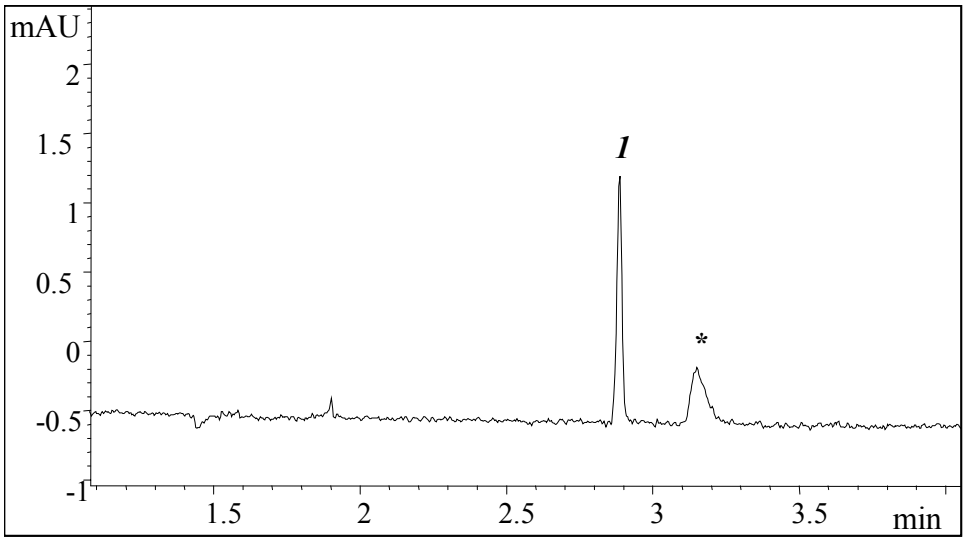

Figure 6.7: A typical electropherogram of a sample of shower cream.
Peaks: (1) Fe(III)-IDS and (*) unknown. Conditions same as given in Fig. 6.4.

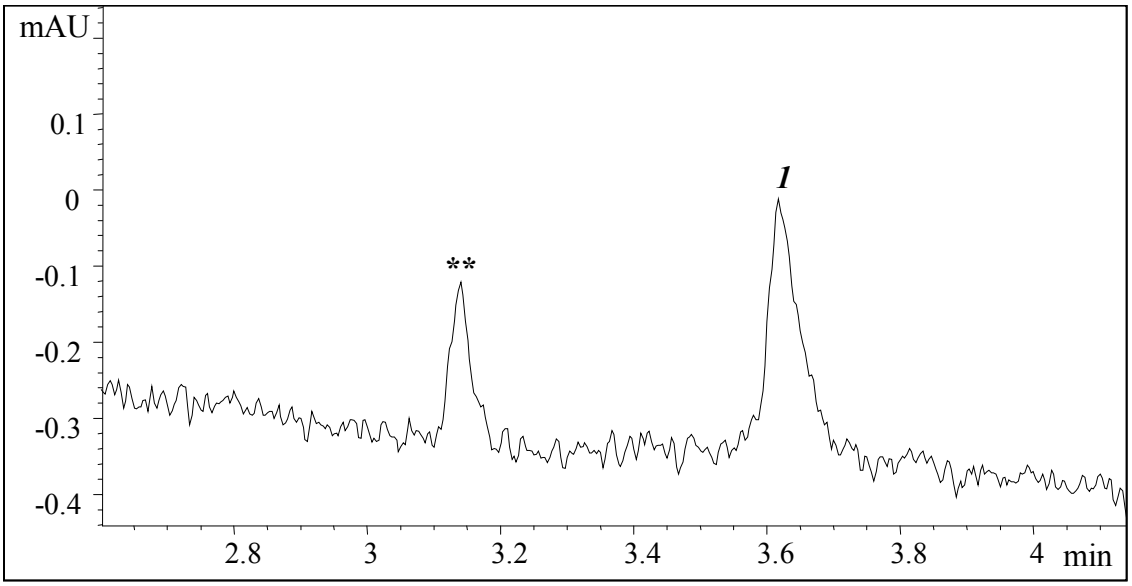

Figure 6.8: A typical electropherogram of a sample of foam bath.
Peaks: (1) Fe(III)-EDTA and (**) unknown. Conditions same as given in Fig. 6.4.

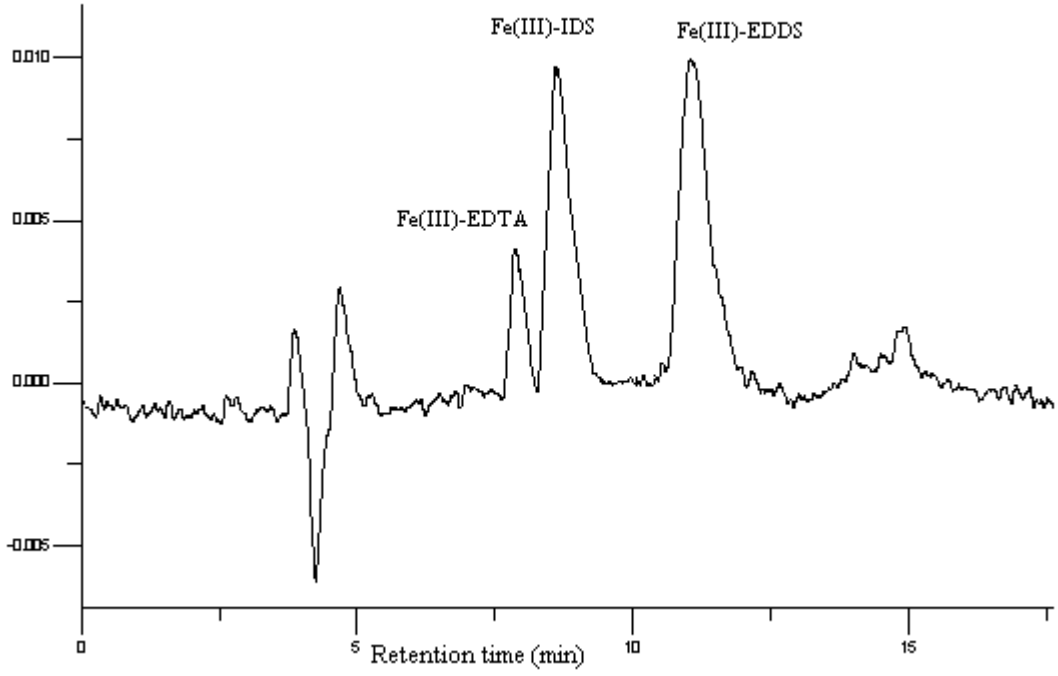

Figure 6.9: A typical chromatogram of a sample of shower cream after spiking with EDTA (0.5 µM), IDS (4µM) and EDDS (8µM).

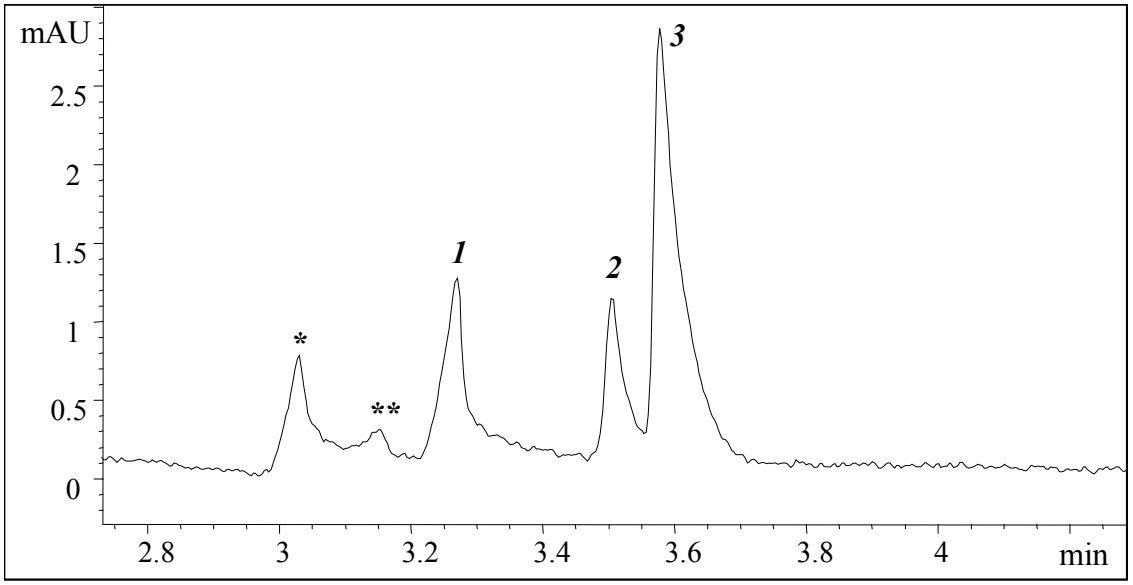

Figure 6.10: A typical electropherogram of a sample of foam bath after spiking with IDS (1.5 mM), EDDS (0.3 mM) and EDTA (0.3 mM). * and ** unknown. For peak identification and conditions please refer Fig. 6.4.

Table 6.4: Determination of Fe complexes of EDTA and IDS in cosmetics

Batch	Sample	Fe(III)-EDTA (% w/w)	RSD (%)	Fe(III)-IDS (% w/w)	RSD (%)
HPLC					
A1	Foam bath	0.21	1.89	--	--
A2	Foam bath	0.18	2.05	--	--
A3	Foam bath	0.25	1.63	--	--
B1	Shower cream	--	--	2.15	1.58
B2	Shower cream	--	--	2.42	1.83
B3	Shower cream	--	--	2.28	1.92
CE					
A1	Foam bath	0.25	1.55	--	--
A2	Foam bath	0.22	1.79	--	--
A3	Foam bath	0.20	1.83	--	--
B1	Shower cream	--	--	2.31	0.56
B2	Shower cream	--	--	2.02	0.72
B3	Shower cream	--	--	2.55	0.63

Table 6.5: Recovery of simultaneous determination of Fe complexes of EDTA, IDS and EDDS in cosmetics by standard addition method

Batch	Name	Fe(III)-EDTA			Fe(III)-IDS			Fe(III)-EDDS		
Recovery		Spiked (µM)	Found (µM)*	Recovery (%)	Spiked (µM)	Found (µM)*	Recovery (%)	Spiked (µM)	Found (µM)*	(%)
HPLC										
A1	Shower cream	0.50	0.44 ± 0.03	88.0	4.0	3.73 ± 0.12	93.3	8.0	7.75 ± 0.09	96.9
		0.75	0.71 ± 0.02	94.7	8.0	8.21 ± 0.03	102.6	16.0	16.09 ± 0.07	100.6
		1.00	0.96 ± 0.04	96.0	15.0	15.18 ± 0.06	101.2	30.0	30.31 ± 0.13	101.0
B1	Foam bath	0.25	0.26 ± 0.02	104.0	10.0	9.8 ± 0.03	98.0	5.0	5.09 ± 0.06	101.8
		0.50	0.48 ± 0.03	96.0	20.0	20.1± 0.08	100.5	10.0	10.23 ± 0.90	102.3
		1.00	1.02 ± 0.02	102.0	40.0	40.4± 0.01	101.0	20.0	20.17 ± 0.15	100.9
CE										
A1	Shower cream	1000	851 ± 2.31	85.1	200	175 ± 3.12	87.5	200	182 ± 2.15	91.0
		1500	1409 ± 3.22	93.9	300	289 ± 3.43	96.3	300	297 ± 4.19	99.0
		3000	2982 ± 3.65	99.4	600	609 ± 3.75	101.5	600	605 ± 3.14	100.8
B1	Foam bath	1000	889 ± 2.14	88.9	200	190 ± 2.33	95.0	200	193 ± 3.57	96.5
		1500	1510 ± 2.82	100.7	300	310 ± 4.12	103.3	300	305 ± 2.68	101.7
		3000	3010 ± 3.29	100.3	600	595 ± 2.45	99.2	600	603 ± 3.35	100.5

* Mean ± SD n=3

6.4 Conclusion

A HPLC and CE method was developed for the simultaneous determination of readily biodegradable chelating agents EDDS and IDS and the non-biodegradable EDTA complexed with Fe(III). The HPLC method displayed lower detection limits than CE. Advantages of CE are shorter analysis time and lower consumption of chemicals. The methods were successfully applied to cosmetic products like shower cream and foam bath for the simultaneous determination of these chelating agents and the results obtained by

both HPLC and CE were comparable with the concentrations of IDS and EDTA in the two products tested. The main advantage of these methods used was the lack of tedious sample preparation. Due to their simplicity the methods could be used routinely not only in quality control laboratories of cosmetic industries but also in environmental/industrial applications to determine these three complexes.

Bibliography

[1] Deacon M, Smyth M.R, Tuinstra L.G.M, ***J. Chromatogr***, 1993, 657, 69.

[2] Sorvari J, Sillanpaa M, Sihvonen M.L, ***Analyst***, 1996, 121, 1335-1339.

[3] Kord A.S, Tumanova I, Matier W.L, ***J. Pharm. Biomed. Anal***, 1995, 13, 575.

[4] http://www.makingcosmetics.com/products/51-antioxidants-EDTA-ethylenediaminetetra-acetic-acid-tetrasodium-salt.htm

[5] Williams D, ***Chem. Br***, 1998, 34, 48-50.

[6] http://www.ospar.org

[7] Loyaux-Lawniczak S, Douch J, Behra P, ***Fresenius J. Anal Chem***, 1999, 364, 727-731.

[8] Bedsworth W.W, Sedlak D.L, ***J. Chromatogr. A***, 2001, 905, 157-162.

[9] Krokidis A.A, Megoulas N.C, Koupparis M.A, ***Anal. Chim. Acta***, 2005, 535, 57.

[10] Suzuki S, Kishimoto K, Amemiya T, Itoh K, Koichi, Nakamura H, ***Kenkyusho Kenkyu Nenpo***, 1993, 44, 85.

[11] Irache J.M, Ezpeleta I, Vega F.A, ***Chromatographia***, 1993, 35, 232.

[12] Metsarinne S, Tuhkanen T, Aksela R, ***Chemosphere***, 2001, 45, 949.

[13] Tandy S, Schulin R, Suter M.J.-F, Nowack B, ***J. Chromatogr. A***, 2005, 1077, 37.

[14] Tandy S, Schulin R, Nowack B, ***J. Chromatogr. Sci***, 2006, 44, 82-85.

[15] Cokesa Z, Knackmuss H.-J, Rieger P.-G, ***Appl. Environ. Microbiol***, 2004, 70, 3941-3947.

[16] Laine P, Matilainen R, ***Anal. Bioanal. Chem***, 2005, 382, 1601.

[17] Padarauskas A, Schwedt G, ***J. Chromatogr. A***, 1997, 773, 351-360.

[18] Harvey S.D, ***J. Chromatogr. A***, 1996, 736, 333-340.

[19] Buchberger W, Mulleder S, ***Mikrochim Acta***, 1995, 119, 103-111.

[20] Laamanen P.-L, Mali A, Matilainen R, ***Anal. Bioanal. Chem***, 2005, 381, 1264-1271.

Chapter 7

Analysis of EDTA in environmental samples using capillary electrophoresis with direct UV detection

7.1 Introduction

Interest in the accurate and precise determination of aminopolycarboxylic acids (APCAs) such as EDTA has become more important because of the increasing need to monitor waste waters following stringent regulation of industrial and agricultural discharges. This is because EDTA occurs widely as a water pollutant since it is mostly used by many industries in aqueous solutions which are discharged after use via wastewater streams and reach the environment. EDTA has been reported as the only anthropogenic organic compound detected in European surface waters at highest concentrations [1] due to its non-readily biodegradability thus can pose a threat to aquatic ecosystem [2]. It can also lead to the mobilization of toxic heavy metals in river sediments [3]. The industrial applications involve complexing metal ions for example in pulp bleaching, electroplating and photographic processing.

Various analytical techniques have been developed for determination of chelating agents for e.g. gas chromatography (GC) [4], liquid chromatography (LC) [5] and ion chromatography mass spectroscopy (IC-MS) [6]. EDTA effluent of municipal wastewater treatment plants (WWTP) in Western Europe analyzed by LC-MS was detected above 10 μg/L [7]. These methods usually rely on the derivatization of the free chelate to a UV-absorbing metal complex and often require complex pretreatment of the samples prior to analysis. Capillary electrophoresis (CE) appears to be an attractive technique with features such as short analysis times, simpler chemistry, high resolution, low electrolyte and sample consumption compared to the latter methods. There are available reports regarding the separation of transition metals ions with EDTA by CE [8-10]. In a more recent work, Laamanen et al [11] studied the determination of chelating agents by CE. Their study involved the use of didecyldimethylammonium bromide (DMDDAB) and

tetradecyltrimethylammonium bromide (TTAB) as flow modifiers. DMDDAB was found to be the best EOF modifier in the separation of eleven chelating agents as their Cu(II) complexes.

In a previous study discussed in Chapter 6 the effect of electroosmotic flow (EOF) modifiers on aminopolycarboxylic acids by CE [12]. We reported the use of CE for the determination of chelating agents using various EOF modifiers, however in that paper our methods were not tested on real samples. In this study we further utilised two of the EOF modifiers namelycetyltrimethylammonium chloride (CTAC) and tetradecyltrimethylammonium chloride (TTAC) for the determination of EDTA in South African river waters and industrial effluents.

7.2 Experimental Details

7.2.1 Chemicals

Copper(II) nitrate standard solution, cetyltrimethylammonium chloride (CTAC), tetradecyltrimethylammonium chloride (TTAC) and ethylenediaminetetraacetic acid disodium salt dehydrate (EDTA) are obtained from Sigma–Aldrich (Steinheim, Germany). Disodium tetraborate decahydrate from Merck (Darmstadt, Germany) was used. Deionized water was prepared by passing distilled water through a Millipore (Bedford, MA, USA) Milli Q water purification system. All reagents were of analytical reagent grade unless stated otherwise.

7.2.2 Instrumentation

All separations were performed with an HP CE instrument as reported before in chapter 2 section 2.2. The capillary cassette temperature was adjusted to 25 °C with air cooling. A separation potential of −25 kV was applied during all separations and samples were introduced by applying a 50 mbar pressure for 2 s. Absorbances at 225, 235 and 245 nm were monitored for the detection of analytes. pH measurements were carried out with combined conductivity/pH meter (Jenway, UK) model 3880 equipped with a combined

glass calomel electrode, which was calibrated using standard buffer solutions (Sigma–Aldrich, Steinheim, Germany) of pH 4.0, 7.0 and 9.2 before measuring the pH of the solutions. All experiments were conducted at 25 °C.

7.2.3 Study site and sample collection

River water and industrial effluents (paper, plating and printer) samples were collected from the City of Cape Town municipality– Scientific Services Department (South Africa) as part of their regional monitoring program. Figure 7.1 shows an overview of the location of some river samples analyzed in this study, sampling points being Ek 3, 5, 9, 17 and 19. Their monitoring points were done between Bottelary and Eerste Rivers in the Western Cape. Industrial effluent samples (i.e. paper, plating and printer) were collected from various industries.

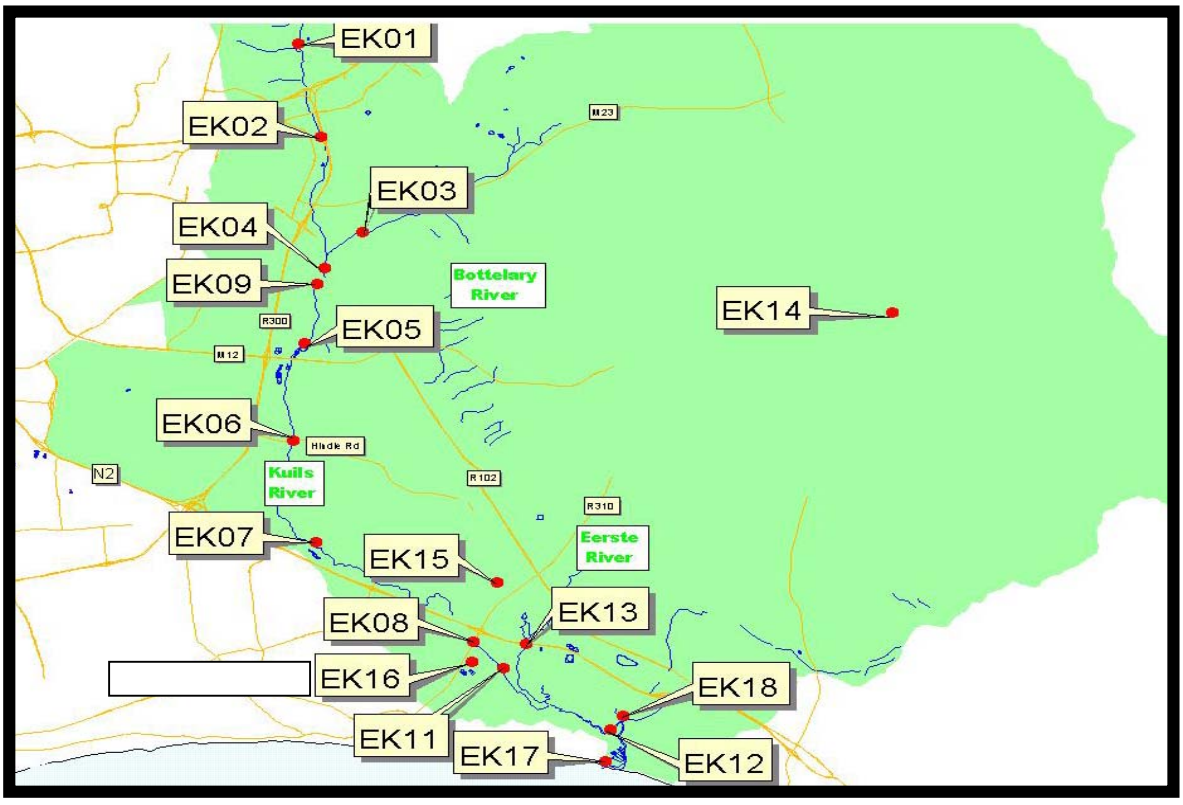

Figure 7.1: Locations of river water sampling sites between the Bottelary and Eerste River.

7.2.4 Solutions and samples

The stock solutions were prepared from EDTA (10 mM) and $Cu(NO_3)_2$ (10 mM) dissolved in background electrolyte (BGE) which consisted of 40 mM tetraborate buffer and 0.3 mM CTAC or TTAC as EOF modifier. Metal complex solutions were prepared by mixing the desired proportions of metal and appropriate complexing agents and diluting with the buffer. In order to analyze EDTA in the environmental samples, all free EDTA and its metal complexes were converted to Cu(II)-EDTA. 10 mL of environmental samples and 5 mM CuEDTA were placed in a volumetric flask and diluted with deionized water. The sample solutions were allowed to stand for three hours to ensure complete complex formation and thermodynamic equilibrium at room temperature. The pH of the sample was then adjusted to the same level as the electrolyte used. The buffer and samples were filtered through a 0.45 μm PVDF membrane filter (Sigma–Aldrich, Steinheim, Germany). It was then directly injected into the CE system for analysis.

The new bare fused silica capillary was rinsed with 0.1 M NaOH for 10 min, then with deionized water for another 10 min and equilibrated with the buffer solution for a further 10 min. In between each injection the capillary was filled with the buffer solution by flushing the entire capillary for 5 min. The sample solution was introduced into the anodic end of the capillary by hydrodynamic injection. A voltage of −25 kV was then applied for separation. After every fourth sample, the capillary was conditioned by flushing it with 0.1 M NaOH (5 min), ultra pure water (10 min) and BGE for 10 min to ensure that the capillary was in good condition throughout the sequence.

7.3 Results and Discussion

EDTA is the most widely used chelating agents because of its ability to form strong complexes with many metal ions. Although EDTA is not toxic to mammals at the concentrations found in the aquatic environment, there has been some concern about its potential to remobilize heavy metals from the decomposition of river sediments and sewage sludge using electrolytic oxidation [13]. As a result, knowledge of the environmental quantity of EDTA and other ligands is vital for understanding their

environmental fate. This is an extension study based on the previous work done by us [12]. The suitability of the CE method was checked on the analysis of EDTA as Cu(II) complex in the South African environmental samples.

Chelating agents do not occur as free acids in environmental samples but complexes with different metal ions. The analysis of EDTA in thirteen environmental samples was investigated utilizing 40 mM tetraborate buffer and 0.3 mM CTAC or TTAC as background electrolyte at pH 6. The effect of varying the concentration and pH of tetraborate as background electrolyte (BGE) in the analysis of chelating agents was tested earlier [12]. Speciation profiles of the negatively charged complex $CuEDTA^{2-}$ modelled by Joint Expert Speciation System (JESS) program has stability in the pH range of 4-10 [14], therefore the chosen pH for this work was within this range. We investigated CTAC and TTAC to test our previous methods used on the analysis of environmental samples because these modifiers are scarcely utilized in the determination of chelating agents.

In order to analyze EDTA in environmental samples, all free EDTA and its metal complexes were converted to $CuEDTA^{2-}$ before CE analysis. Better peak shapes were obtained when CTAC was used as EOF modifier compared to TTAC. The electropherogram of river water sample Ek 3 complexed with CuEDTA separated in less 4 min is illustrated in Figure 7.2A. The first sharp peak eluting at 1.5 min is due to the nitrate peak. EDTA in environmental samples was analysed by the standard addition method i.e. EDTA was identified by spiking a standard CuEDTA complex solution (Fig. 7.2B). Other metal ions in the sample did not interfere with the measurement of EDTA.

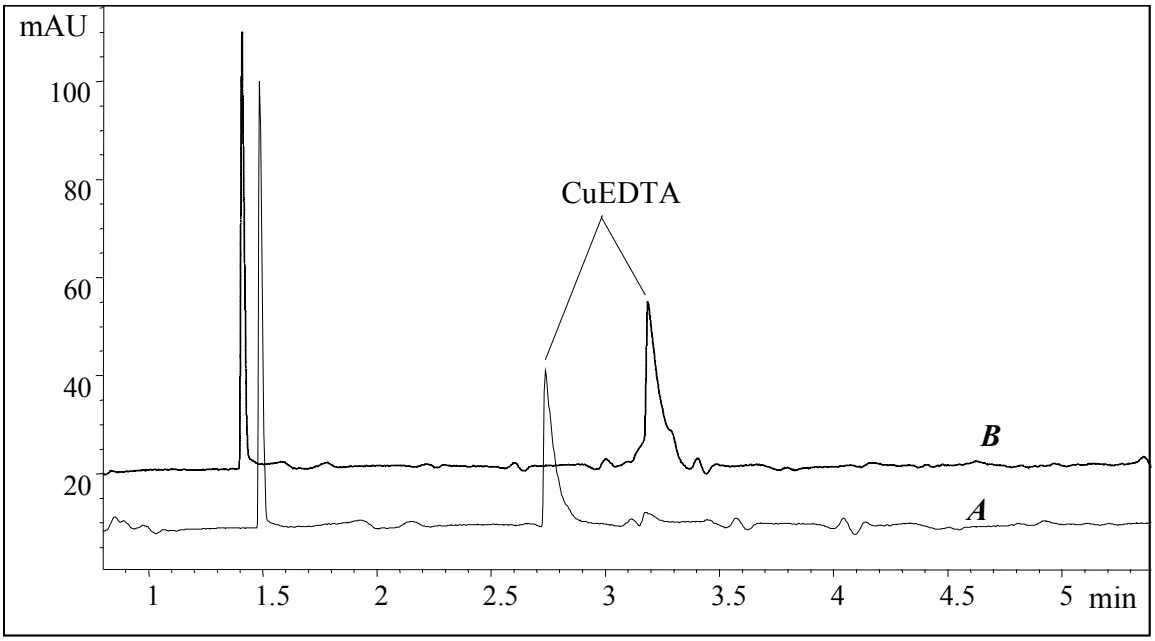

Figure 7.2: Electropherograms of river water sample Ek 3, (A) complexed with CuEDTA; (B) spiked with CuEDTA. Conditions: 40 mM tetraborate buffer and 0.3 mM CTAC at pH 6 (with NaOH), applied voltage -25 kV, temperature 25 ºC, hydrodynamic sample injection for 2s applying 50 mbar pressure, detection at 235 nm.

The data for analysis of environmental samples is summarized in Table 7.1. The analytical parameters of the methods using TTAC and CTAC were evaluated and their concentrations are compared with ICP data (Table 7.2). The migration times were different for all the samples but the variability of migration times did not affect the identification of the analytes because peak patterns remain the same. The reason for this behaviour may be due to different matrixes in all samples. Repeatability of peak areas was ≤ 5.5 and ≤ 2.70 % for migration times. The linearity was tested in the concentration range 0.4-5 mM for a standard solution of CuEDTA complex. The calibration curves based on the corrected peak areas were linear in the concentration range tested and the correlation coefficients (R^2) were ≥ 0.9850 respectively. The limit of detection (LOD) was determined from repeated injections of diluted solution standard, at a signal-to-noise ratio (S/N) of 3. The data presented were the average of the four injections of the sample or the standard. The LODs were 30 μM when CTAC was used and 45 μM for TTAC.

Paper mill samples did not contain measurable concentrations of EDTA, but with the sample matrix the ICP measurements were possible.

Table 7.1: Analytical parameters of environmental samples using CTAC and TTAC as modifiers in CE

Sample type	RSDs (Migration time)		RSDs (Peak area)		R^2	
	CTAC	TTAC	CTAC	TTAC	CTAC	TTAC
River water						
Ek 3	2.52	0.44	4.19	5.51	0.995	0.994
Ek5	ND	ND	ND	ND	ND	ND
Ek 9	ND	0.48	ND	1.05	ND	0.992
Ek 17	ND	ND	ND	ND	ND	ND
Ek 19	ND	ND	ND	ND	ND	ND
Paper A	2.63	0.29	1.78	1.85	0.995	0.997
Paper B	0.67	1.65	3.70	0.98	0.987	0.968
Plating A	0.42	1.54	5.53	4.61	0.996	0.991
Plating B	0.45	0.59	1.01	2.04	0.991	0.985
Plating C	0.11	1.72	2.17	3.15	0.978	0.994
Printer A	0.29	ND	1.97	ND	0.985	ND
Printer B	0.48	ND	3.50	ND	0.992	ND
Printer C	1.16	ND	3.71	ND	0.990	ND

Number of replicates = 4, ND = not detected

EDTA concentrations could only be determined by CE for the samples upstream of Bottelary River i.e. Ek 3 and 9. Ek 3 is located next to the residential area and 1 km away from the viticulture wastewater treatment plant. There is a wastewater treatment plant 50 m away from Ek 9. In the residential areas most people make use of the household products which contain EDTA as part of the ingredients and it is also used in most industries. EDTA therefore find its way into the river water and it was not detected in the downstream samples of the river because it was below the limit of detection of the CE

method. The results indicate that the concentrations varied by the type of environmental samples being analyzed, with the highest concentrations in river sample Ek 3.

Table 7.2: Concentration (mM) of EDTA found in some South African environmental samples using CE compared to ICP.

Sample type	concentration of EDTA (mM)		
	CE (CTAC)	CE (TTAC)	ICP
River water			
Ek 3	0.4795	0.4964	0.6135
Ek5	ND	ND	0.3820
Ek 9	ND	0.2578	0.3774
Ek 17	ND	ND	ND
Ek 19	ND	ND	0.3889
Paper A	0.2945	0.3163	ND
Paper B	0.3492	0.2491	ND
Plating A	0.3184	0.2913	0.3922
Plating B	0.2859	0.3047	0.4161
Plating C	0.3261	0.3384	0.4362
Printer A	0.3072	ND	0.4325
Printer B	0.3346	ND	0.4029
Printer C	0.3528	ND	0.4196

Number of replicates = 4, ND = not detected

7.4 Conclusion

EDTA is extensively being used as chelating agent in many industrial and domestic applications for many years and is released to the environment through sewage treatment plants. The CE methods proved to be suitable for the determination of EDTA in environmental samples and reasonable resolution was achieved without matrix

intereference. When CTAC was utilized as EOF modifier most environmental samples were determined.

The river sample Ek 3 showed the highest concentration of EDTA as compared to other samples. This is attributed to the fact that Ek 3 is located near residential area and wastewater treatment plant. It was also expected that Ek 9 would have a high concentration of EDTA because of it is 50 m away location from wastewater treatment plant. This was not the case in our study and the reason might be that another chelating agent other than EDTA is used in the plant or they use it is in small quantities during their processes. The obtained CE and ICP data are of special importance from an environmental point of view. There is also a need to investigate more on the concentration levels of other chelating agents in South African rivers especially the ones that flow close to industries using CE as a method for analysis due to its simplicity.

Bibliography

[1] Quintana J. B, Reemtsma T, ***J Chromatogr A***, 2007, 1145, 110-117.

[2] Nowack B, ***Environ. Sci. Technol***, 2002, 36, 4009-4016.

[3] Xue H, Sigg L, Kari F. G, ***Environ Sci Technol***, 1995, 29, 59-68.

[4] Sillanpää M, Sihvonene M.L, ***Talanta***, 1997, 44, 1487-1497.

[5] Laine P, Matilainen R, ***Anal.Bioanal.Chem***, 2005, 382, 1601-.

[6] Knepper T P, Werner A, Bogenschütz G, ***J Chromatogr A***, 2005, 1085, 240-246.

[7] Reemtsa T, Weiss S, Mueller J, Petrovic M, Gonzalez S, Barcelo D, Ventura F, Knepper T P, ***Environ Sci Technol***, 2006, 40, 5451.

[8] Carbonaro R.F, Stone A.T, ***Anal. Chem***, 2005, 77, 155-164.

[9] Laamanen P.-L, Busi S, Lahtinen M, Matilainen R, ***J Chromatogr A***, 2005, 1095, 164-171.

[10] Katata L, Nagaraju V, Crouch A.M, ***Anal. Chim. Acta***, 2006, 579, 177-184.

[11] Laamanen P.-L, Matilainen R, ***Anal. Chim. Acta***, 2007, 584 (1), 136-144.

[12] Katata L, Crouch A.M, "The effect of various electrophoretic flow modifiers and anions on the separation efficiency of aminopolycarboxylic acids (EDTA, EDDS

and IDS) by capillary electrophoresis" manuscript to be submitted for publication.

[13] Kari F.G, Giger W, ***Water Res***, 1996, 30, 122-134.

[14] Khotseng L.E, PhD thesis, University of Stellenbosch, South Africa, 2004

Chapter 8

8 General conclusions and future recommendations

8.1 General conclusions

As demonstrated in this thesis CE can be successfully used as an analytical tool for the analysis of APCAs especially readily biodegradable complexes. It also showed the possibility to separate labile metal-IDS complexes at various pH levels and concentrations, although some of the peaks could not be identified in the electropherograms. JESS speciation data was compared with the obtained results and validated the presence of some metal-IDS species.

The time analysis study of ML complexes gave an interesting perspective of the behaviour of complexes at various pH levels and time intervals. As usual CuDTPA and CuEDDS showed a great stability over the analysis time and this was in agreement with the results found in the literature. The study is important as it gave an analyst an idea of the eventual fate of various ML complexes in the aqueous media. This information can help especially environmentalists about the fate of chelating agents in the environment.

A mixture of different metal ions complexed with chelating agents i.e. IDS, EDDS and EDTA was also achieved by CE. The use of pH buffers with weak complex properties like MES and MOPSO is highly recommended when separating a mixture of ML complexes as this was impossible in our case when tetraborate buffer was used. In chapter 5, CE and HPLC method was developed for the determination of EDDS, IDS and non-readily biodegradable EDTA complexed with Fe(III). The methods were further applied to the analysis of EDTA and IDS in shower cream and bath foam. Due to their comparability of the CE to the preferred routinely used HPLC, CE shows to be a promising tool that can be used in quality control laboratories of environmental, cosmetic and many more industries to determine chelating agents.

This work demonstrated the utility of CE in studying the behaviour of various EOF modifiers on the separation of a mixture of CuEDTA, CuEDDS and CuIDS complexes. The length of the alkyl chain and counter anion of the modifiers played a major role in the separation process of the CuL complexes. CTAC was then used to test the applicability of the method in various South African environmental samples such as river water and industrial effluents. The method can assist in monitoring the concentration of chelating agents in natural waters and industrial effluents.

8.2 Future recommendations

A follow-up study is required where CE is coupled with MS. This would help to identify most of the unknown species observed during analysis of ML complexes especially for the obtained results in Chapter 2 and 3. This is because there is no literature available in the CE-MS of readily biodegradable chelating complexes like EDDS and IDS. Although an attempt was made in Belgium (Prof Pat Sandra's laboratory, Gent University) for the CE-MS analysis of readily biodegradable metal ligand complexes but due to limited time spent there our results were not conclusive, therefore a thorough investigation needs to be done. This work would aid in predictions of the environmental behaviour of contaminant metal ions with chelating agent.